The chemokine CCL2/CCR2 signaling mediates cancer associated fibroblasts-cancer cells interaction and promotes basal-like breast cancer progression

By

Min Yao

Submitted to the graduate degree program in Pathology and Laboratory Medicine and the Graduate Faculty of the University of Kansas in partial fulfillment of the requirements for the degree of Doctor of Philosophy.

Chair: Nikki Cheng, Ph.D.

Fang Fan, M.D., Ph.D.

Patrick E. Fields, Ph.D.

Timothy A. Fields, M.D., Ph.D.

Joan Lewis Wambi, Ph.D.

Date Defended: 27 September 2017

The dissertation committee for Min Yao certifies that this is the approved version of the following dissertation:

The chemokine CCL2/CCR2 signaling mediates cancer associated fibroblasts-cancer cells interaction and promotes basal-like breast cancer progression

_____

Chair: Nikki Cheng, Ph.D.

Date Approved: 12 October 2017

Abstract

Breast cancer is the most common cancer diagnosed in women in the United States. The basal-like breast cancer subtype represents about 12% of breast cancer and has the worst outcome in patients due to lack of effective therapies. Tumor stroma plays an important role in cancer progression. Cancer associated fibroblasts (CAFs) are the most abundant stromal cells in breast cancer, but their function in cancer progression has not been fully understood. We previously identified that the chemokine CCL2 was highly expressed in breast cancer associated fibroblasts. CCL2 is known to recruit monocyte/macrophage and promotes cancer progression. We previously found that recombinant CCL2 can directly signal to breast cancer cells and promote cell survival and invasion *in vitro*. In this study, we aimed to determine the functional importance of CCL2 signaling mediated fibroblast-cancer cell interactions in the breast cancer progression. We evaluated the expression of CCL2 and fibroblast marker Fsp1 in breast cancer tissue microarray containing 427 samples by immunohistochemistry. Expression of CCL2 and Fsp1 were co-upregulated in invasive ductal carcinoma compared to normal breast. High stromal CCL2 expression associated with reduced recurrence free survival in the basal-like subtype. Further data mining in the breast cancer TCGA and METABRIC datasets revealed that the CCL2/CCR2 pair expressed highest in the basal-like subtype. We confirmed high CCL2 expression from CAFs isolated from primary human and mouse breast cancer samples. CAFs with high CCL2 expression significantly promoted xenograft growth when co-grated with human basal-like breast cancer MCF10A-CA1D cell line. Reduction of CCL2 expression by CRISPR mutation or shRNA knockdown in human or mouse CAFs significantly reduced tumor growth in the co-graft model. Fibroblasts condition medium or recombinant CCL2 directly promoted CA1D cancer cell growth *in vitro*. Mutation of the CCL2 receptor CCR2 receptor in CA1D

cancer cell significantly reduced cancer cells growth *in vitro* and *in vivo* in response to CCL2 stimulation. The CCL2/CCR2 signaling activated PKC and SRC pathways in cancer cells, and contributed to growth promotion. We aimed to test the therapeutic efficacy by blocking CCL2 in breast cancer mouse model through continuous delivery of CCL2 neutralizing antibody. Despite the steady delivery of the antibody, CCL2 blocking did not significantly affect tumor progression. Examination of CCL2 level in blood and tumor sites revealed that CCL2 blocking significantly induced higher free CCL2 level, which may contribute to lack of efficacy. In summary, our studies have showed that CCL2 derived from cancer associated fibroblasts plays an important role in basal-like breast cancer progression. Direct signaling to cancer cells via CCR2 is an important mechanism in CCL2 function. Thus, the CCL2/CCR2 signaling may serve as potential therapeutic targets in basal-like breast cancer. CCL2 blocking by neutralizing antibody can lead to undesired increased CCL2 level, and alternative targeting approaches are needed to achieve therapeutic efficacy.

Acknowledgements

There are so many people to thank for my doctoral studies. For those who know my history in graduate studies, it has been a long and rough path. Without that help, I cannot come and stand here today. I had a hard time in my first graduate studies. It did not work out very well, and I had to graduate with a Master's degree after four years of graduate work in the lab. I had long been interested in biological research, but this failure was a heavy blow to me. I began to doubt myself, was research in science a real good fit for me? However, I still recalled my excitement when reading scientific literature, discussing ideas, or achieving tiny discoveries in the lab. I decided to give myself another try and re-started my Ph.D. studies in Department of Pathology. After another four years, I am standing here to defend today.

First of all, I would like to thank my mentor, Dr. Nikki Cheng. I was so grateful that Nikki gave me an opportunity to do a rotation in her lab and decided to take me as a graduate student later, back in 2013. I am also so lucky to find out that Nikki is a great mentor. Without her, I cannot come here today. For those who do not know Nikki much, she may seem a little too serious, does not smile or talk much. But inside the lab, she is really helpful and supportive. She always encourages me, opens to new methods and ideas, and trains me in data analysis and interpretation. She works very hard, often stays late at night and in the weekend, serving an inspiring model of a scientist. Though extremely busy, she spends lots of time and efforts in supporting students besides research. She supported me in multiple grant applications and taking additional classes. She also supported a lot in my career developments. I have discussed with her many times about career interests and future plan. She is always helpful and insightful. She helped write very supportive recommendation letters. Among all her mentoring efforts, I would like to specifically mention one example which I remember all the time. One time during my

first attempt in grant writing, she helped revise my draft of research proposal, and found my written English was very poor, containing lots of grammar errors. She decided to show me how to make corrections and improve written English in front of a computer, literally, words by words, sentence by sentence. It took us one Friday night and one Saturday afternoon to finish a three- page proposal. After that, she bought and gave me a grammar book which I still keep today. My English has improved much since then, but I never forgot this special occasion that she took such great efforts in helping me. It is in Nikki's lab that I regain my confidence, strengthen my interest in science, and look forward to continuing. Without Nikki's support, I think all those will be impossible. I feel so lucky to have her as my mentor, and I would like to recommend her to all graduate students for training.

I would like to thank my committee members, for their help in my research and career development. I would like to thank Dr. Timothy Fields. He always asks critical questions and gives good suggestions. He also helps in my career development and writes a supportive reference letter. I would like to thank Dr. Patrick Fields. He is not only my committee member, but also a collaborator. I have worked in his lab to generate the CRISPR/Cas 9 mutant. He is always very encouraging and supportive in my research. I have a lot of discussions with him on career development. So many times he just walked into our lab, pat on my shoulder, and said to me, "Hey, Min, I think you should consider professor XX as potential postdoc mentor". My committee member Dr. Fan Fang is breast cancer pathologist. It is really helpful to get insights from her on the clinical side. I have bothered her so many times, by bringing her slides and asking for help for histology under the microscope. I would like to thank Dr. Joan Wambi. She is also an expert in breast cancer, gives nice suggestions, and supports my research and career

development. I also would like to thank my former committee, Dr. Adams Krieg. He is also very encouraging and helpful, and I am sorry to see him move away to a different institution.

I would like to thank members of the Cheng laboratory. First of all, I would like to thank Wei Fang. He is a senior postdoc in the lab, and is like my second mentor. He is very critical and insightful, and provides many good suggestions for my research. He is always very helpful with experimental technique. He also functions as a lab manager, and helps take care of all the supporting issues with research. Beyond research, I always enjoy talking with him, sports, jokes, everything, like a close friend. I would like to thank my fellow students, Gage Brummer and Diana Acevedo. They are all inspiring me in their own ways in pursuing scientific research and career. I have enjoyed discussions and collaborations with them. I would like to thank the technician Curtis Smart. He has worked with me for over a year, and helped me with many experiments. I would like to thank all formal lab members, especially former graduate student An Zou and postdoctoral fellow Benford Mafuvadze, for their help and support.

I would like to thank a few collaborators in my thesis studies. Firstly, I would like to thank Dr. Vincent Staggs and Dr. Wendy He from Biostatistics Department. Dr. Staggs helped with the initial survival analysis in the tissue microarray studies, and kindly shared me his SAS code. I took Dr. He's survival class, and from her, I learned the survival analysis and SAS programming. Secondly, I would like to thank my classmate and friend Dr. Nehemiah Alvarez from Dr. Patrick Fields's lab in the collaboration on CRISPR/Cas9. Nehemiah helped me in the generation of the CCR2 mutant cell lines and learn the CRISPR/Cas9 technology. We became close friends after the collaboration. Lastly, I would like to thank Dr. Shixiang Huang from Baylor College of Medicine. Her group helped us in analyzing samples using reverse phase protein array.

In addition, I would like to thank a few laboratories and individual in KUMC that help me in my studies. I would like to thank Dr. Roy Jensen lab for sharing the basal-like breast cell lines, and many research equipment. I would like to thank Dr. Jeremy Chien for providing me the CRISPR/Cas9 vectors. I would like to thank Dr. Katherine Fields for sharing the THP-1 cell line with me. I would like to thank the Histology, Flow cytometry and Rodent Search Facility core facilities for their supports in my research.

I would like to thank Dr. Mary Markiewicz for her help in my career development. I took tumor immunology class from her, and the immunology journal club under her supervision. She also provides lots of suggestions in searching for postdoctoral mentors in the area of tumor immunology. I would like to thank Dr. Thomas Yankee and Dr. Michael Parmely for their suggestions in my career development. I also would like to thank Dr. Benyi Li for his support for me and my wife Tina.

I would like to thank my family in China for supporting me all the years, especially, my father, mother, and my sister. I own my whole life to their love. It has been tough for me to not visit them often while I am here in U.S., but they never stop their continual encouragement and supports.

Most importantly, I would like to thank my wife Tina (Qingting Hu). She does a lot for me and for the family. We met here in KUMC when she came for an exchange scholar program. We fall in love and get married. She decided to stay with me in U.S. and gave up her original career to become a doctor in China. My life is completely changed since met with her. She takes very good care of me and makes sure I look clean and tidy. She is always supportive and encouraging, especially in times when I am felling low. Also, she inspires me in her own way in

getting adjusted to new life in U.S. She studies very hard in learning the English language. She has good skills in research, and actually publishes more papers than I do. In fact, she helps many experiments in my thesis studies. I cannot express enough my appreciation and love toward my wife. It coincides that my defense day is also the birthday of my wife. I hope my passing of defense can be one small birthday gift for all her support and love.

I would like to thank the Pathology Department and KUMC for their support in my study and research here. I also thank all my friends, church families, and everyone who has helped and inspired in my studies here in Kansas City.

My thesis study is funded by American Cancer Society (RSG-13-182-01-CSM). I also receive a pilot grant from Pathology Department. Without those funds, this research is not possible,

All my words fall short in expressing my thanks and gratitude for all the people involved in my doctoral studies. I sincerely hope my training here will help prepare me in making more scientific contributions in fighting cancers in the long term, in another way to say thank you.

Table of contents

List of figures and tables

Chapter I: Background

Chapter II: Expression of CCL2 and fibroblast marker Fsp1 in breast cancer

Chapter III: Function of the CCL2/CCR2 signaling in fibroblasts and breast cancer cells interaction

Chapter IV: Therapeutic targeting the CCL2 signaling in breast cancer model

Chapter V: Conclusion and Discussion

Chapter I: Background

Breast cancer

Epidemiology

Breast cancer is the most common form of cancer diagnosed in women in U.S., with an estimated 252,710 new cases of invasive breast cancer diagnosed in 2017, accounting for 30% of total cancer incidences in women (1). Breast cancer is the second leading cause of cancer deaths in women, with estimated 40, 610 cases in 2017 (1). It is generally estimated that one in eight women will have breast cancer in her life time, and about one-third of those will die of breast cancer.

Pathology

Breast cancer rises from epithelial cells lining the milk duct or milk producing lobular units (1,2) and is subdivided into ductal carcinoma or lobular carcinoma based on its anatomical origin (Figure 1). The normal milk duct consists of two layers of epithelial cells. The luminal cells are located inside of the duct and are surrounded by the basal cells on the outside layer. Ductal carcinoma is the most common breast cancer, representing about 80% of invasive breast cancer, while lobular carcinoma represents about 15% (3). Histologically, ductal carcinoma tends to form glandular structures, while lobular carcinoma is less adhesive and often forms individual cell file (4). In these studies, we are mostly focused on invasive ductal carcinoma.

During breast cancer progression, epithelial cells obtain increased proliferation ability due to acquired genomic mutations. When the cancer cells are confined inside the duct, they are called ductal carcinoma in situ (DCIS), which is considered benign neoplasm (Figure 1) (1). When the cancer cells break the basement membrane and invade into surrounding tissue such as fat pad, they are called invasive breast cancer (Figure 1). During disease progression, breast cancer will metastasize to draining lymph nodes of breast and to distant organs such as lung,

bone and brain. The disease progression and metastasis significantly affect breast cancer patient outcome. During 2005-2011, about 61% breast cancers are diagnosed in localized stage, 32% in regional stage (metastasis to local breast tissue or lymph node), and 6% in distant metastasis stage (metastasis to distant organs). The five-year survival rate is 99% for breast cancer in localized stage, 85% for regional stage, and 26% for distant stage (1).

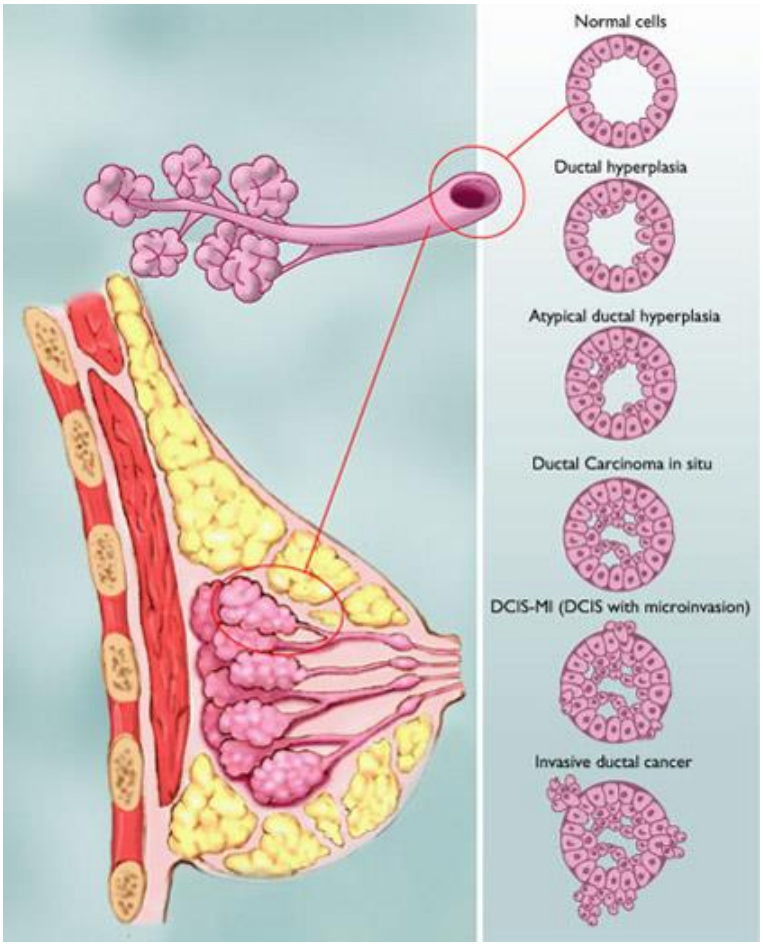

Figure 1. Illustration of breast cancer pathogenesis and progression. Image is downloaded from breastcancer.org website. Link: http://www.breastcancer.org/pictures/types/dcis/dcis_range?utm_medium=OBWidget&utm_source=OB

Stage and Molecular Subtype

Breast cancer is often detected by mammogram and palpation of lumps. The disease is confirmed by biopsy and clinical pathology. Breast cancer is often diagnosed using classical TNM stages, combining information of tumor size and histology (T), local lymph node infiltration (N) and distant metastasis (M) (5). The TNM staging system divides breast cancer into four stages (stage I to IV), with increased disease burden with increased cancer stage. For example, stage I breast cancers are small in size, and contain no or few local lymph node infiltration. The tumor size and number/area of lymph node infiltration increases from stage I to stage III, while stage IV breast cancer contains distant metastasis (5).

Breast cancer is a complex disease and can be further divided into different molecular subtypes, which are helpful in prognosis and treatment. Historically, breast cancers are divided into five molecular subtypes based on microarray profiling--luminal A, luminal B, Her2, basal-like and normal like subtypes (6,7). A simplified commercial diagnostic kit has been developed to subtype breast cancer by analyzing a list of 50 genes expression (PAM50) (8,9). The most convenient method used in the clinic is analyzing expression of three molecular markers: estrogen receptor (ER), progesterone receptor (PR) and Her2 overexpression. ER and PR are analyzed by immunohistochemistry, and Her2 is analyzed by both immunohistochemistry and DNA fluorescent in situ hybridization. Cell proliferation status (characterized by Ki67 expression) is also used in subtyping. In this method (10), luminal A (70%) is defined by expression either ER+ or PR+, and Her2-, and low in Ki67 expressing; luminal B subtype (10%) is defined by expression either ER+ or PR+, and high Ki67 expressing; Her2 subtype (15%) is defined by Her2+; triple negative subtype (12%) is defined by ER-, PR- and Her2-.

The term basal-like breast cancer is derived from expression profiling analysis (microarray or PAM50). Basal-like breast cancer is often characterized by expressing of basal cytokeratin (CK5/6, CK14), similar to the basal epithelial cells (6). Luminal breast cancers (luminal A and luminal B) express markers similar to luminal epithelial cells, such as cytokeratin 19 (6). The triple negative breast cancer is characterized by lacking expression of ER, PR and Her2. About 71% triple negative breast cancers are basal-like breast cancer by microarray profiling. Similarly, about 77% molecular basal-like breast cancers are triple negative (11,12). In this thesis, basal-like breast cancer and triple negative breast cancers are used exchangeable unless specified.

Prognosis and Treatment

The prognosis and treatment of breast cancer are critically dependent on the cancer stage and molecular subtype (1). When breast cancer is diagnosed as localized disease (Stage I to III), surgical removal of cancer is often performed. When only partial breast containing tumor is removed, it is called lumpectomy; when the whole breast is removed, it is called mastectomy. Surgery is often followed by radiation, chemotherapy or targeted therapy. In metastatic breast cancer (Stage IV), systematic treatments, such as chemotherapy or targeted therapy are often used. ER+ breast cancer can be treated with hormone targeted therapy, such as tamoxifen to block ER function. In postmenopausal women with ER+ breast cancer, aromatase inhibitors are used as a targeted therapy to block synthesis of estrogen ligand by aromatase. In Her2 positive breast cancer, Her2 targeted therapies are used, such as Her2 blocking antibody (Herceptin) or chemical inhibitors (Lapatinib).

Luminal and Her2+ breast cancer have relative good survival outcome due to available targeted therapy. In contrast, the triple negative breast cancer does not respond to those targeted

therapies due to loss of expression of ER and Her2, and has the worst patient outcome (7,13). For example, in one study on correlation of clinical outcome with molecular subtype defined by PAM50, the five-year survival rate for basal-like subtype is about 87%, compared to 99% for luminal A and 95% for luminal B or Her2 subtypes (8). Thus, studying the molecular mechanism of basal-like breast cancer progression is critical in identifying potential therapeutic targets.

Cancer associated fibroblasts

The stromal environment has emerged as a critical factor in tumor progression (14). Tumor stroma consists of extracellular matrix and stromal cells. Cancer associated fibroblasts (CAFs) are the most abundant cell types in tumor microenvironment. CAFs are often regarded as activated fibroblasts, as they share common features of activated fibroblasts in inflammatory condition, such as increased proliferation, secretion of soluble factors and extracellular matrix remodeling activity (15). CAFs are a heterogeneous cell population, and they can originate from bone marrow cells, tissue residual fibroblasts and epithelial to mesenchymal transition of tumor cells (16). A number of markers are commonly used to label CAFs, including fibroblast specific protein 1 (Fsp1), fibroblast activation protein (FAP), a-smooth muscle actin (SMA), podoplanin, PGDFRβ (15). However, all of those markers are not fibroblast exclusive, and each of them only labels a subpopulation of fibroblasts (17).

Accumulation of CAFs has been reported in multiple cancer types, such as breast cancer, pancreatic cancer, and lung cancer (15). Fibroblasts accumulation is generally associated with unfavorable outcome in cancer patients (15). However, fibroblasts labelled with different molecular markers are associated with different clinical outcome. For example, accumulation of fibroblasts expressing markers of a-SMA (18), PDGFRβ (19) or podoplanin (20) has been reported to associate with unfavorable outcome in breast cancer. However, accumulation of

fibroblasts expressing FAP marker has been reported to associate with good outcome in breast cancer (21). Those studies indicate different lineages of fibroblasts may function differently in cancer.

The function of fibroblasts in cancer progression is often studied by using mouse genetic models and co-culture and co-transplantation studies (15). In mouse genetic models, genetic modulation of factors in fibroblasts provides physiological relevant insights. For example, conditional knockout of TGFβII receptor in Fsp1+ fibroblast lineage by a Cre recombinase expressed under Fsp1 promoter, led to spontaneous tumor formation in prostate and forestomach, indicating a critical role of fibroblasts in controlling tumor formation (22). In another study, genetic ablation of FAP positive fibroblasts in pancreatic cancer model led to a better response to immunotherapy (23). However, other studies using genetic depletion of a-SMA expressing CAFs in mouse pancreatic cancer model have resulted in accelerated disease progression, indicating an unexpected tumor suppression role (24,25). However, the genetic models are limited by the lacking of fibroblast specific Cre recombinase expression, as most of the fibroblasts Cre mouse lines mentioned above also expressed in other cell lineages. A complimentary method is using CAFs isolated from tumor samples and studying their function using fibroblast-cancer cell co-culture and co-transplantation models. Those studies also provided important insights in the roles of CAFs in cancer growth and metastasis, such as promoting angiogenesis and cancer cell invasion (15). The fibroblasts heterogenicity and multiple functions indicate a complex role in cancer progression. A better understanding of CAFs function is needed in order to develop fibroblasts targeted therapy in cancer.

Chemokine CCL2 signaling and functions

Chemokines are small soluble proteins (8-10 kDa) that regulate homing and recruitment of immune cells through formation of molecular gradients (26). Chemokines are highly conserved between mice and humans. They play important roles in regulating immune cell trafficking and endothelial sprouting during embryonic development, wound healing and infections (26). Currently, more than 47 ligands and 23 receptors have been identified and classified into the multiple categories, depending on the spacing of the cysteine motif present at the N terminus of the chemokine ligand (26).

CCL2 belongs to the C-C class of chemokines, which contain two pairs of conserved cysteine residues. Also known as Monocyte Chemoattractant Protein 1 (MCP-1), CCL2 is a potent chemokine in inducing monocyte migration (27). CCL2 can bind to multiple receptors including CCR2, CCR4 and CCR5 *in vitro*, but it has the highest binding affinity with CCR2 (27,28). In mouse model, knockout of CCL2 and CCR2 show similarly phenotype in defects in monocyte migration (29,30). Besides CCL2, CCL7 also binds with CCR2 receptor and functions in the process of monocyte recruitment. CCL7 knockout mouse also shows defect in monocyte migration (31). Those studies suggest that CCL2 and CCL7 function non-redundantly in recruiting monocyte in mouse functioning through CCR2 receptor.

Overexpression of CCL2 has been implicated in inflammatory diseases, including rheumatoid arthritis, macular degeneration, diabetes and atherosclerosis (27,32). CCL2 is overexpressed in the epithelium and stroma of numerous cancer types, including gliomas, prostate cancers, ovarian cancers and breast cancers, and expression correlates with recruitment of macrophages (32-34). CCL2 expression correlates with tumor grade and unfavorable patient prognosis from studies of tumor biopsies and blood serum levels of cancer patients (32).

Expression of CCL2 in cancer has been observed in multiple cell types, including epithelial cancer cells, fibroblasts, endothelial cells, and macrophages (32). However, the contribution of each individual cellular source of CCL2 is undefined. A few studies indicate an unequal contribution of different sources. In one clinical association study, the authors reported that stromal CCL2 significantly associated unfavorable outcome in breast cancer, while epithelial CCL2 did not (35). In a breast cancer xenograft mouse model, CCL2 from human cancer cells or mouse stromal cells both functioned in promoting lung metastasis, revealed from CCL2 blockade studies using human or mouse specific CCL2 neutralizing antibody (36). Grafting breast cancer cells into CCL2 mutant mouse hosts also resulted in reduced primary tumor growth and metastasis, compared to wildtype control (37). All those studies indicate that the stromal cells are important cellular sources of CCL2. Early studies in our laboratory showed that CAFs with TGFβII knockout produced a significantly higher level of chemokine CCL2, and promoted mammary tumor cells metastasis (38). In following up studies with human breast cancer samples, increased expression of CCL2 was observed in cancer cells and stromal cells (39). Those studies indicate that cancer associated fibroblasts may serve as an important cellular source of chemokine CCL2 in breast cancer progression.

The majority of CCL2 function in breast cancer is focused on immune cell recruitments. In lung metastasis model, CCL2 has been shown to induce inflammatory monocyte migration and promote vascular permeability through VEGF expression. This promotes cancer cells extravasation and increases lung metastasis (36). Inhibition of CCL2 by blocking antibody reduces lung metastasis (36). CCL2 expression in primary breast cancer is also associated with macrophage infiltration and angiogenesis (37,40). CCL2 can also recruit immunosuppressive myeloid derived suppressor cells, and inhibits anti-tumor immunity (41).

The expression of receptor CCR2 has been reported in multiple cancer cells (39,42-44), indicating a potential role for CCL2 signaling to cancer cells. A few *in vitro* studies have shown that CCL2 can signal directly to cancer cells. An earlier study in our laboratory reported that recombinant CCL2 promoted breast cancer cells invasion and survival *in vitro* (39). CCL2 has been reported to promote cancer stem cells formation in Her2+ breast cancer cells *in vitro* (45). However, the functional importance of CCL2 signaling to cancer cells has not been directly tested *in vivo*. Most *in vivo* studies are performed with CCL2 knockdown or blocking (36,40,45), thus those results cannot distinguish the CCL2 effects on stromal immune cells or cancer cells.

Hypothesis and outline of contents

Those preliminary studies led us to hypothesize that **CCL2 derived from cancer associated fibroblasts promotes breast cancer progression by signaling to cancer cells via CCR2** (Figure 2). In the following three chapters, we have addressed this hypothesis through both human cancer samples analysis and mouse models studies. We briefly summarize the contents of the following four chapters as below:

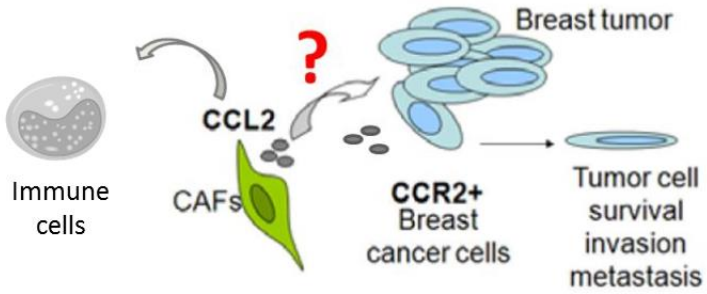

Figure 2. Overall hypothesis and model.

Chapter II: Expression of CCL2 and fibroblast marker Fsp1 in breast cancer

In this chapter, we have evaluated the prognostic significance of CCL2 protein expression in breast cancer subtypes, in relation to its expression in the epithelium or stroma, or in relation to Fibroblast Specific Protein 1 (Fsp1), a mesenchymal marker. Immunohistochemistry analysis of tissue microarrays revealed that CCL2 significantly correlated with Fsp1 expression in the stroma and tumor epithelium of invasive ductal carcinoma. In the overall breast cancer cohort (n=427), CCL2 and Fsp1 expression in whole tissues, stroma and epithelium were inversely associated with cancer stage and tumor size. When factoring in molecular subtype, stromal CCL2 was observed to be most highly expressed in Basal-like breast cancers. By Cox Regression Modeling, stromal CCL2, but not stromal Fsp1 expression was significantly associated with decreased recurrence free survival. Furthermore, stromal CCL2 (HR= 7.51 p=0.007) was associated with a greater hazard than cancer stage (HR=2.54, p=0.045) and tumor grade (HR=0.41, p=.0871). These studies indicate that stromal CCL2 is associated with decreased recurrence free survival in patients with basal-like breast cancer, with important implications on the use of stromal markers for predicting patient prognosis.

Chapter III: Function of the CCL2/CCR2 signaling in fibroblasts and breast cancer cells interaction

In this chapter, we have studied the function of chemokine CCL2 derived from cancer associated fibroblasts, and the role of direct CCL2/CCR2 signaling in basal-like breast cancer cells. Our studies indicate that fibroblast mediated CCL2/CCR2 signaling promotes the growth of basal-like breast cancers independent of these stromal responses. Knockdown of CCL2 in fibroblasts or knockout of CCR2 in breast cancer cells abrogates fibroblast mediated growth of MCF10CA1d breast cancer cells, independently of macrophage recruitment or tumor angiogenesis. *In vitro*, MCF10CA1d cells grow less dense, when treated with conditioned

medium from stromal cells deficient in CCL2. SRC or PKC inhibitors block CCL2/CCR2 mediated growth of breast cancer cells. Datamining analysis indicates that CCL2 and CCR2 are most highly expressed in basal-like breast cancers. These studies demonstrate a novel mechanism regulating basal-like breast cancer progression involving CCL2/CCR2 signaling in cancer cells. Thus, the CCL2/CCR2 signaling may serve as potential therapeutic targets in basal-like breast cancer.

Chapter IV: Therapeutic targeting the CCL2 signaling in breast cancer model

In this chapter, we have investigated the effects of continuous delivery of human CCL2 neutralizing antibodies on breast cancer progression. Nude mice bearing MCF10CA1d breast tumor xenografts were implanted with osmotic pumps containing control IgG or anti-CCL2, and analyzed for CCL2 levels, and tumor progression over 4 weeks. Despite inhibiting CCL2-induced migration *in vitro*, CCL2 neutralizing antibodies did not significantly affect tumor growth, invasion, macrophage recruitment or tumor angiogenesis. CCL2 antibodies did not affect murine CCL2 levels but significantly increased human CCL2 levels in circulating blood and tumor interstitial fluid. CCL2 neutralizing antibodies reduced CCL2 levels in cultured cells short-term at high concentrations. ELISA analysis of CCL2 in cultured fibroblasts and breast cancer cells revealed that the neutralizing antibodies sequestered CCL2 in the media. CCL2 levels were restored once the antibodies were removed. These studies reveal limitations in CCL2 neutralizing antibodies as a therapeutic agent, with important implications for translating CCL2 targeting to the clinic.

Chapter V: Conclusion and Discussion

In this chapter, we have highlighted the overall importance of our founding and the potential applications. In addition, we will also discuss the limitations of our studies and additional questions not addressed in our studies. We also propose follow up studies and future directions derived from these studies.

Chapter II: Expression of CCL2 and fibroblast marker Fsp1 in breast cancer

Contents in this chapter have been published in:

Yao, M., E. Yu, V. Staggs, F. Fan and N. Cheng (2016). "Elevated expression of chemokine C-C ligand 2 in stroma is associated with recurrent basal-like breast cancers." Mod Pathol **29**(8): 810-823.

Introduction

Treatment of breast cancer is complicated by the presence of different molecular subtypes. These subtypes include: Luminal A, Luminal B, Her2 overexpressing (Her2+) and Basal-like breast cancers. Histologically, these subtypes are classified by the status of estrogen receptor (ER), progesterone receptor (PR), Her2, and cell proliferative index (46-49). Conventional prognostic indicators such as grade and stage do not accurately predict patient prognosis for all of the different molecular subtypes (50,51), indicating the need to identify prognostic factors unique to each subtype.

Recent studies demonstrate that the stroma of invasive breast cancers express high levels of Chemokine C-C Ligand 2 (CCL2). Previous studies have primarily examined CCL2 expression for its association with macrophages in breast cancer and patient prognosis and have reported different results (35,52,53). In previous studies, we demonstrated an important biological role for CCL2 overexpression in breast cancer cells and in fibroblasts in regulating tumor progression (38,54). These studies suggest that multiple factors could affect the prognostic relevance of CCL2 expression in breast cancer.

In these studies, we employed several novel approaches to evaluate the prognostic significance of CCL2 expression in breast cancer. Here, we employed a software based approach to evaluate the prognostic significance of CCL2 protein expression in breast cancer subtypes, in relation to its expression in the epithelium or stroma, or in relation to Fsp1, a mesenchymal marker. Immunohistochemistry analysis of tissue microarrays revealed that CCL2 significantly correlated with Fsp1 expression in the stroma and tumor epithelium of invasive ductal carcinoma. In the overall breast cancer cohort, CCL2 and Fsp1 expression in whole tissues, stroma and epithelium were inversely associated with cancer stage and tumor size. When

factoring in molecular subtype, stromal CCL2 was observed to be most highly expressed in Basal-like breast cancers. By Cox Regression Modeling, stromal CCL2, but not stromal Fsp1 expression was significantly associated with decreased recurrence free survival. Furthermore, stromal CCL2 (HR= 7.51 p=0.007) was associated with a greater hazard than cancer stage (HR=2.54, p=0.045) and tumor grade (HR=0.41, p=.0871). Our studies have important implications on the use of stromal markers for predicting prognosis of patients with Basal-like breast cancer.

Materials and methods

Patient samples

A total of 12 prognostic tissue microarray slides (6 slides in duplicate) were obtained from the National Cancer Institute Cancer Diagnostics Program. Each array slide contained 90-100 breast cancer core samples and 5 normal breast tissue cores, 3 fibroadenoma cores, and 20 control core samples comprised of prostate, colon and salivary gland and endometrium tissues. De-identified carcinoma or matching normal adjacent tissue samples were collected from patients who were diagnosed with breast cancer between 1985 and 1997, prior to adjuvant therapy. The majority of those patients (85%) received adjuvant radiation, chemo- or hormone therapy, or a combination of therapies. The mean follow-up time was 104 months, with a maximal follow-up time of 276 months. Pathology reports included information on: clinical diagnosis, treatment regimen, age, stage, tumor size, grade, lymph node status, mitotic score and intensity of biomarker staining for ER, PR and Her2. Patient outcome included information on: metastasis, recurrence, survival and follow-up time.

5 de-identified normal breast tissue samples and 32 core samples of stage I-IV breast ductal carcinoma were obtained in duplicate from the Biospecimen Core Repository at the University of Kansas Medical Center. This cohort included pathology information on: age, stage, grade, tumor size, Ki67 expression and intensity of biomarker staining for ER, PR and Her2. Outcome information included: status on survival, recurrence, and number of recurrences. Treatment information was not available.

The clinical pathologic features of both datasets are summarized (Table 1). When the patient datasets were combined, the mean age of patients was 59 years, with a mean follow-up time of 8.7 years.

Immunohistochemistry

Tissue microarray slides were de-paraffined and rehydrated through a series of xylenes and 100%, 95%, 70% and 50% ethanol. For CCL2 immunostaining, slides underwent antigen retrieval through low pressure cooking in 2M urea for 2 min. Peroxidases were quenched for 30 minutes in PBS containing 3% H202 and 10% Methanol, and blocked in PBS containing 3% Fetal bovine serum for 1 hour. Slides were incubated with goat anti-human CCL2 antibody at a 1:100 dilution (cat no. sc-1304, Santa Cruz Biotechnology, Santa Cruz, CA) overnight in blocking buffer, and with biotinylated horse anti-goat antibody(Vector Laboratory, BH-9500, 1:1000) in room temperature for two hours. For Fsp1 immunostaining, slides underwent antigen retrieval through low pressure cooking in 10 mM sodium citrate pH 6.8 for 2 minutes. After peroxidase quenching and blocking, slides were incubated with rabbit anti-Fsp1 at a 1:3 dilution (cat no. ab-27427, Abcam, Cambridge, MA) in blocking buffer overnight, and then with peroxidase conjugated goat anti-rabbit antibody at a 1:1000(cat no. 611-1302, Rockland

Immunochemicals, Pottstown, PA) for 2 hours at room temperature. Expression of CCL2 and Fsp1 proteins were detected with streptavidin-peroxidase (cat no. PK-6100, Vector Laboratories, Burlingame, CA) and 3,3'-diaminobenzidine (DAB) substrate. Slides were counterstained with Harris's hematoxylin, dehydrated and mounted with Cytoseal (cat no. 8312-4, Thermo Fisher Scientific, Lenexa, KS). Images were acquired using a Motic AE31 inverted microscope with camera and Q capture software.

For immunofluorescence staining, CCL2 expression was detected through incubation with secondary donkey anti-goat conjugated to Alexa Flour-488 at a 1:1000 dilution (cat no. R37118, Thermo Fisher Scientific). To detect Fsp1, slides were incubated with secondary rabbit biotinylated antibodies, conjugated to streptavidin- Alexa Flour-568 (cat no. s-11226, Thermo Fisher Scientific). Slides were counterstained with DAPI and mounted in PBS containing 50% glycerol.

Image quantification

Images of immunohistochemistry staining were acquired at 10x magnification using a Motic AE31 inverted microscope with Infinity 2-1x color digital camera. Software analysis of biomarker expression in breast tissues was performed using methods previously described (55). Images were first imported into Adobe Photoshop. Color and exposure of images were normalized using auto-contrast. Tumor epithelium was distinguished from the stroma by differences in nuclear and cellular morphology, and tissue architecture. To select for specific tissues, the lasso tool was to select and crop out stroma or epithelium. The stromal tissues were labeled as "total stromal area" while the epithelial tissues were labeled as "total epithelial area." DAB staining, identified as brown, was selected using the Magic Wand tool in the Color Range

Window, with a specificity range of 66. Selected pixels were copied to a new window and saved as a separate file. Images were opened in Image J software (NIH) and converted to greyscale. Background pixels resulting from luminosity of bright field images were removed by threshold adjustment. Images were the subject to particle analysis. DAB staining and total areas were expressed as particle area values of arbitrary units. Positive DAB values were normalized total stromal or epithelial values.

Statistical analysis

Sample populations did not fit a Gaussian distribution, and were observed to be uneven. The uneven characteristic was due to two factors. Information on prognostic factors was not provided for all patients within the two cohorts. In addition, some tissue samples on the tissue microarray did not adhere to the slide during staining. As such, protein expression values and their relationships to clinical data were analyzed using non-parametric methods. Statistical analyses were performed using Graphpad Software and SAS.

The samples from the two cohorts were combined. Comparison of two groups with discrete variables was performed using Wilcoxon Two-Sample Test. Tests for association between CCL2 and Fsp1 were performed using Spearman Correlation Analysis. Analysis of three or more groups was performed using Kruskal-Wallis Test with Dunn's post-hoc comparison between groups. Cox regression model for non-proportional hazards was used for univariate and multivariate analysis. Expression levels of CCL2 and Fsp1 in the Cox regression model were transformed by multiplying values by 10 so that values were greater than 1. Statistical significance was determined by $p < 0.05$. Factors approaching significance were

further selected for multi-variate analysis. *p<0.05, **p<0.01, ***p<0.001, unless otherwise specified.

Ethics statements

The tissues collected for these studies were de-identified and classified as "Exempted" according to regulations set forth by the Human Research Protection Program (ethics committee) at the University of Kansas Medical Center (#080193). Written informed consent for tissue collection was obtained by the Biospecimen core repository. Tissue samples were de-identified prior to distribution to the investigators. Existing medical records were used in compliance with the regulations of the University of Kansas Medical Center and National Cancer Institute. These regulations are aligned with the World Medical Association Declaration of Helsinki.

Results

CCL2 and Fsp1 are co-expressed in breast cancer

To characterize the expression patterns of CCL2 and Fsp1 in breast cancer, we performed immunohistochemistry staining on breast cancer tissue microarray obtained from the National Cancer Diagnostics Program and the University of Kansas Medical Center Biospecimen Core Repository. To circumvent possible bias caused by visual scoring of tissues, we utilized an Image J software based approach to quantify protein expression (55). Expression patterns were compared among normal breast tissues, fibroadenoma tissues, which are non-malignant breast lesions, and invasive breast carcinoma tissues. Of the invasive breast cancer cases, 91% were comprised of invasive ductal carcinoma and 9% were diagnosed as invasive lobular carcinoma. Expression CCL2 and Fsp1 proteins were detected in the stroma and epithelium of normal breast tissues, fibroadenoma, invasive lobular carcinoma and invasive ductal carcinoma (Figure 3A).

When quantified in whole tissues, CCL2 and Fsp1 were most highly expressed in invasive ductal carcinoma tissues, compared to the other tissue types (Figures 3B-C). By Spearman correlation analysis, CCL2 was significantly associated with Fsp1 expression in whole tissues, in the stroma and in the epithelium of invasive ductal carcinoma (Figures 4A-C). By co-immunofluorescence staining of invasive ductal carcinoma samples, CCL2 was found to significantly overlap with Fsp1 expression in the stroma and tumor epithelium (Figure 4D). These data demonstrate significant associations between CCL2 and Fsp1 expression in invasive ductal carcinoma.

Table 1. Clinical-pathological features of tumor samples in the NCI and KUMC TMAs combined.

Factors	Sample size (% of total)
Age (years)	
<50	130 (30%)
>=50	297 (70%)
Histology type	
Ductal	388 (91%)
Lobular	38 (9%)
Unknown	1 (0.2%)
T stage	
T1	90 (21%)
T2	196 (46%)
T3	88 (21%)
T4	42 (10%)
Unknown	11 (3%)
N stage	
N0	92 (22%)
N1	266 (63%)
N2	54 (13%)
N3	3 (1%)
Unknown	12 (3%)
Grade	
I	61 (14%)
II	197 (46%)
III	167 (39%)
Unknown	2 (0.5%)
ER status	
Negative	145 (34%)
Positive	271 (63%)
Unknown	11 (3%)
PR status	
Negative	168 (39%)
Positive	247 (58%)
Unknown	12 (3%)
Her2 status	
Normal	339 (79%)
Overexpression	76 (18%)
Unknown	12 (3%)

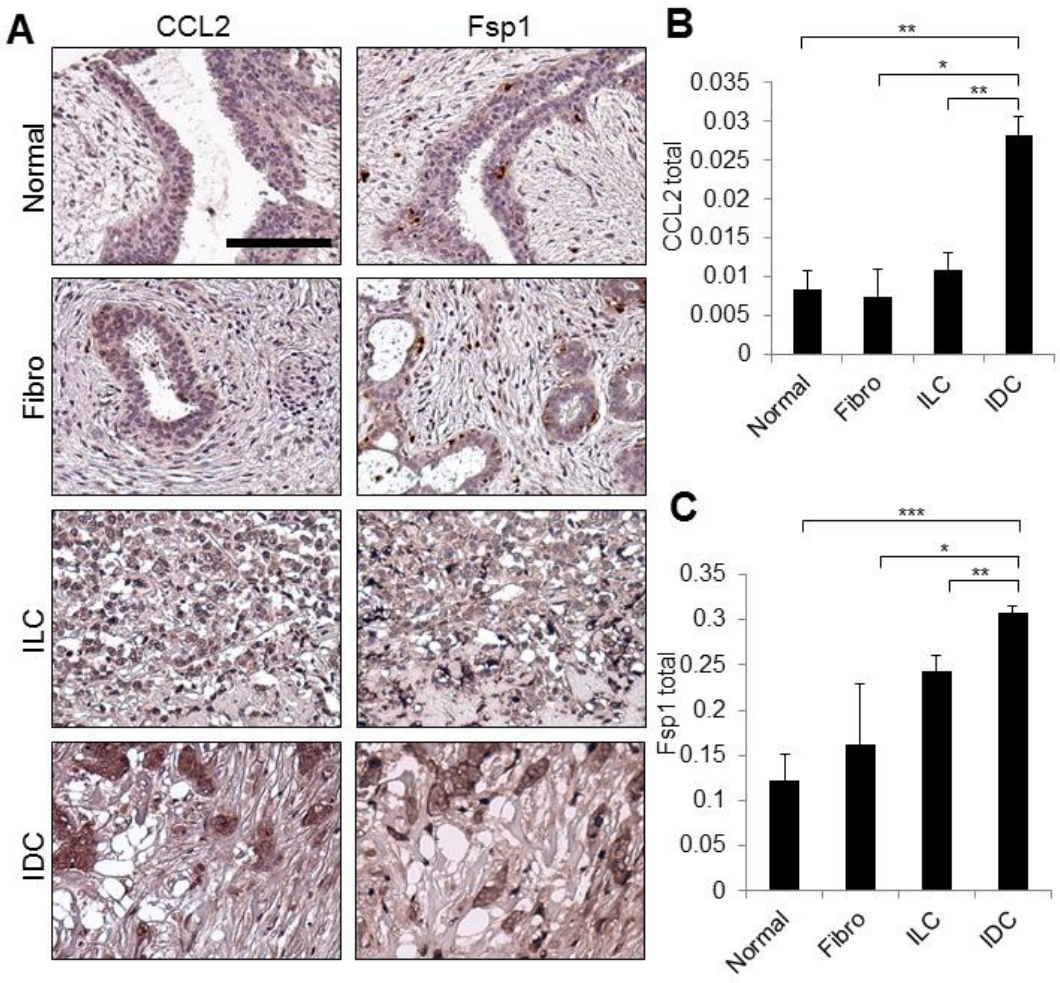

Figure 3. Expression of CCL2 and Fsp1 proteins in breast tissues. TMAs containing samples of normal breast (n=20), fibroadenoma (Fibro, n=9), invasive lobular carcinoma (ILC, n=38) and invasive ductal carcinoma (IDC, n=388) breast cancer were immunostained for CCL2 and Fsp1. Expression levels were quantified by Image J; arbitrary units are shown. (**A**) Representative images of CCL2 and Fsp1 expression. Scale bar= 100 microns. Comparison of CCL2 (**B**) and Fsp1 (**C**) expression among different groups using Kruskal-Wallis Test with Dunn's post-hoc comparison. Statistical significance was determined by *p<0.05; **p<0.01, ***p<0.001.

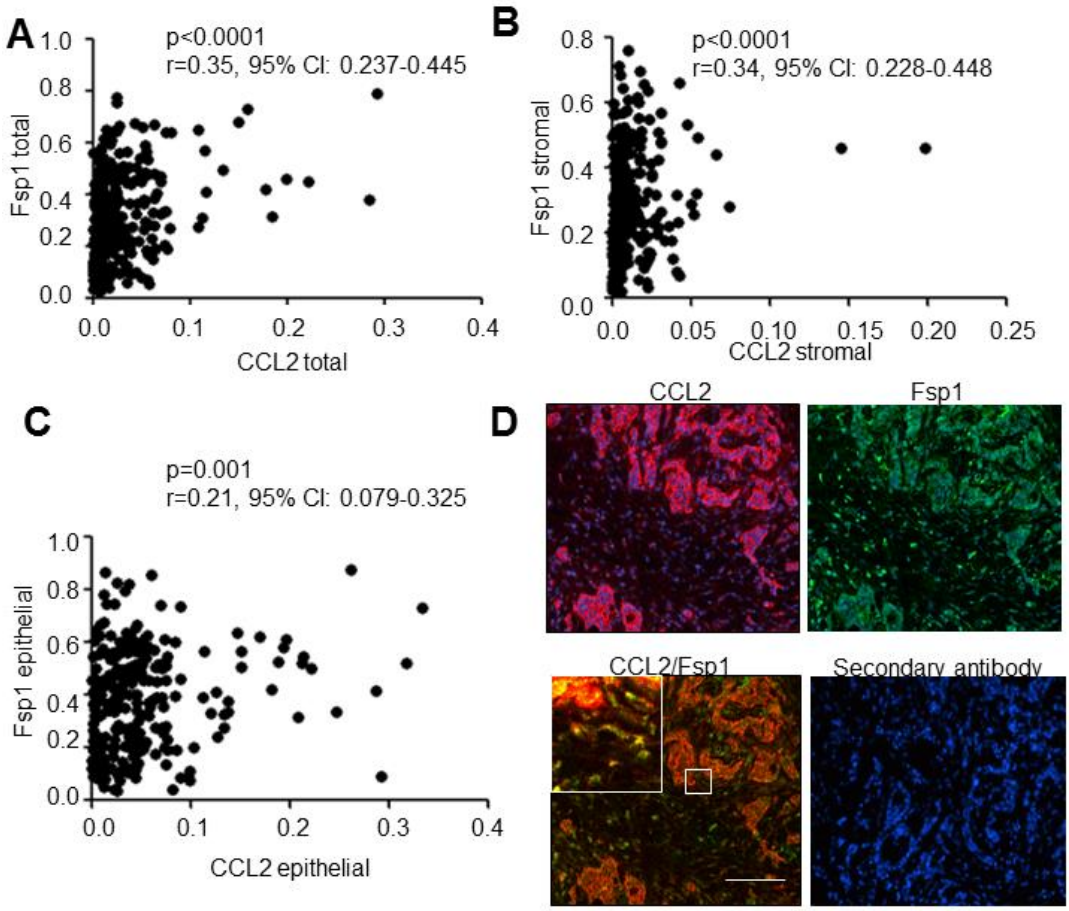

Figure 4. CCL2 is significantly associated with Fsp1 expression in IDC. Associations between CCL2 and Fsp1 expression in whole tissue (total) (**A**), stroma (**B**) or epithelium (**C**) in IDC were analyzed by Spearman Correlation analysis. Statistical significance was determined by $p<0.05$. Correlation co-efficient (r) and 95% confidence interval (95% CI) are shown. (**D).** Co-immunofluorescence staining for CCL2 and Fsp1 in IDC. Magnified inset shows overlapping staining. Secondary antibody staining only is shown as negative control. Scale bar= 400 microns.

CCL2 and Fsp1 expression do not significantly associate with patient outcome in the overall cohort

We then analyzed for associations between CCL2 or Fsp1 with commonly used prognostic factors in IDC. Whole tissue (total) expression of CCL2 and Fsp1 inversely correlated with overall stage and T stage (Figures 5A-B). Total Fsp1 but not total CCL2 expression inversely correlated with N stage (Figure 5C). Total expression of CCL2 and Fsp1 was not associated with tumor grade, ER, PR or Her2 status (Table 2). Similarly, stromal and epithelial expression of CCL2 and Fsp1 negatively correlated with overall stage and T stage (Tables 3 and 4). In contrast to total CCL2 expression, stromal CCL2 expression negatively correlated with Her2 overexpression. In contrast to total Fsp1 expression, epithelial Fsp1 positively correlated with ER and PR status (Tables 3 and 4). In summary, these data indicate that CCL2 and Fsp1 inversely associate with stage and tumor size, and that associations with ER, PR and Her2 status are dependent on tissue specific patterns of expression. We next determined whether CCL2 and Fsp1 expression were associated with patient outcome. To adjust for multiple variables that might affect the association of CCL2 and Fsp1 expression with patient outcome, univariate Cox regression analysis was first performed for overall survival (Table 5). Tumor size, lymph node status and histologic grade were associated with decreased overall survival, with Hazard Ratios of 1.58 or more and p-values of less than 0.01. Among adjuvant therapies as possible factors, chemotherapy was associated with decreased overall survival (HR=1.42, p=0.046). Radiation therapy and hormone treatment were not significantly associated with overall survival. Among expression of biomarkers, the absence of ER and PR significantly associated with decreased overall survival, with Hazard Ratios of 1.84 or more, and p-values less than 0.001.

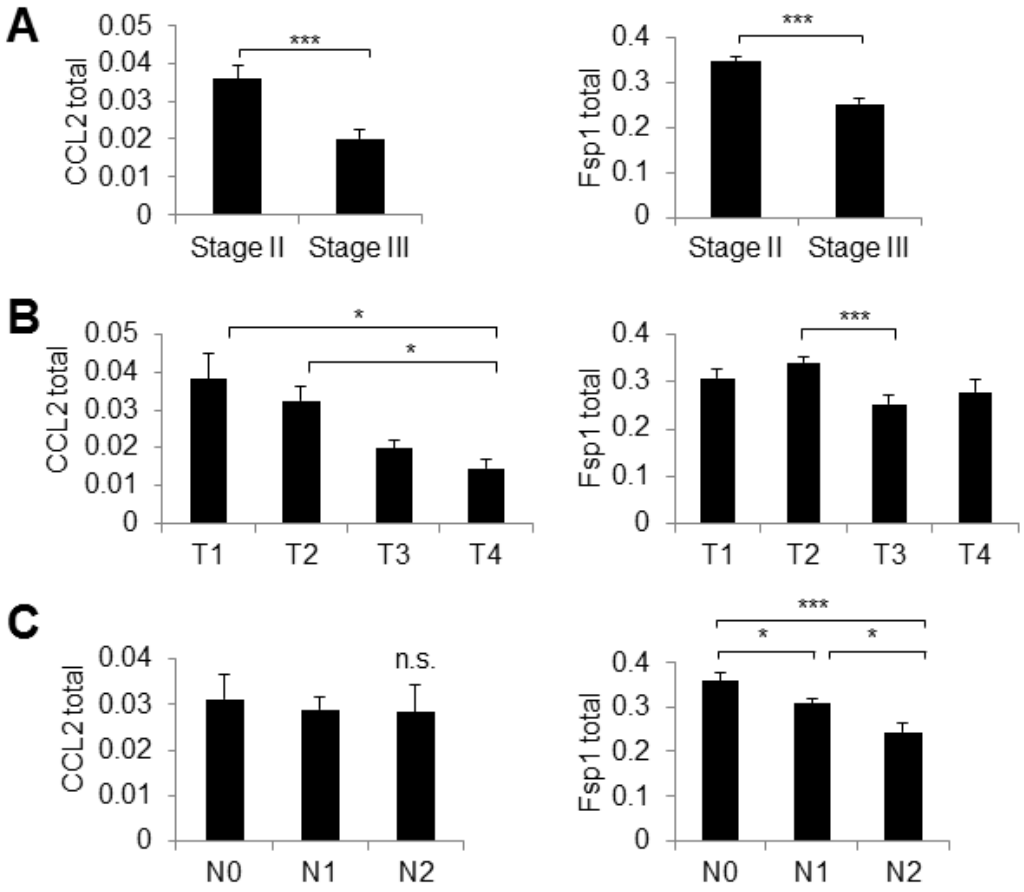

Figure 5. CCL2 and Fsp1 proteins are associated with overall stage and T stage in IDC. Total CCL2 and Fsp1 expression were analyzed for associations with overall stage (**A**), T stage (**B**) and N stage (**C**). Statistical analysis was performed using Mann-Whitney' test (overall stage) or Kruskal-Wallis Test with Dunn's post-hoc comparison (T stage and N stage). Statistical significance was determined by *p<0.05; **p<0.05, ***p<0.001 and n.s. = not significant.

Table 2. Associations of total CCL2 and Fsp1 expression with clinico-pathological factors. Univariate analyses were performed using Mann Whitney Test for two groups or Kruskal-Wallis Test with Dunn's post-hoc comparisons for three or more groups. Statistical significance was determined by $p<0.05$.

Factors	CCL2 total			Fsp1 total		
	N	Mean expression value	p-value	N	Mean expression value	p-value
Stage						
II	173	0.036	<0.0001	213	0.347	<0.0001
III	130	0.020		139	0.252	
T stage						
T1	68	0.038	0.002	76	0.308	0.001
T2	138	0.033		169	0.341	
T3	65	0.020		73	0.253	
T4	36	0.015		38	0.278	
N stage						
N0	59	0.031	0.613	78	0.359	0.001
N1	201	0.029		226	0.308	
N2	43	0.028		48	0.245	
Grade						
I	41	0.020	0.679	47	0.319	0.470
II	135	0.028		159	0.297	
III	139	0.031		158	0.316	
ER status						
Negative	122	0.028	0.565	130	0.311	0.907
Positive	188	0.029		226	0.309	
PR status						
Negative	133	0.027	0.214	148	0.306	0.627
Positive	177	0.030				

				207	0.314	
Her2 status						
Normal	248	0.030	0.072	284	0.315	0.302
Overexpression	62	0.025		71	0.294	

Table 3. Associations of stromal CCL2 and Fsp1 expression with clinico-pathological factors. Univariate analyses were performed using Mann Whitney Test for two groups or Kruskal-Wallis Test with Dunn's post-hoc comparisons for three or more groups. Statistical significance was determined by $p<0.05$.

Factors	CCL2 stromal			Fsp1 stromal		
	N	Mean expression value	p-value	N	Mean expression value	p-value
Stage						
II	152	0.016	<0.0001	201	0.320	<0.0001
III	121	0.007		131	0.225	
T stage						
T1	62	0.015	<0.0001	74	0.284	0.001
T2	121	0.015		158	0.312	
T3	59	0.006		70	0.223	
T4	35	0.005		38	0.278	
N stage						
N0	51	0.014	0.407	71	0.336	<0.001
N1	182	0.012		217	0.281	
N2	40	0.011		44	0.215	
Grade						
I	40	0.011	0.517	47	0.274	0.254
II	125	0.012		154	0.270	
III	120	0.012		143	0.296	
ER status						
Negative	106	0.012	0.203	118	0.295	0.319
Positive	174	0.012		218	0.276	
PR status						
Negative	118	0.012	0.117	136	0.281	0.689
Positive	162	0.012		199	0.285	
Her2 status						
Normal	225	0.013	0.039	270	0.289	0.325
Overexpression	55	0.009		65	0.264	

Table 4. Associations of epithelial CCL2 and Fsp1 expression with clinic-pathological factors. Univariate analyses were performed using Mann Whitney Test for two groups or Kruskal-Wallis Test with Dunn's post-hoc comparisons for three or more groups Statistical significance was determined by $p<0.05$.

Factors	CCL2 epithelial			Fsp1 epithelial		
	N	Mean expression value	p - value	N	Mean expression value	p- value
Stage						
II	157	0.062	<0.0001	180	0.421	<0.0001
III	123	0.035		120	0.319	
T stage						
T1	61	0.069	0.000	71	0.394	0.002
T2	126	0.054		140	0.411	
T3	62	0.036		60	0.322	
T4	35	0.027		33	0.324	
N stage						
N0	57	0.052	0.749	68	0.398	0.051
N1	184	0.050		187	0.389	
N2	39	0.050		45	0.321	
Grade						
I	35	0.043	0.459	41	0.447	0.049
II	125	0.054		135	0.373	
III	132	0.046		136	0.367	
ER status						
Negative	112	0.043	0.106	110	0.351	0.034
Positive	176	0.053		196	0.399	
PR status						
Negative	120	0.043	0.057	127	0.355	0.043
Positive	168	0.054		178	0.401	
Her2 status						
Normal	234	0.051	0.258	246	0.386	0.530
Overexpression	54	0.043		59	0.365	

Table 5. Univariate Cox Regression model on the association of CCL2 and Fsp1 expression with outcome of patients with IDC. The Hazard Ratio (HR) was calculated from the Cox Proportional Hazard Regression Model. 95% confidence interval (CI) of the calculated HR is shown. Statistical significance was determined by $p<0.05$.

	Overall survival				Recurrence free survival			
Factors	**HR**	**95% CI**		**p-value**	**HR**	**95% CI**		**p-value**
T stage								
T1	1.00	0.99	1.02	0.644	1.00	0.99	1.01	0.965
T2	1.59	0.95	2.67		1.62	1.01	2.58	
T3	3.64	2.12	6.23		2.39	1.40	4.07	
T4	1.97	0.97	3.98		2.30	1.20	4.41	
N stage								
N0	1.00				1.00			
N1	1.58	0.98	2.54	0.002	1.38	0.89	2.14	<0.001
N2	2.89	1.61	5.21		2.99	1.72	5.19	
Grade								
I	1.00				1.00			
II	3.79	1.64	8.75	0.002	2.24	1.18	4.25	0.009
III	4.62	2.00	10.65		2.69	1.42	5.09	
Chemotherapy								
No	1.00			0.046	1.00			0.037
Yes	1.42	1.01	2.02		1.43	1.02	2.00	
Radiation therapy								
No	1.00			0.513	1.00			0.114
Yes	1.13	0.79	1.61		1.32	0.94	1.85	
Hormone therapy								
No	1.00			0.635	1.00			0.563
Yes	0.92	0.65	1.30		1.10	0.79	1.53	
ER status								
Positive	1.00			<0.001	1.00			0.001
Negative	1.92	1.37	2.70		1.75	1.26	2.44	
PR status								

Positive	1.00			<0.001	1.00			0.002
Negative	1.84	1.32	2.58		1.70	1.22	2.37	
Her2 status								
Normal	1.00			0.127	1.00			0.134
Overexpression	1.37	0.91	2.06		1.35	0.91	2.01	
CCL2 total	0.01	0.00	2.83	0.111	0.01	0.00	2.25	0.096
CCL2 stromal	1.01	0.36	2.85	0.984	1.37	0.52	3.59	0.522
CCL2 epithelial	0.03	0.00	1.59	0.085	0.03	0.00	1.19	0.062
Fsp1 total	0.55	0.19	1.58	0.266	0.60	0.22	1.68	0.334
Fsp1 stromal	0.51	0.17	1.49	0.218	0.53	0.19	1.51	0.235
Fsp1 epithelial	0.55	0.19	1.59	0.273	0.78	0.29	2.11	0.620

Expression of CCL2 and Fsp1 proteins in whole tissue, stroma and epithelium were not associated with overall survival. We next examined for associations with recurrence free survival (Table 5). Tumor size, lymph node status and histologic grade were associated with decreased recurrence free survival with Hazard Ratios of 1.38 or more and p-values less than 0.01. Chemotherapy, but not anti-hormonal or radiation therapy, was associated with decreased relapse-free survival with Hazard Ratio of 1.43 and p=0.037. ER and PR, but not Her2 were associated with decreased recurrence free survival with Hazard Ratios of 1.70 or more, and p-values of less than 0.01. Expression of CCL2 and Fsp1 proteins in whole tissue, stroma and epithelium were not associated with recurrence free survival. In summary, CCL2 and Fsp1 expression in IDC does not associate with patient outcome.

Stromal CCL2 associates with decreased relapse-free survival in patients with Basal-like breast cancer

Given the heterogeneity of breast cancer, and some associations with hormone receptor status, it was possible that expression of CCL2 and Fsp1 proteins were associated with breast subtype. Therefore, we compared expression patterns of CCL2 and Fsp1 in normal breast, Luminal A, Luminal B, Her2+ and Basal-like breast cancers. Luminal A breast cancers were identified as ER+ and/or PR+, Her2- and low Ki67 (<14%) or mitotic index (<2). Luminal B breast cancers were defined by expression of ER and/or PR, expression of Her2+ and high Ki67 (>14%) or mitotic index (>2). Her2+ breast cancers were identified as ER-, PR- and strongly Her2+, while Basal-like breast cancers were defined by the absence of ER, PR and Her2 expression (46-49).

Luminal A, Luminal B and Basal-like breast cancers showed significantly higher levels of CCL2 and Fsp1 expression in whole tissues, compared to normal breast tissues (Figure 6A). There were no significant differences in epithelial CCL2 and Fsp1 expression among the different tissue types (Figure 6B). We observed a significant increase in expression of stromal CCL2 and stromal Fsp1 in Luminal A, Luminal B and Basal-like breast cancers (Figure 6C), compared to normal breast tissues. These data indicate that a significant source of CCL2 and Fsp1 expression originated from the stroma among the different breast cancer subtypes.

CCL2 and Fsp1 were further analyzed for associations with patient outcome among the different breast cancer subtypes. By univariate Cox Regression Analysis, expression of CCL2 and Fsp1 proteins in whole tissues, stroma or epithelium were not associated with outcome of patients with Luminal A, Luminal B or Her2 overexpressing breast cancers (Table 6). For patients with Basal-like breast cancer, total and stromal Fsp1 expression were marginally associated with decreased overall survival, by univariate Cox Regression analysis (Table 7), but did not show any significant associations with patient outcome when adjusted for multiple factors (Table 8 and 9). By univariate and multivariate Cox Regression analyses, stromal CCL2 was associated with decreased recurrence free survival of patients with Basal-like breast cancer (Table 10). Furthermore, stromal CCL2 (HR= 7.51 p=0.007) was associated with a greater hazard than cancer stage (HR=2.54, p=0.045) and tumor grade (HR=0.41, p=.0871) (Table 10). We also found that chemotherapy treatment was associated with a higher hazard than the absence of chemotherapy, a trend that was also reported in previous studies (56). In summary, these data demonstrate that stromal CCL2 expression is associated with decreased recurrence free survival in patients with Basal-like breast cancers.

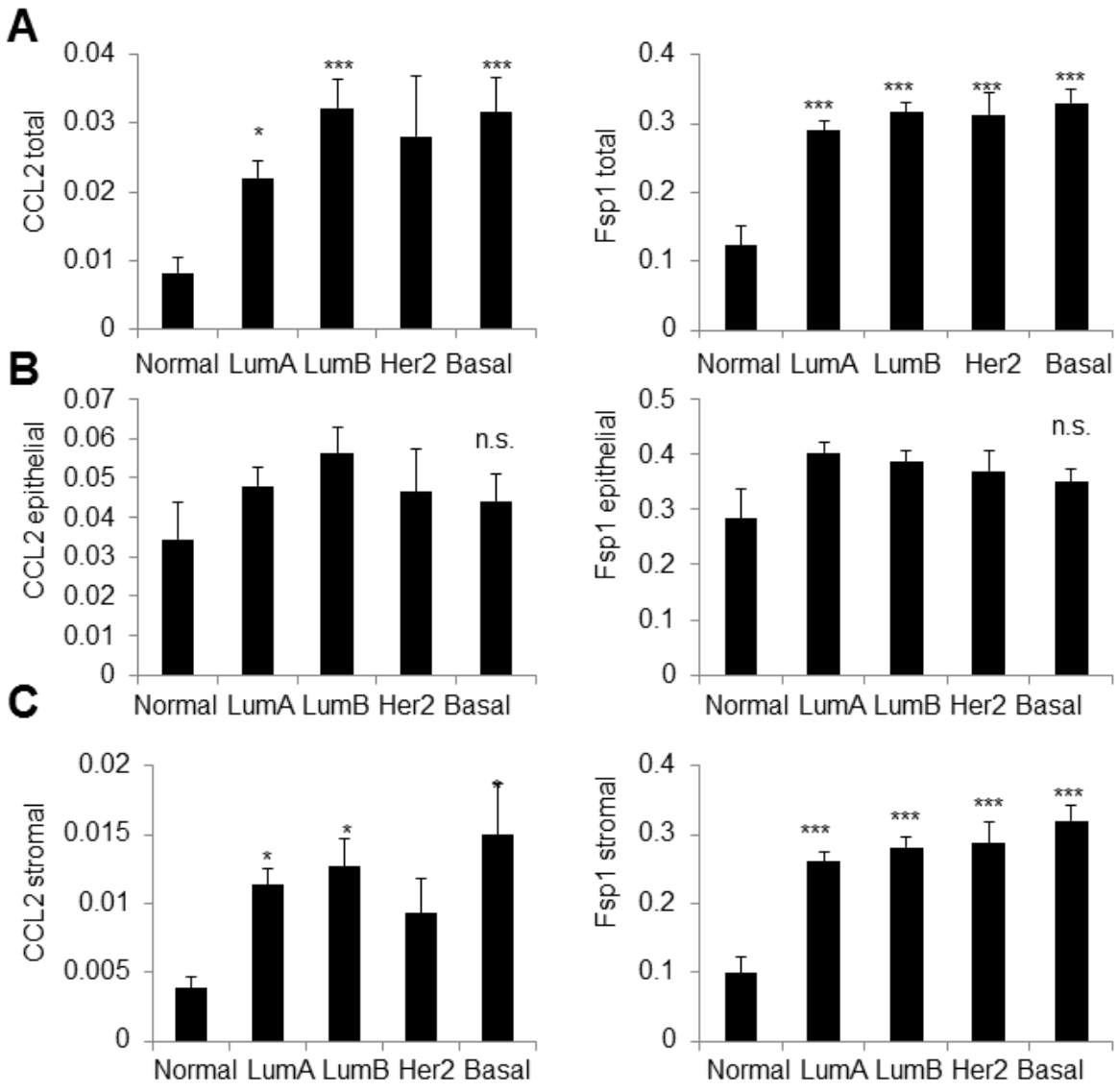

Figure 6. Associations of CCL2 and Fsp1 proteins with molecular subtypes. Expression levels of CCL2 and Fsp1 in whole tissue (**A**), epithelium **(B)** and stromal(**C**) were examined in: normal breast tissues (n=20), Luminal A (n=135), Luminal B (n=113), Her2+ (n=42) or Basal-like (n=75) breast cancers. Statistical analysis was performed using Kruskal-Wallis Test with Dunn's post-hoc comparison. Statistical significance was determined by $p<0.05$; *$p<0.05$, **$p<0.01$, ***$p<0.001$, n.s. = not significant.

Table 6. Associations of CCL2 and Fsp1 expression with outcome for patients with Luminal A, Luminal B or Her2+ breast cancers. Associations of CCL2 and Fsp1 with overall survival and recurrence free survival were determined using univariate Cox Regression analysis. 95% confidence interval (CI) of the calculated Hazard Ratio (HR) is shown. Statistical significance was determined by $p<0.05$.

	Factor	Overall survival				Recurrence free survival			
		HR	95% CI		p-value	HR	95% CI		p-value
LumA	CCL2 total	0.02	0.00	32455.83	0.582	0.02	0.00	5081.37	0.535
	CCL2 stromal	0.33	0.01	11.45	0.538	1.39	0.10	19.65	0.806
	CCL2 epithelial	0.62	0.00	2208.55	0.908	0.05	0.00	250.25	0.493
	Fsp1 total	1.60	0.19	13.51	0.665	1.13	0.15	8.49	0.903
	Fsp1 stromal	0.68	0.07	6.21	0.729	0.52	0.06	4.24	0.543
	Fsp1 epithelial	1.99	0.23	16.90	0.529	2.41	0.35	16.61	0.371
LumB	CCL2 total	0.02	0.00	116.90	0.369	0.01	0.00	48.28	0.269
	CCL2 stromal	0.59	0.10	3.68	0.575	0.54	0.09	3.25	0.499
	CCL2 epithelial	0.03	0.00	11.69	0.253	0.03	0.00	8.67	0.230
	Fsp1 total	0.76	0.11	5.25	0.779	0.83	0.13	5.47	0.844
	Fsp1 stromal	0.92	0.13	6.32	0.932	0.73	0.11	4.85	0.743
	Fsp1 epithelial	0.40	0.07	2.40	0.317	0.70	0.13	3.86	0.684
Her2+	CCL2 total	0.00	0.00	904.47	0.235	0.00	0.00	700.93	0.269
	CCL2 stromal	1.01	0.06	18.43	0.993	9.17	0.24	350.51	0.233
	CCL2 epithelial	0.01	0.00	427.02	0.372	0.01	0.00	214.89	0.352
	Fsp1 total	0.15	0.01	1.98	0.151	0.30	0.03	3.36	0.328
	Fsp1 stromal	0.16	0.01	2.39	0.183	0.39	0.03	5.59	0.485
	Fsp1 epithelial	0.37	0.03	5.11	0.459	0.42	0.03	5.04	0.490

Table 7. Associations of CCL2 and Fsp1 expression with patient outcome in Basal-like breast cancers. Associations of CCL2 and Fsp1 with overall survival and recurrence free survival were determined using univariate Cox Regression analysis. 95% confidence interval (CI) of the estimated Hazard Ratio (HR) is shown. Statistical significance was determined by $p<0.05$.

Factors	Overall survival				Recurrence free survival			
	HR	95% CI		p-value	HR	95% CI		p-value
CCL2 total	0.05	0.00	764.46	0.544	0.06	0.00	1103.32	0.573
CCL2 stromal	1.61	0.55	4.76	0.386	5.28	1.31	21.25	0.019
CCL2 epithelial	0.02	0.00	69.49	0.333	0.01	0.00	38.31	0.246
Fsp1 total	0.13	0.02	1.19	0.071	0.28	0.04	2.31	0.239
Fsp1 stromal	0.15	0.02	1.31	0.086	0.31	0.04	2.28	0.250
Fsp1 epithelial	0.36	0.03	4.16	0.417	0.66	0.06	7.27	0.734

Table 8. Univariate and Multivariate Cox Regression Analyses on the association of total Fsp1 expression with overall survival in patients with Basal-like breast cancers. 95% confidence interval (CI) of the calculated Hazard Ratio (HR) is shown. Statistical significance was determined by $p<0.05$.

Factor	Univariate analysis				Multivariate analysis			
	HR	95% CI		p-value	HR	95% CI		p- value
Age	1.00	0.97	1.02	0.636	-			
Stage								
II	1.00			0.082	1.00			0.738
III	1.81	0.93	3.53		1.132	0.546	2.347	
Grade								
I	0.00	0.00			-			
II	1.00			0.871	-			
III	0.83	0.41	1.67		-			
Chemotherapy								
No	1.00			0.050	1.00			0.117
Yes	2.29	1.00	5.25		2.103	0.829	5.33	
Radiation therapy								
No	1.00			0.060				0.081
Yes	1.94	0.97	3.85		1.974	0.919	4.238	
Hormone therapy								
No	1.00			0.953	-			
Yes	1.06	0.15	7.77		-			
Fsp1 total	0.13	0.02	1.19	0.071	0.196	0.02	1.909	0.160

Table 9. Univariate and Multivariate Cox Regression Analyses on the association of stromal Fsp1 expression with overall survival in patients with Basal-like breast cancers. 95% confidence interval (CI) of the calculated Hazard Ratio (HR) and p-value is shown. Statistical significance was determined by $p<0.05$.

Factor	Univariate analysis				Multivariate analysis			
	HR	95% CI		p- value	HR	95% CI		p- value
Age	1.00	0.97	1.02	0.636	-			
Stage								
II	1.00			0.082	1.00			0.567
III	1.81	0.93	3.53		1.26	0.57	2.78	
Grade								
I	0.00	0.00			-			
II	1.00			0.871	-			
III	0.83	0.41	1.67		-			
Chemotherapy								
No	1.00			0.050	1.00			0.022
Yes	2.29	1.00	5.25		4.19	1.23	14.25	
Radiation therapy								
No	1.00			0.060	1.00			0.567
Yes	1.94	0.97	3.85		1.64	0.71	3.76	
Hormone therapy								
No	1.00			0.953	-			
Yes	1.06	0.15	7.77		-			
Fsp1 stromal	0.15	0.02	1.31	0.086	0.26	0.03	2.47	0.241

Table 10. Univariate and multivariate Cox Regression analyses on the association of stromal CCL2 expression with recurrence free survival of patients with Basal-like breast cancers. Association of CCL2 and recurrence free survival was determined by Cox univariate or multi-variate regression analysis. Hazard Ratio (HR), 95% confidence interval (CI) of the calculated HR is shown. Statistical significance was determined by $p<0.05$.

Factor	Univariate				Multivariate			
	HR	95% CI		p-value	HR	95% CI		p-value
Age	0.99	0.96	1.01	0.242	-			
Stage								
II	1.00			0.065	1.00			0.048
III	1.88	0.96	3.67		2.45	1.01	5.95	
Grade								
I	0.00	0.00	0.00		-			
II	1.00			0.958	-			
III	0.90	0.44	1.84		-			
Chemo-therapy								
					1.00			
No	1.00			0.015				0.034
Yes	2.98	1.23	7.19		3.73	1.10	12.58	
Radiation therapy								
No	1.00			0.102	-			
Yes	1.80	0.89	3.62		-			
Hormone therapy								
No	1.00			0.656	-			
Yes	0.82	0.34	1.98		-			
CCL2 stromal	5.28	1.31	21.25	0.019	7.51	1.72	32.91	0.007

Discussion

Despite the importance of the stroma in animal models of breast cancer, the use of stromal biomarkers in the clinical setting remains to be validated. In these studies, we report that stromal CCL2 expression correlates with worse relapse-free survival in Basal-like breast cancer and was independent of stromal Fsp1 or other commonly recognized prognostic factors such as grade.

While CCL2 is expressed in the stroma and epithelium of breast tissues, and significantly correlates with Fsp1 expression in the overall cohort, we show that only stromal CCL2 is a significant prognostic factor in recurrent Basal-like breast cancers. We did not observe a significant association between CCL2 expression in whole tissues, stroma or epithelium with patient outcome in the overall cohort. These studies contrast with previous studies showing that CCL2 expression correlated with poor patient prognosis regardless of molecular subtype (35,52). It is possible that different experimental designs contributed to the different results. We utilized an Image J software approach to quantify protein expression in patient samples collected from US patients (n=427). Previous studies utilized smaller sample sizes (n=128-150), collected from Japanese patients (35,52). One study used an ELISA approach to analyze breast tumor samples (52). Another study relied on visual scoring of samples during immunohistochemistry analysis (35). It is possible that regional differences affect expression of CCL2 in patients. It would be of interest in the future to determine whether demographics affect CCL2 expression in cancer patients.

Interestingly, we observed that high level CCL2 expression in the overall cohort was inversely associated with T stage or N stage, which would be associated with good prognosis. In contrast stromal CCL2 expression was associated with poor prognosis in patients with Basal-like

breast cancer. We noted that a large number of cases in the overall cohort were Luminal A and B breast cancer, (n= 248) compared to Basal-like breast cancers which were mainly stage III breast cancers (n=75). Patients with Luminal breast cancer show a more favorable prognosis than Basal-like breast cancer (46,47). Thus, the discrepancy may be due to the large proportion of Luminal breast cancer cases, which were consistent with the overall diagnostic trends in the US (57,58), but may have skewed the associations of CCL2 in the overall cohort. While CCL2 expression was not significant in Her2+ breast cancers in our studies, a recent study of 32 Her2+ breast cancer patients reported that high levels of serum CCL2 associated with favorable outcome in patients vaccinated against Her2 antigen (59). High CCL2 expression could predict a more favorable outcome if examined in a therapeutic context. These studies suggest different complex roles for CCL2 among different subtypes of breast cancer.

In addition to fibroblastic cells, CCL2 was expressed in infiltrating cells in our patient samples, consistent with previous studies [32, 35]. It is likely that fibroblasts and macrophages together, constitute a major source of CCL2 expression in breast cancer stroma. Despite the similarities in expression patterns, stromal CCL2 but not stromal Fsp1, was associated with decreased recurrence free survival of Basal-like breast cancer patients. We observed a small but not statistically significant association between total Fsp1 (HR=0.13, p=0.071) and stromal Fsp1 expression (HR=0.15, p=0.086) with favorable overall survival, opposite results of stromal CCL2. These results further suggest that stromal CCL2 expression is independent of Fsp1 expression in Basal-like breast cancers. These results are consistent to one recent study reporting that high expression of Fsp1 in the stroma correlated with favorable overall survival and increased relapse-free survival in the overall cohort in univariate analyses (60).

In summary, our studies demonstrate an association between poor outcome in Basal-like breast cancer and CCL2 expression in the stroma. These studies demonstrate that stromal markers may be useful predicting prognosis for specific breast cancer subtypes.

Chapter III: Function of the CCL2/CCR2 signaling in fibroblasts and breast cancer cells interaction

Contents in this chapter are currently in preparation for submission.

Introduction

Stromal CCL2 expression correlated with poor prognosis for patients with basal-like breast cancers (61). In animal models, antibody neutralization of CCL2 inhibits growth and metastasis of breast tumor xenografts correlating with decreased macrophage recruitment (35,36,38). While the majority of studies on CCL2/CCR2 signaling in breast cancer have focused on its role in regulating immune cell recruitment, recent studies have suggested an immune independent function for CCL2/CCR2 signaling. CCR2 is overexpressed in breast cancer cells, and is important for CCL2 induced cell motility and survival (39). CCL2 neutralization inhibits fibroblast induced tumor cell invasion (62). While CCL2 may be overexpressed in the tumor (35,61), these studies suggest that CCL2/CCR2 signaling to breast cancer cells mediated by fibroblasts may play an important role in breast cancer progression, independent of the immune system.

In these studies, we sought to characterize the role of autocrine and paracrine CCL2/CCR2 signaling in progression of basal-like breast cancers using the MCF10CA1d xenograft mouse models (63,64). Co-grafting MCF10CA1d breast cancer cells with cancer associated fibroblasts enhanced breast tumor growth, which was abrogated by knockdown of CCL2 in the stroma or knockout of epithelial CCR2. The reduction in breast tumor growth was independent of macrophage recruitment or tumor angiogenesis. Knockout of CCR2 alone had minimal effects on cancer cells survival or proliferation, but ablated stromal conditional medium or recombinant CCL2 induced proliferation. The SRC or PKC pathways activated by CCL2 signaling contributed to CCL2/CCR2 mediated growth of breast cancer cells. Comparison among different molecular subtypes through datamining revealed CCL2 and CCR2 were most highly expressed in basal-like breast cancers. These studies reveal fibroblasts are an important source of

CCL2 production, and regulate basal-like breast cancer growth through CCL2/CCR2 signaling in breast cancer cells. Thus, the CCL2/CCR2 signaling may serve as potential therapeutic targets in basal-like breast cancer.

Materials and methods

Cell lines and culture

The human breast cancer cell line MCF10CA1d (63,64) was kindly provided by Fred Miller, Ph.D. (University of Michigan). MCF10A-DCIS.com was kindly provided by Fariba Behbod, Pharm. D., Ph.D. (University of Kansas Medical Center). BT-20, MDA-MB-436, MDA-MB-468 and HCC1937 were kindly provided by Roy Jensen, M.D. (University of Kansas Medical Center). MDA-MB-231was purchased from ATCC. MDA-MB-436 was cultured in Leibovitz's L-15 medium, supplemented with 10% fetal bovine serum (FBS). MDA-MB-436 was cultured in L-15 medium, supplemented with 10%FBS, 10 ug/ml insulin and 16 ug/ml glutathione. BT-20 cells were cultured in Eagle's Minimal Essential Medium and supplemented with 10%FBS. All other cell lines were cultured in Dulbecco's Modified Eagle Medium (DMEM) containing 10% FBS, 2mM L-glutamate and 1% penicillin-streptomycin. Primary human breast cancer fibroblasts (CAF) and normal adjacent fibroblasts (NAF) were obtained from invasive breast carcinoma tissue samples obtained from University of Kansa Medical Center Biospecimen Repository. Mouse mammary fibroblasts were derived from MMTV-PyMT transgenic mice (65), or tumor- free mice. Fibroblasts were isolated from tissues as previously reported (66). Purity of fibroblasts was assessed by DNA genotyping and for positive expression of Fsp1, a-SMA and N-cadherin, but absence of other cell lineage markers. Fibroblasts were immortalized by transfection of hTert prior to ablation studies, using approaches previously

described (67). All cell lines were confirmed mycoplasma free using the mycoplasma detection kit (Lonza, #LT07-703).

Orthotopic transplantation tumor model

Female athymic nude mice ($FoxN1^{nu/nu}$) 6-8 weeks old were purchased from Charles River. Breast cancer cells and fibroblasts were orthotopically transplanted using approaches previously reported (68). Briefly, 100,000 cancer cells and 250,000 fibroblasts were seeded into 50 ul Rat Tail Collagen type I overnight. In cancer cell graft alone, only 10^5 cancer cells were used. Mice were anesthetized with 1-3% isoflurane. An incision was made into the skin flap to expose the #4-5 mammary glands. A pocket was made underneath the mammary lymph node using spring scissors and the collagen plug was inserted into the pocket. Wounds were closed by gut absorbable suture. Mice were monitored twice a week. Mice were sacrificed at approximately 6 weeks of age when the control tumors grew 1.5 cm in diameter, the largest allowable size allowed by the Institutional Animal Care and Use Committee (IACUC). All animal procedures were approved by IACUC under AAALAC guidelines.

Lung whole mount staining

Lung metastasis was analyzed by lung whole mount staining as reported before (69). Briefly, lungs were fixed in 10% neutral formalin overnight, dehydrated through 70%, 95% and 100% ethanol, and cleared in xylene overnight in 4^{o}C. Lungs were then rehydrated through ethanol gradients, stained with hematoxylin for 10min, and de-stained with 1%HCL in water for 20min. Lung metastasis was then counted under the microscope with 200 magnifications.

CCL2 ELISA

10^4 human or mouse fibroblasts were seeded overnight into 24-well plate, and changed into serum free DMEM medium for 24h. Conditioned medium was assayed for human CCL2 (Peprotech, #900-K31) or murine CCL2 expression (Peprotech, #900-126)

shRNA knockdown

Stable cell lines were generated by transduction of lentivirus expressing shRNA. Lentivirus was produced by co-transfection of shRNA and packaging vectors (psMD2.G and psPAX2) into HEK293T cells, using methods previously described (70). Lentiviral vectors were obtained from Origene with shRNA targeting sequence as follows. murine CCL2 (TL501987): 5'-ACGTGTTGGCTCAGCCAGATGCAGTTAAC-3', human shRNA1: 5'-TATAGAAGAATCACCAGCAGCAAGTGTCC-3', human shRNA2:5'-AGAAGCTGTGATCTTCAAGACCATTGTGG-3'. Scramble control shRNA (TR30021) sequence was not provided.

CRISPR/Cas9 gene ablation

Lentivirus vector expressing Cas 9 and blasticidin selection marker was obtained from Jeremy Chien, Ph.D. (University of Kansa Medical Center), originally developed by Feng Zhang, Ph.D. (MIT)(71). Guide RNA (gRNA) for human CCL2 was: 5'-GTACCTGGCTGAGCGAGCCCT-3'. gRNA for CCR2 was 5'-TTCACAGGGCTGTATCACAT-3' . For CCL2 gene ablation, the gRNA for human CCL2 was cloned into the lentivirus vector pLKO5.sgRNA.EFS.GFP (72) (Addgene, #57822) using BsmBI restriction enzymes. Fibroblast cells were transduced with Cas9 lentivirus one time, treated with 4 ug/ml blasticidin (Invitrogen, #R210-01), followed by transduction with lentivirus expressing gRNA or empty vector. Cells were sorted by flow cytometry for GFP and were cultured in a 96

well plate seeded at 0.5 cell per well. For CCR2 gene ablation, the gRNA was cloned into the pL-CRISPR.EFS.GFP vector (72) (Addgene, #57818), a lentivirus vector containing both the Cas9 and GFP reporter, using BsmBI restriction enzyme. MCF10CA1d Cells were transduced with the lentivirus one time, flow sorted by GFP and seeded into 6-well plates at 1000 cells per well. Individual colonies were manually picked and seeded into a 96-well plate. Colonies were screened for CCR2 gene alternation by PCR with primers flanking the targeting site: Forward 5'-ACATGCTGGTCGTCCTCATC-3', Reverse 5'-: AAACCAGCCGAGACTTCCTG-3'. PCR was performed at annealing temperature of 67^{o}C for 30 cycles with 20 ng genomic DNA templates. DNA from mutant clones was further confirmed by sequencing (GENEWIZ).

Flow cytometry

Adherent cells were lifted off plates using Accutase (Millipore Sigma, #SCR005) at 37^{0}C. Cells were washed in PBS, incubated with anti-CCR2-PE at a 1:10 dilution (R&D Systems, #FAB151P) for 1 hour. Cells were washed in PBS and read by flow cytometer using a BD LSRII instrument.

Generation of conditioned medium:

1 million cancer cells or fibroblasts were seeded into a 10 cm dish in DMEM/10% FBS. Medium was collected after 24h, centrifuged and filtered through 0.45um to eliminate cell debris before use.

2D Cell proliferation assay

Cells were seeded overnight into a 96-well plate overnight (500 cells/well) in triplicate in DMEM/10% FBS. The next day, cells were incubated with fresh DMEM/10% FBS in the

presence or absence of: 200ng/ml human recombinant CCL2 (Peprotech, #300-04), DMSO, SRC inhibitor PP2 at 10uM or 20uM (AdipoGen, #AG-CRI-3563), PKC inhibitor Go6983 at 5uM or 10 uM (Cayman Chemical, #13311). In conditioned medium studies, conditioned medium was used instead. Cells were fixed in 10% formalin, stained with crystal violet, extracted with 10% acetic acid, and quantified at OD590.

3D spheroid assay

Tumor spheroids were established using conditions previously described (73). Briefly, 96-well plates were coated with 40 ul of matrix containing 1:1 ratio of collagen (Corning, #354236) and Growth Factor Reduced Matrigel (Corning, #354230). MCF10CA1d cancer cells were seeded at 1000 cells per well in 200 ul DMEM/10%FBS containing 2.5% matrigel. The media was replaced with conditioned medium every 2 days for to 6 days. Bright field images of cell spheres were taken every two days using an EVOS FL-Auto imaging system at 10X magnification. Sphere size was quantified using Image J.

Western blot

Cancer cells were seeded at 200,000 cells/well in a 6-well plate overnight in DMEM/10% FBS, serum deprived overnight, and incubated with serum free media in the presence or absence of 200 ng/ml recombinant human CCL2. For inhibitor studies, cells were incubated with DMSO, PP2 and G06983 and CCL2 together for 15 minutes. Cells were washed twice with cold PBS and lysed with RIPA buffer containing protease inhibitor and phosphatase inhibitors. 20-25 ug proteins were resolved on SDS-PAGE gels, transferred to nitrocellulose membranes. Membranes were blocked in 5% milk and incubated with primary antibodies at 1:1000 dilution: p-PKC (pan, βII Ser660, CST, #9371), p-SRC (Tyr416, CST, #6943), SRC (CST, #2123), p-AKT (Ser473,

CST, #4060), AKT (R&D, #MAB2053), p-ERK (Thr202/Tyr204, CST, #4370), ERK (CST, 9107), p-SMAD3 (Ser423/425, CST, 9520), SMAD3 (CST, #9523) and ACTIN (Sigma, #A5441). Corresponding HRP conjugated secondary antibodies (anti-mouse or anti-rabbit) at 1:2000 dilution were used.

Histology/immunohistochemistry

Tumor samples were fixed in 10% formalin overnight, paraffin embedded and sectioned at 5- micron thickness. For H&E stain, sections were incubated in hematoxylin for 3 minutes and counter stained with eosin for 3 minutes. For immunostaining, sections were heated in 10mM sodium citrate at low pressure for 20 minutes using a pressure cooker to de-crosslink antigens. Peroxidases were quenched in water containing 10% methanol and 10% hydrogen peroxidase. Slides were blocked in PBS containing 5% FBS for 1 hour, incubated at 1:100 dilution with primary antibodies: anti-human cytokeratin 5 (ThermoFisher, #MA5-12596), Ki67 (Santa Cruz, #sc15402), cleaved Caspase-3 (CST, #9661), von William Factor (Chemicon, #AB7356), Arginase I (Santa Cruz, #sc-20150), LC3b (CST, #3868). Samples were stained with corresponding biotinylated anti-rabbit or anti-mouse secondary antibodies at 1:500 dilution. Sections were incubated with streptavidin-HRP (Vector Lab., #PK-6100). Antigens were detected using DAB substrate (Vector Lab., #SK-4100). Slides were counter-stained with hematoxylin, dehydrated and mounted with Cytoseal (Thermo Fisher, #348976). Images were captured using EVOS FL-Auto microscope, 4 random images at 100 or 200x magnification. Expression was quantified using Image J as previously described (69).

Datamining

Datasets were downloaded from cBioportal (http://www.cbioportal.org/). The TCGA dataset (74)(n=825) and the METABRIC dataset (75,76) (n=2509) were analyzed for CCL2 and CCR2 expression. Breast cancer subtype was defined by PAM50.

Statistical analysis

Statistical analysis was performed using GraphPad software. Two tailed Student T test was used for two group comparison. One Way ANOVA with Bonferroni post-hoc comparison was used for multiple group comparison. Correlation of CCL2 and CCR2 expression was analyzed using Pearson's correlation test. Statistical significance was determined by $p<0.05$.

Results

Fibroblast mediated growth of basal-like breast tumor xenografts correlates with CCL2 expression

In recent studies, we demonstrated that CCL2 expression in breast cancer stroma correlated with accumulate of fibroblastic cells, and was associated with poor prognosis for patients with basal-like breast cancer (61). To further understand the role of CAF derived CCL2 on progression of basal-like breast cancers, we isolated multiple primary CAFs from human breast cancer biopsy and mouse mammary tumors. Characterization of those fibroblasts confirmed they expressed fibroblast markers Fsp1, a-SMA and N-cadherin, but lacked expression markers of other cell lineages (Figure 7). Examination of chemokine CCL2 expression by ELISA revealed both human and mouse fibroblasts expressing higher level of CCL2, compared to common breast cancer cell lines and normal breast epithelial cell line (Figure 7 and 8), though variation of CCL2 expression was observed among individual

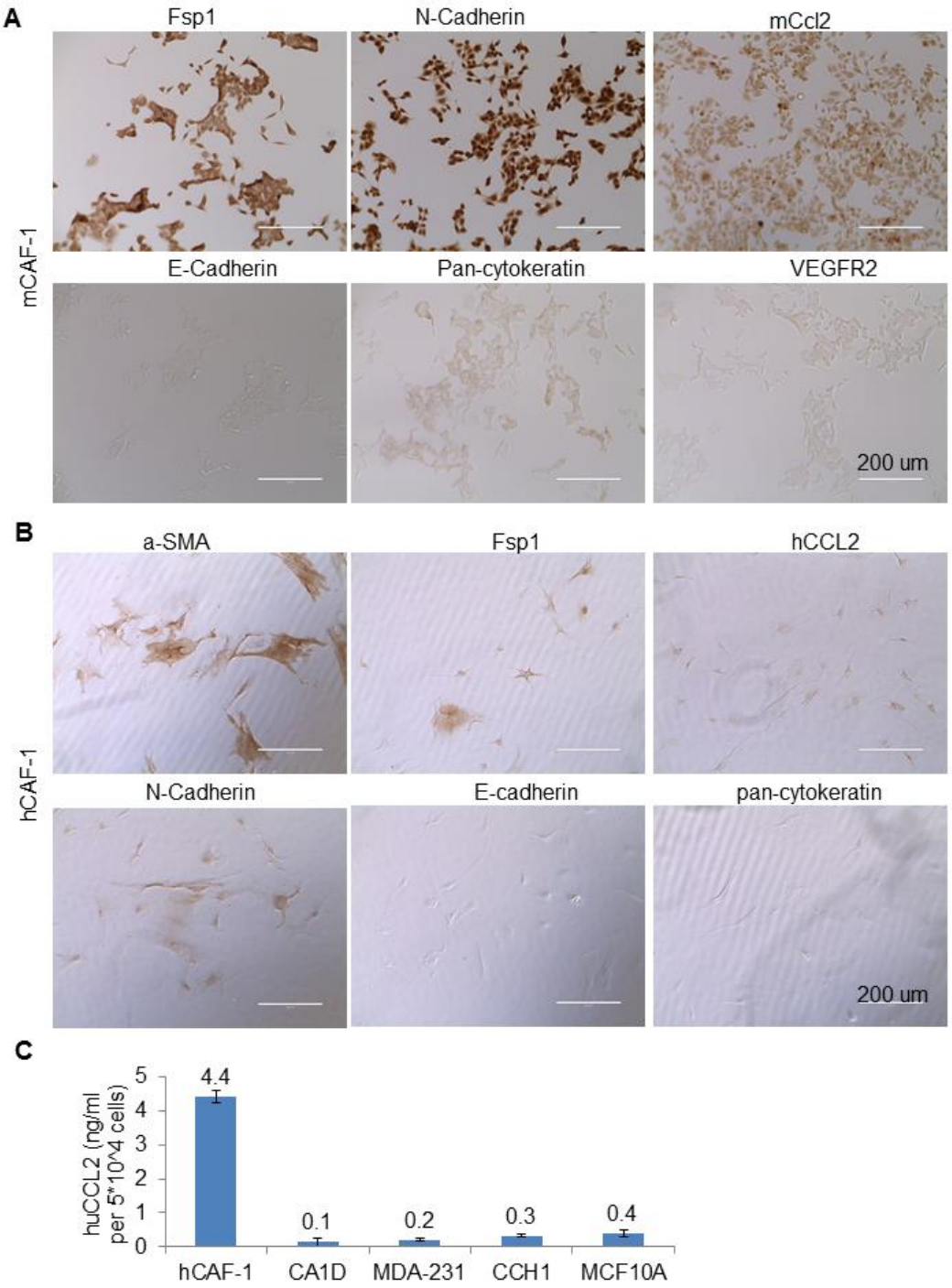

Figure 7. Molecular characterization of CAFs and CCL2 expression. Immunohistochemistry staining of mouse mCAF-1 (**A**) and human hCAF-1 (**B**) using markers of mesenchymal (Fsp1, N-Cadherin, a-SMA), epithelial (E-cadherin, pan-cytokeratin) or endothelial (VEGFR2) lineages and CCL2. (**C**) CCL2 expression determined by ELISA in various human breast cancer cell lines or normal epithelial cell (MCF10A). Condition medium was collected from 5*10^4 cells. hCAF-1 was used for comparison.

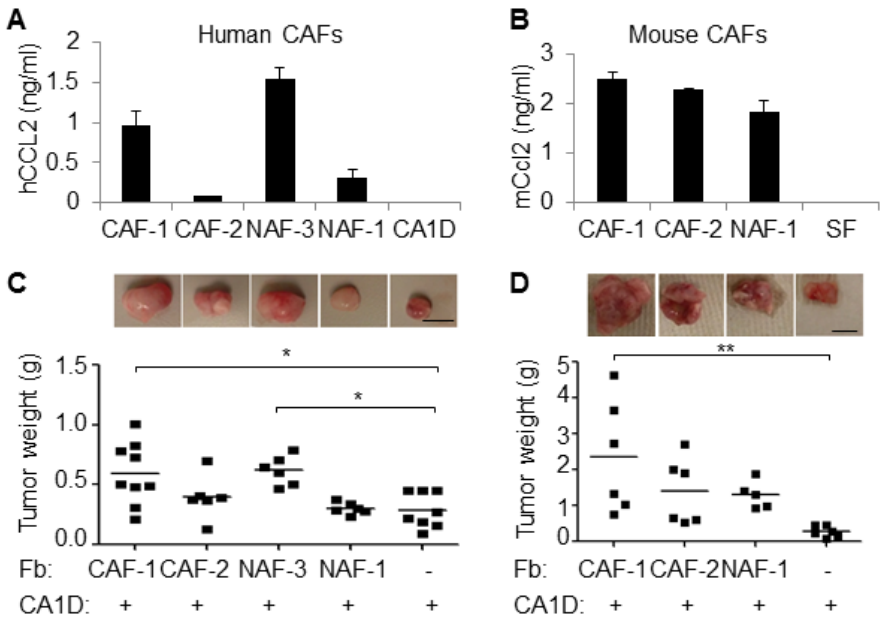

Figure 8. Breast cancer associated fibroblasts with high CCL2 expression promoted CA1D tumor growth. (A) Human CCL2 expression level in primary breast cancer associated fibroblasts (CAF) and normal fibroblasts (NAF) determined by ELSIA per 10^4 cells. (**B**) Mouse CCL2 expression in CAFs and NAF, serum free medium (SF) used as control. Tumor weight of CA1D cancer cells co-grafted with human CAFs or NAFs(**C**), or mouse CAFs or NAFs (**D**), compared with cancer cell alone after four weeks inoculation. Each dot represents one mouse, and representative tumor images were shown above. Scale bar=1cm. One way ANNOVA was used for statistical analysis. *p<0.05, **p<0.01.

human samples. We co-transplanted human or mouse fibroblasts with the human basal breast cancer cell line MCF10CA1d, which was derived from Ras transformation of MCF10A breast epithelial cells (63,64). Co-transplantation with human fibroblasts revealed that CAF-1 and NAF-3 significantly increased primary tumor growth over MCF10CA1d alone, correlating with high CCL2 expression (Figure 8A-B). Similarly, murine CAF-1 significantly increased the growth of primary MCF10CA1d xenografts, correlated with a high murine CCL2 expression (Figure 8B and D). Histological analysis revealed that grafting of tumor cells alone or with fibroblasts resulted in formation of high grade, invasive tumors with few glandular structures (Figure 9A). The majority of the tumor tissue was comprised of CK5+ breast epithelial cells (Figure 9B), consistent with cytokeratin expression of basal-like breast cancers (6). Grafting of MCF10CA1d cells alone or with fibroblasts did not result in macroscopic lung metastasis as determine whole mount staining (Figure 9C). In summary, these data indicate that CAFs increase tumor growth but do not significantly affect metastasis of MCF10CA1d tumor xenografts.

Ablation of stromal CCL2 expression inhibits growth and survival of basal-like breast tumor xenografts

In previous studies, we found that CCL2 was expressed in both the tumor epithelium and stroma (61). To determine the functional contribution of CCL2 on primary tumor growth, we examined the effects of CCL2 deficiency in fibroblasts and MCF10CA1d cells. CCL2 was knocked out in human CAFs (hCAF-1) by CRISPR/Cas9 (77) through targeting N-terminal of CCL2 protein (Figure 10A). Two CCL2 deficient clones (mut-7, mut-22) were generated and determined by ELISA (Figure 10A). Control or CCL2 deficient fibroblasts were then co-grafted with MCF10CA1d cells and examined for changes in tumor growth. Co-grafting of mut-7 or mut-22

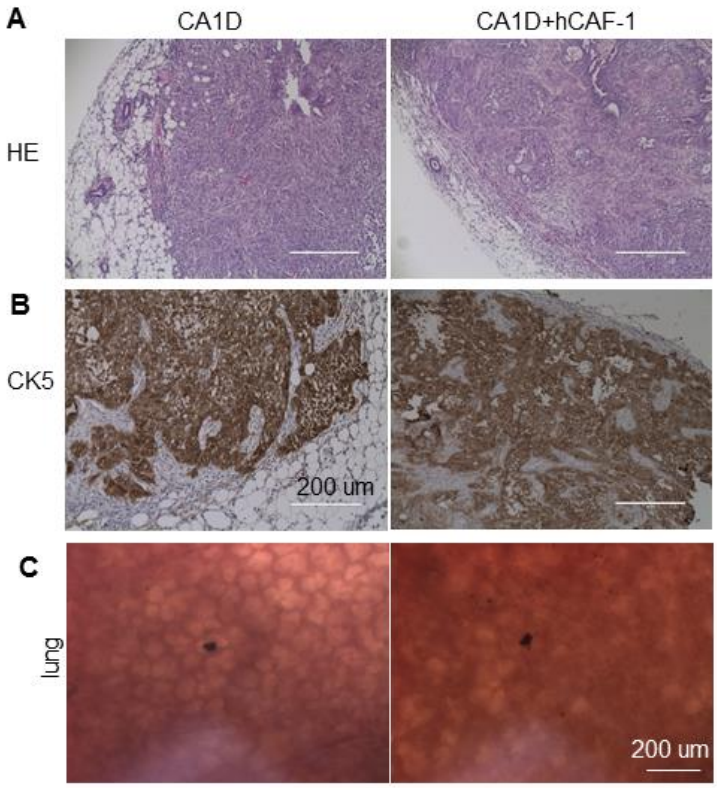

Figure 9. Histology and cancer cells identification in the co-graft tumor model. Tumor sections from CA1D or CA1D+hCAF-1 stained with hematoxylin-eosin (**A**), and immunohistochemistry stained with human specific cytokeratin 5 (CK5) (**B**). (**C**) Examples of lung micro-metastasis by lung whole amount staining. Scale bar is 200 um.

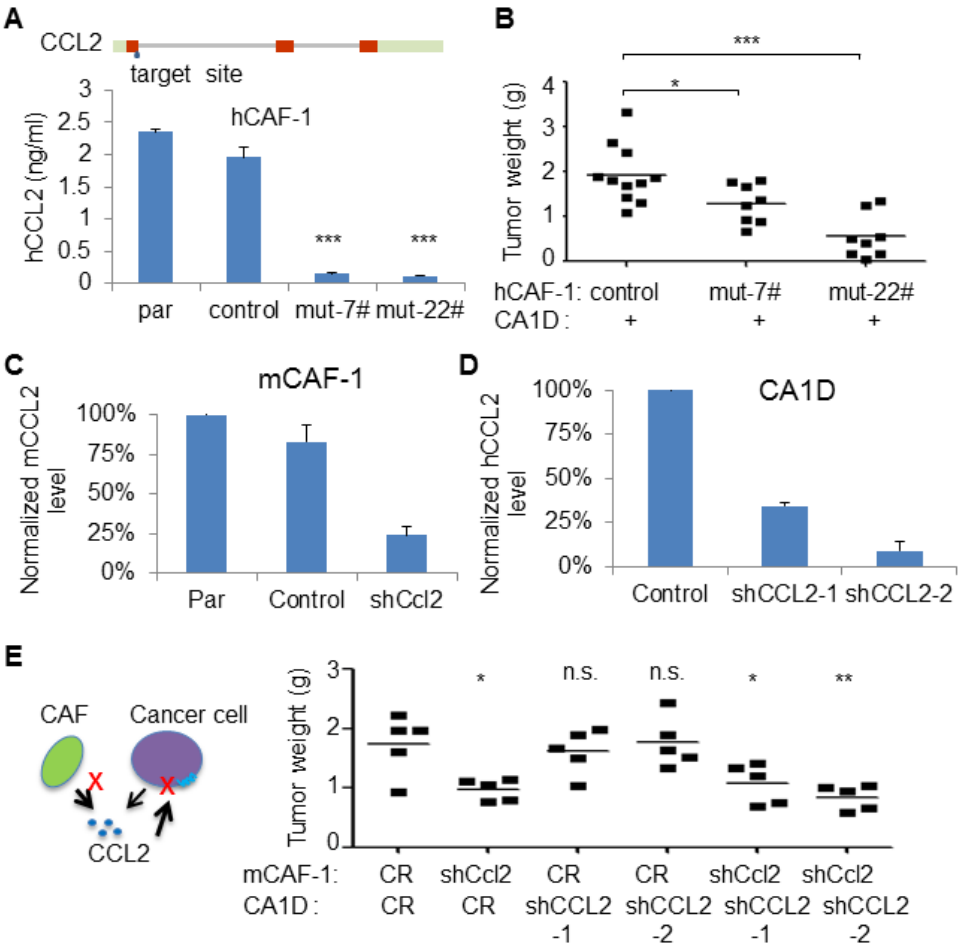

Figure 10. CCL2 derived from cancer associated fibroblasts contributed to CA1D tumor growth. (A) CCL2 expression in human CAF-1 with targeted mutation by CRISPR/Cas9. Arrow indicates gRNA target site in the first coding exon (red). CCL2 expression from mutant clones (7# and 22#) was compared to control clone or parental cell line (par). (**B**) Tumor weight of CA1D co-grafted with control or CCL2 mutant CAF-1 after 6 weeks inoculation. (**C**) Scheme of CCL2 knockdown in mouse CAF-1 or CA1D cells. Tumor weight of co-graft model with CCL2 knockdown in mCAF-1 (shCcl2) or CA1D cancer cells (shCCL2-1 and shCCL2-2). Each group was compared to control shRNA (CR) in mCAF-1 and CA1D. Tumor was grafted for four weeks, with five mice per group. One way ANNOVA was used for statistical analysis. *p<0.05, **p<0.01, ***p<0.001, n.s. p>=0.05. Determination of CCL2 knockdown efficiency in mCAF-1 (**D**) or human CA1D (**E**) determined by mouse or human CCL2 ELISA. CCL2 expression level was normalized to parental or control shRNA.

hCAF-1 clones resulted in a significant decrease in tumor growth over time compared to co-grafting with control hCAF-1 cells (Figure 10B). To further confirm this study, CCL2 expression was knocked down in murine CAF-1 (mCAF-1) and in MCF10CA1d breast cancer cells by stable shRNA expression. This resulted in a 60-80% decreased in CCL2 expression in mCAF-1 (Figure 10C) or MCF10CA1d cells (Figure 10D) compared to control shRNA cells. Breast cancer cells co-grafted with CCL2 deficient mCAF-1 cells showed a significant decrease in tumor mass compared to co-grafting with control CAF-1 cells, while CCL2 deficient MCF10CA1d cells co-grafted with control mCAF-1 did not (Figure 10E). Co-grafting with CCL2 deficient MCF10CA1d cells with CCL2 deficient CAF-1 cells did not further affect tumor mass (Figure 10E). These data indicate that CCL2 derived from murine CAFs but not from MCF10CA1d cells is important for primary tumor growth. In summary, our studies demonstrate that CCL2 derived from fibroblasts regulate breast cancer growth.

We further evaluated the effects of stromal CCL2 ablation on the primary tumor proliferation and survival through histology. By H&E stain, MCF10CA1d tumors co-grafted with control or CCL2 shRNAs fibroblasts both showed significant areas of central necrosis. Quantification of these areas revealed no significant differences in necrosis between the groups (Figure 11A). By immunohistochemistry, stromal CCL2 deficiency did not significantly affect tumor cell proliferation as indicated by PCNA staining (Figure 11B), but did significantly increase cleaved caspase-3 expression and LC3B immunostaining, indicating increased apoptosis and autophagy (Figure 11C-D). While CCL2 is known is associated with increased levels of M2 macrophages (69) and tumor angiogenesis (78), there were no significant changes in M2 macrophage levels or blood vessel density in the primary tumor, as determined by

immunostaining for arginase I and VWF8 (Figure 12A-B). These data indicate that stromal CCL2 mediated tumor growth

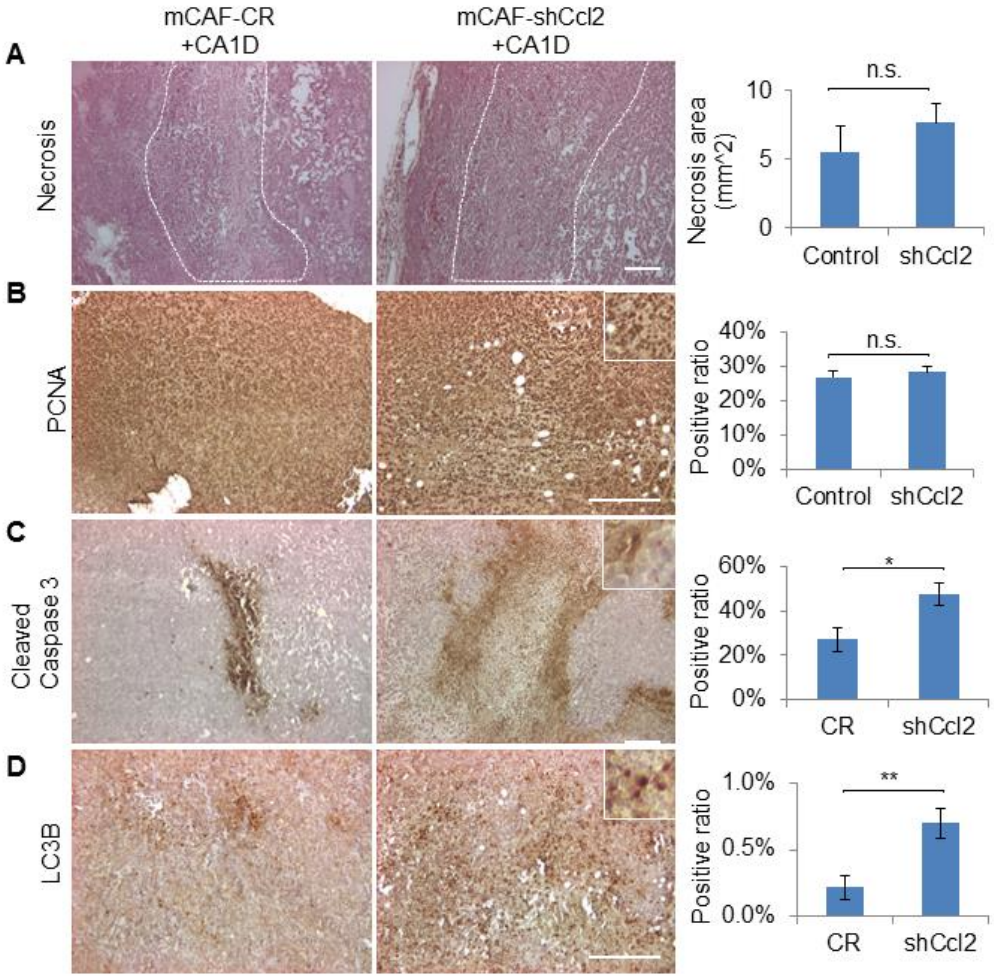

Figure 11. CCL2 knockdown in cancer associated fibroblasts associated with increased expression of apoptosis and autophagy markers. Comparison of necrosis by hematoxylin-eosin staining (**A**) or molecular markers between CA1D co-grafted with control (CR) or CCL2 knockdown(shCcl2) mouse CAF-1 by immunohistochemistry with PCNA (**B**), LC3b (**C**) and cleaved caspase-3 (**D**). Necrosis area in (A) were circled by dotted white line. Inserts in B-D showed the magnified picture of staining. Scale bar represented 400 um. Student T test was used for statistical analysis. *p<0.05, **p<0.01, and n.s. (p>=0.05).

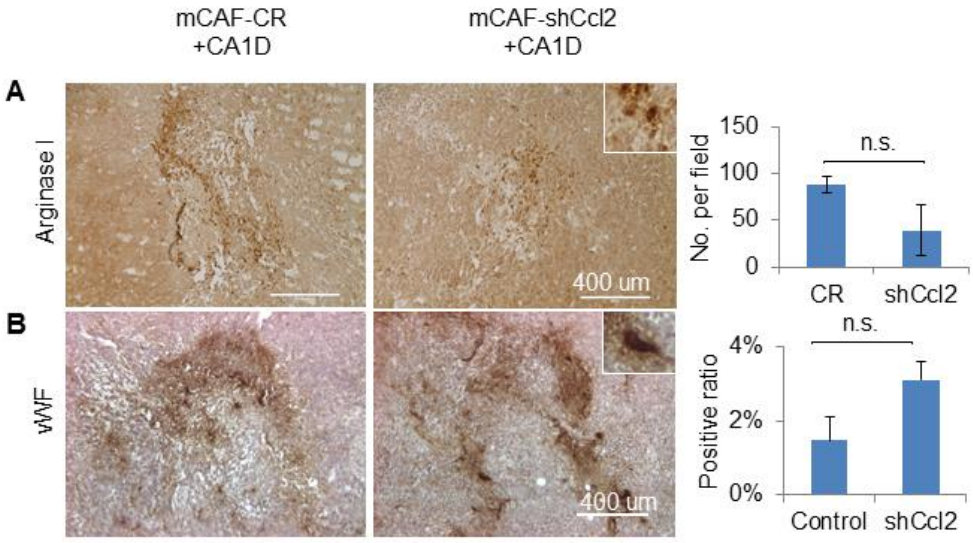

Figure 12. CCL2 knockdown in cancer associated fibroblasts did not significantly affect M2 macrophage infiltration and angiogenesis. Comparison of stromal cell markers between CA1D co-grafted with control (CR) or CCL2 knockdown(shCcl2) mouse CAF-1, using M2 macrophage marker Arginase I (**A**) and angiogenesis marker vWF (**B**). Student T test was used for statistical analysis. n.s. ($p>=0.05$).

is associated with cell survival, and is independent of tumor angiogenesis and macrophage recruitment.

CCL2 derived from fibroblasts signals directly to breast cancer cells to mediate cell growth

To determine whether CCL2 derived from CAFs directly signaled to breast cancer cells, we utilized *in vitro* cell culture systems. MCF10CA1d breast cancer cells cultured in a monolayer were treated with conditioned medium from hCAF-1 cells or recombinant CCL2, and showed a significant increase in cell density as determined by crystal violet staining (Figure 13A-B). Interestingly, CCL2 mediated cell growth was associated with the serum concentration used for incubation, as treatment of breast cancer cells with CCL2 in 1% FBS resulted in a small but not significant increase in cell density (Figure 13B). 3-dimensional (3D) cultures were used to more closely mimic conditioned in tumor tissues (73). Similar to 2D culture, MCF10CA1d cells treated with fibroblast conditioned medium showed an increase in spheroid growth over time (Figure 13C-D). MCF10CA1d spheroids treated with conditioned medium from CCL2 deficient hCAF-1 cells resulted in significantly decreased spheroid size over time, compared to control hCAF-1 cells (Figure 13E). The effect of CCL2 deficient fibroblast condition medium can be rescued by adding back of recombinant CCL2 (Figure 13F). These data indicate that CCL2 derived from fibroblasts acts directly on MCF10CA1d breast cancer cells to mediate growth over time.

CCR2 knockout inhibits CCL2 mediated breast cancer growth

In previous studies, we showed that CCR2 was overexpressed in breast cancer cells, correlating with tumorigenicity (39).

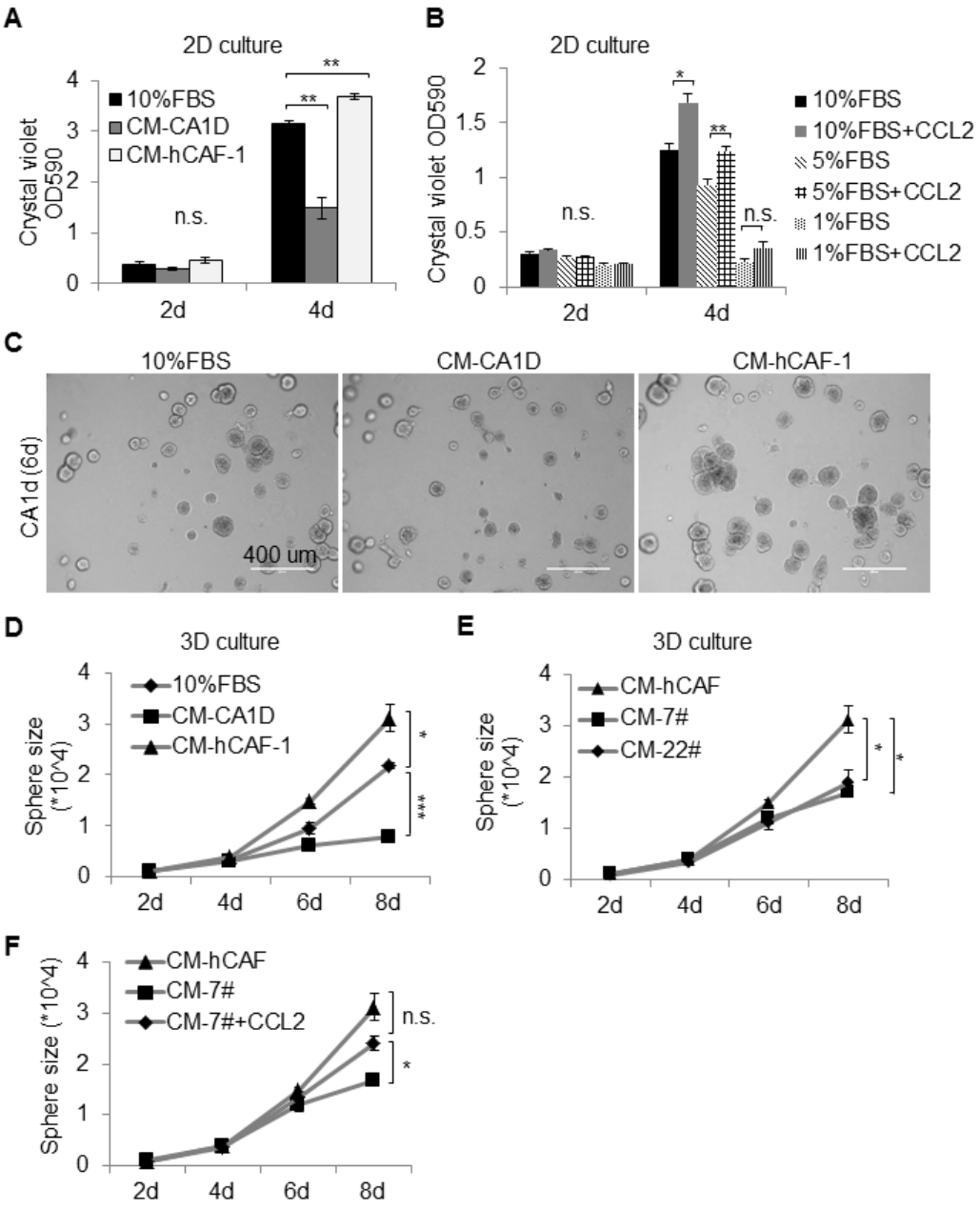

Figure 13. CCL2 derived from cancer associated fibroblasts promoted MCF10CA1d growth *in vitro*. (A) Comparison of CA1d cell proliferation in 2-dimensional culture in regular medium (10%FBS), or in condition medium from CA1d (CM-CA1D) or human CAF-1 (CM-hCAF-1) . Cell number was quantified by crystal violet staining. (**B**) Effect of recombinant CCL2 (200 ng/ml) in CA1d cell proliferation in 2D in different serum medium. (**C**) Representative images of CA1d spheres in 3-dimensional culture for 6 days. Comparison of CA1d sphere size during 8-day 3-dimensional culture in conditional medium (**D**), CCL2 mutant fibroblasts condition medium(7# and 22#) **(E**) or mut-7# fibroblasts condition medium with added recombinant CCL2 (200 ng/ml) (**F**). One way ANNOVA was used for statistical analysis. *p<0.05, **p<0.01, ***p<0.001, n.s. p>=0.05.

To further determine the significance of epithelial CCR2 expression to CAF mediated breast tumor growth, we knocked out CCR2 in MCF10CA1d breast cancer cells by CRISPR/Cas9, targeting the third transmembrane domain of CCR2 protein (Figure 14A). PCR screening identified two mutant clones F1 and G10, both of which possessed deletion and/or insertion in the coding region and resulted frame shift of the CCR2 protein (Figure 14B-C). Flow cytometry analysis of cell surface receptor expression indicated a 75 % reduction in CCR2 expression in the G1 mutant, while the F1 mutant showed 10% reduction in CCR2 expression (Figure 15A). It is likely that the F1 mutant clones expressed a truncated CCR2 protein on the membrane surface that may be recognized by CCR2 antibody. However, the resulting frameshift in the coding region generated a premature stop codon, resulting in mutants lacking a C-terminal region (Figure 15C). As such, we expected these mutants to abrogate CCR2 signaling, despite residual CCR2 expression. To control for specificity of CRISPR/Cas9 targeting, a wildtype clone (WT A1), which possessed an intact CCR2 gene, was identified by PCR and confirmed by sequencing (Figure 15B-C). Grafting of F1 or G10 cells alone showed a small but significant reduction in tumor growth compared to WT A1 cells. Co-grafting of F1 or G10 cells with hCAF1s resulted in a significant reduction in hCAF1 mediated tumor growth, compared to co-grafting of hCAF1 with WT A1 control breast cancer cells (Figure 3-9B). The 3D culture of CCR2 deficient MCF10CA1d breast cancer (F1, G10) alone did not result in significant changes to spheroid size (Figure 15C). 2D culture of F1 or G10 cells alone did not affect cell density (Figure 3-9D). However, treatment of F1 or G10 cells in 3D culture with hCAF1 conditioned medium resulted in smaller spheroids compared to the treatment of WT A1 cells (Figure 15C). Treatment of F1 or G10 cells cultured in 2D with hCAF conditioned medium showed a significant decreased in cell density compared to the treatment of WT A1 control cells (Figure 15D). These data indicate that

hCAF mediated growth of MCF10CA1d breast cancer cells through CCR2 dependent mechanisms.

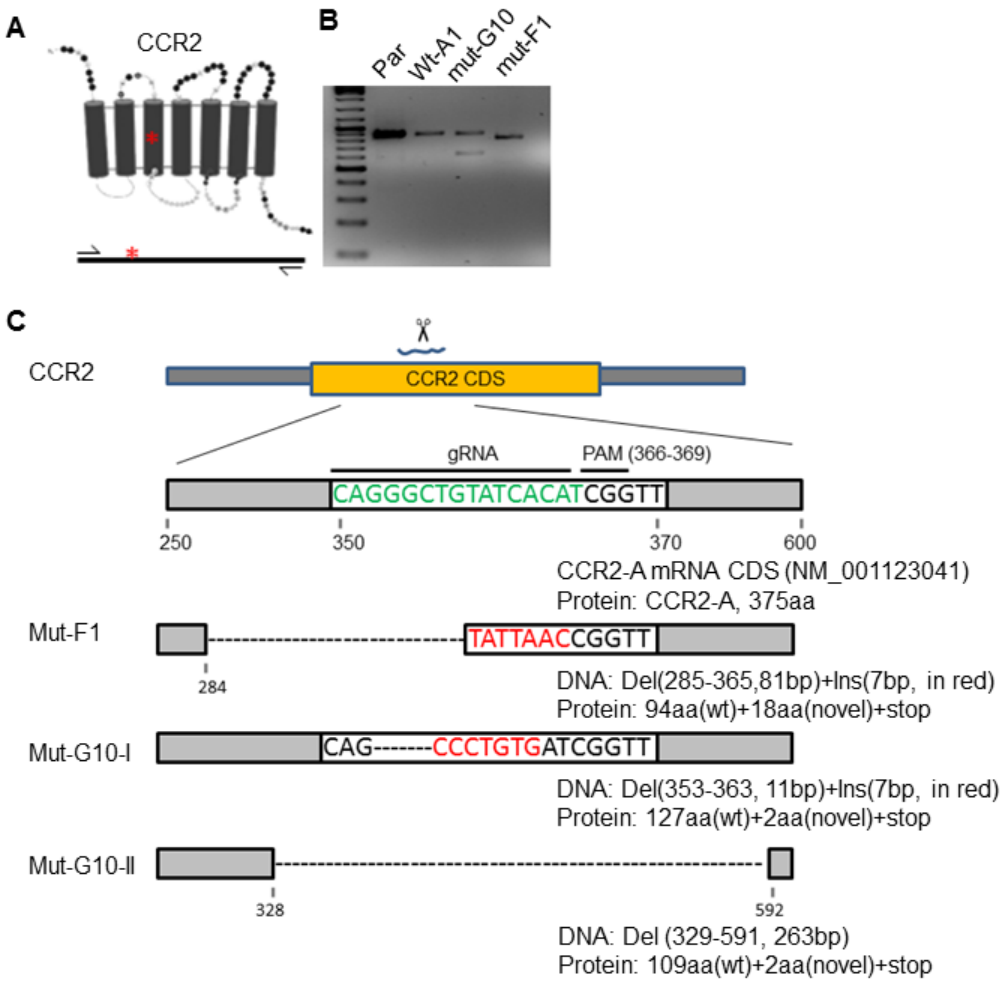

Figure 14. Screening and characterization of CCR2 mutant CA1D cell lines. (**A**) Illustration of CCR2 gRNA targeting site and PCR screening method. Red asterisk indicated the gRNA target site. (**B**) Identification of CCR2 mutant CA1D cell lines by PCR screening of genomic DNA from different cell colonies, showing the DNA size shift of mutant clone G10 and F1 compared to parental cell line or wildtype clone A1. (**C**) DNA sequence detail of CCR2 mutant F1 and G10 clones. CCR2-A CDS sequence was used as reference to detail mutation sites. Note the gRNA target region in on common region of CCR2-A and CCR2-B, so both isoform will be mutated. The mutated CCR2 protein sequence was predicted from the DNA sequence.

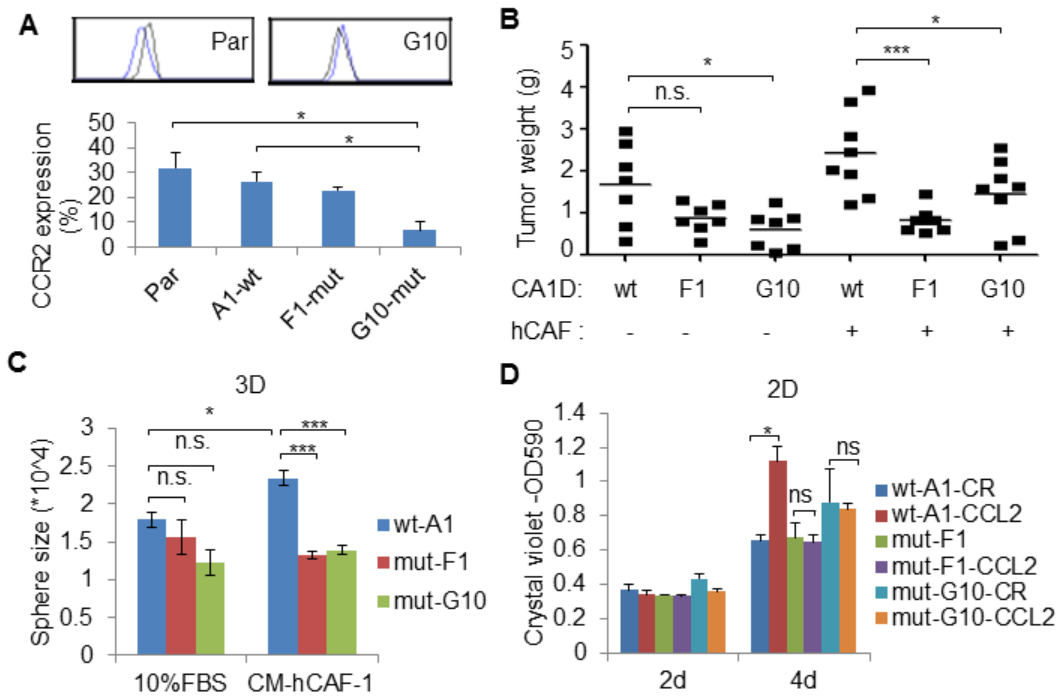

Figure 15. CCR2 mutant CA1D cancer cells lost response to CCL2 stimulated tumor progression. (**A**) Flow cytometry analysis of CCR2 surface expression on wildtype and mutant clones. Expression value is overton subtraction in population comparison. Top insert showed example of overlay between isotype control (blue) vs CCR2-PE (grey). (**B**) Comparison of tumor weight after grafting CCR2 mutant cancer cells alone, or in combination with human CAF-1 for 6 weeks *in vivo*. (**C**) Comparison of sphere growth for CCR2 mutants and wildtype control in response to fibroblast condition medium in 3D culture. (**D**) Comparison of cell proliferation for CCR2 mutants and wildtype control in response to CCL2 stimulation in 2D culture. One way ANNOVA was used for statistical analysis. *p<0.05, **p<0.01, ***p<0.001, n.s. p>=0.05.

CCL2/CCR2 signaling mediates breast cancer growth through PKC and SRC signaling pathways

To determine the signaling mechanisms through which CCL2/CCR2 mediated breast tumor growth, we examined the candidate pathways observed to be regulated by chemokine signaling (79), including PI3K/AKT, PKC and SRC pathways. MCF10CA1d breast cancer cells were treated with CCL2 over time and analyzed for phosphor-protein expression by immunoblot analysis. CCL2 did not affect phosphor-AKT expression or SMAD3 (Figure 16). CCL2 treatment significantly increased the level of pan phosphor-PKC (βII Ser600) and phosphor-SRC (Try416) expression starting at 2 min and peaking at 15 min, relative to untreated cells (Figure 17A). CCR2 knockout inhibited CCL2 induced phosphorylation of SRC and PKC, compared to WT A1 cells. Interestingly, CCR2 mutants appeared to show a higher basal level expression of phosphor SRC and PKC, in the absence of stimulation (Figure 17B). We further confirmed by over-expressing CCR2 in CA1D cell lines. CCR2 over-expression was sufficient to induce SRC and PKC phosphorylation without CCL2 ligand treatment, and lead to increased cell proliferation (Figure 18A-B).

To determine the relevance of PKC and SRC activation to CCL2 induced cell growth, we treated MCF10CA1d breast cancer cells with PP2, a small chemical SRC inhibitor (80,81), or with the pan PKC inhibitor G06983 (82). PP2 treatment inhibited CCL2 induced phosphor-SRC in a dose-dependent manner (Figure 18C). G06983 treatment increased phosphor-PKC level (Figure 18C), which is consistent with previous studies showing that G06983 binding to PKC, prevented its degradation (83). PP2 or G06983 treatment over 2 days did not significantly affect cell density of MCF10CA1d breast cancer cells. However, after 4 days, PKC or SRC inhibition notably inhibited the growth of MCF10CA1d breast cancer cells

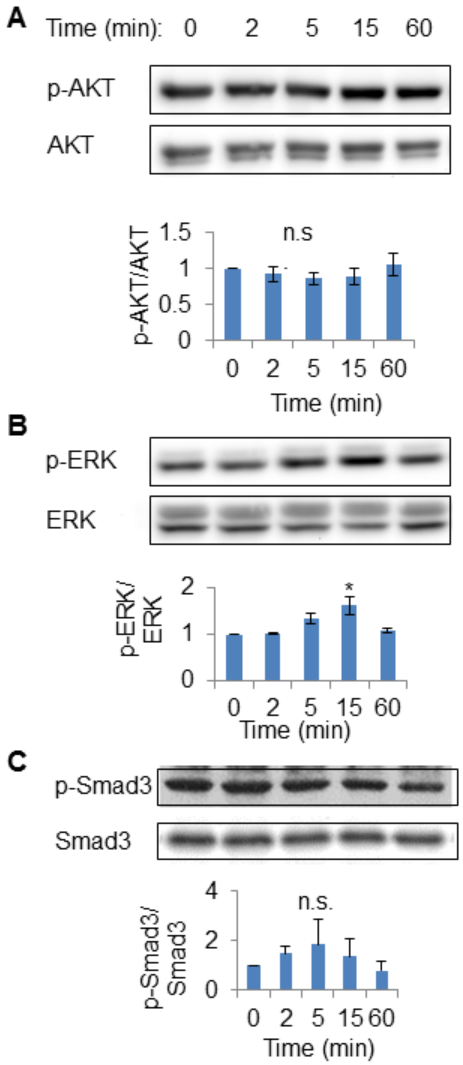

Figure 16. CCL2 signaling does not activate AKT and Smad3 pathways.
Representative images showing the AKT (**A**), ERK/MAPK (**B**) and SMAD3 (**C**) pathways activation during CCL2 stimulation over 1h window time course. Quantification showed results from three independent results. Phosphorylation signal was normalized to total protein and compared to 0 min. One way ANNOVA was used for statistical analysis. *p<0.05, **p<0.01, ***p<0.001, n.s. p>=0.05.

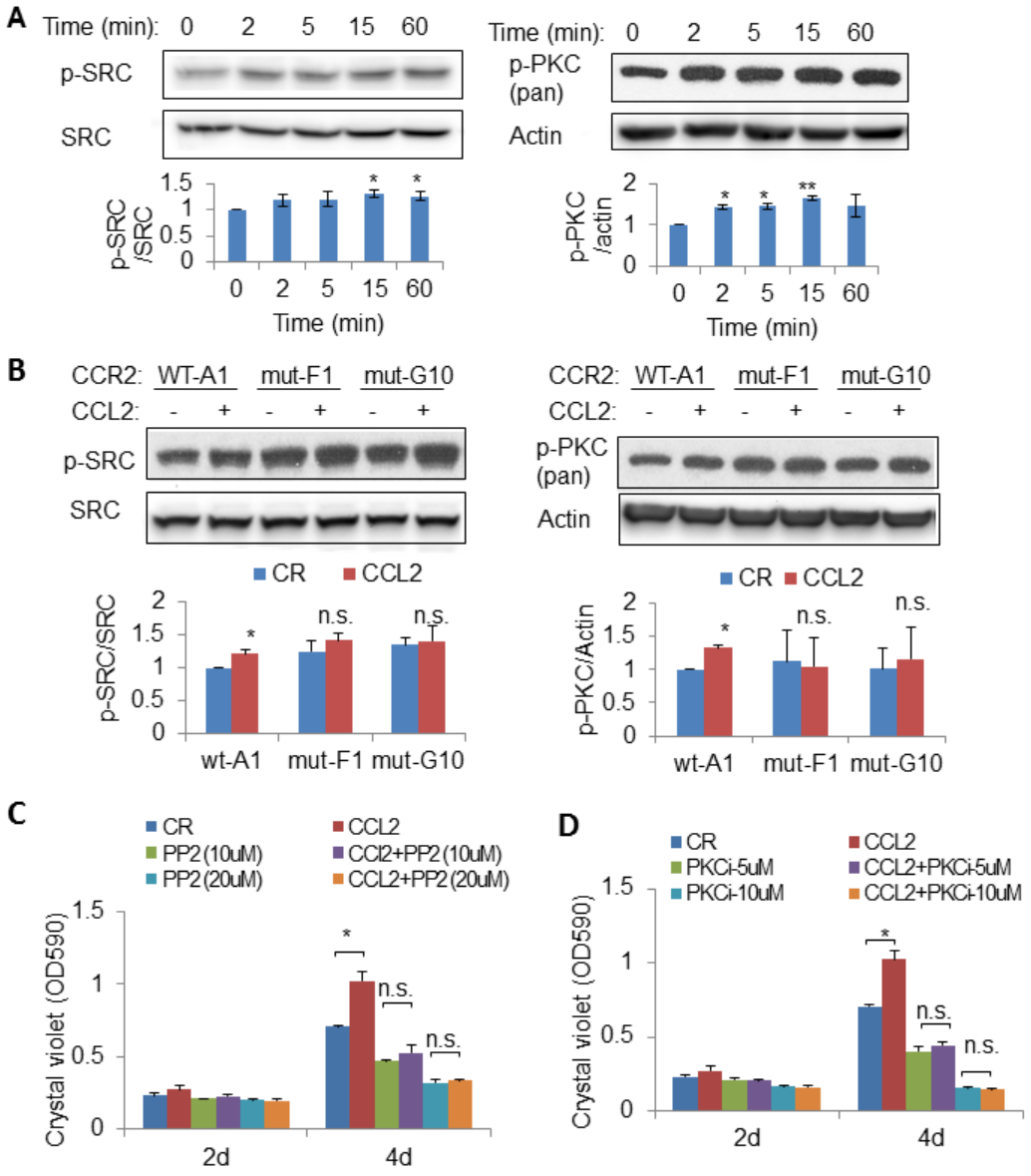

Figure 17. PKC and SRC pathways function downstream of CCL2 signaling in promoting CA1D cell proliferation. (A) Time course studies of SRC and PKC pathways activation by CCL2 stimulation (200 ng/ml) in CA1D cancer cells. (**B**) CCR2 mutant CA1D cancer cells stimulated with CCL2. (**C**) The effect of SRC inhibition by PP2 inhibitor on CA1D cell proliferation during CCL2 treatment. **(D**) The effect of PKC pathway inhibition by G06983 in CA1D cell proliferation during CCL2 stimulation. One way ANNOVA was used for statistical analysis. *p<0.05, **p<0.01, ***p<0.001, n.s. p>=0.05.

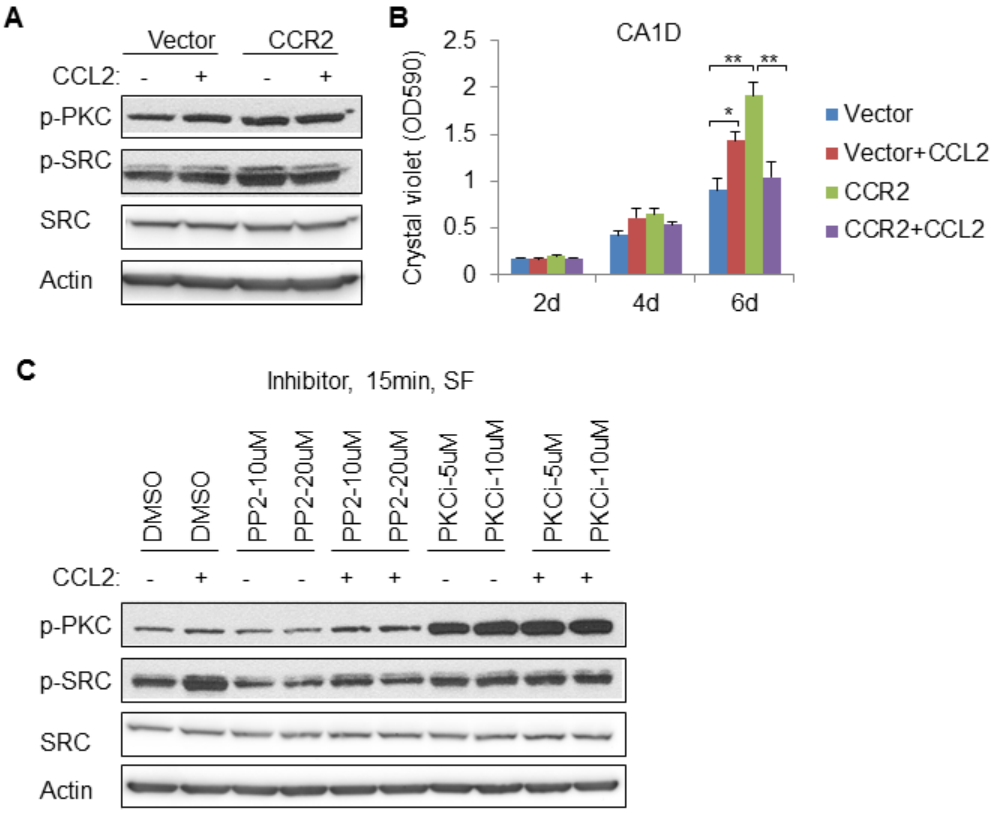

Figure 18. CCL2 signaling and SRC and PKC pathways. (A) The effect of CCR2 overexpression on PKC and SRC pathways in CA1D cell lines with/without CCL2 treatment for 15 min. (**B**) The effect of CCR2 over-expression in CA1D cell proliferation in 6-day time window. (**C**) Western blot examination of the effect of SRC inhibitor PP2 and PKC inhibitor G06983 on different dosages on p-SRC and p-PKC. Treatment was done in serum free medium for 15min. One way ANNOVA was used for statistical analysis. *p<0.05, **p<0.01, ***p<0.001, n.s. p>=0.05.

inhibited CCL2 induced growth of MCF10CA1d cells (Figure 17C-D). These data indicate that CCL2 mediated breast cancer cell growth through PKC and SRC dependent mechanisms.

CCL2 and CCR2 expression are co-upregulated in basal-like breast cancers

In previous studies, we showed that stromal CCL2 was elevated in basal-like breast cancers (61). To determine the clinical significance of CCL2 and CCR2 expression, we analyzed cancer genomic datasets for co-expression among breast cancer subtypes. CCL2 gene amplification was present in about 3% patient samples across all major breast cancer datasets, while genetic alternations for CCR2 gene were present less than 1% (Figure 19). When we examined RNA expression in the TCGA dataset (74) (n=520), CCL2 and CCR2 were both significantly higher in basal-like subtype compared to luminal subtypes (Figure 20A). Higher expression of CCL2 and CCR2 in basal-like breast cancers was confirmed in a second independent dataset (METABRIC (75,76), n=1904) (Figure 20B). Furthermore, CCL2 gene expression significantly correlated with CCR2 expression in basal-like breast cancers in the TCGA and METABRIC datasets (Figure 20C-D). These data indicate that CCL2 and CCR2 co-expression are associated with the basal-like breast cancer subtype.

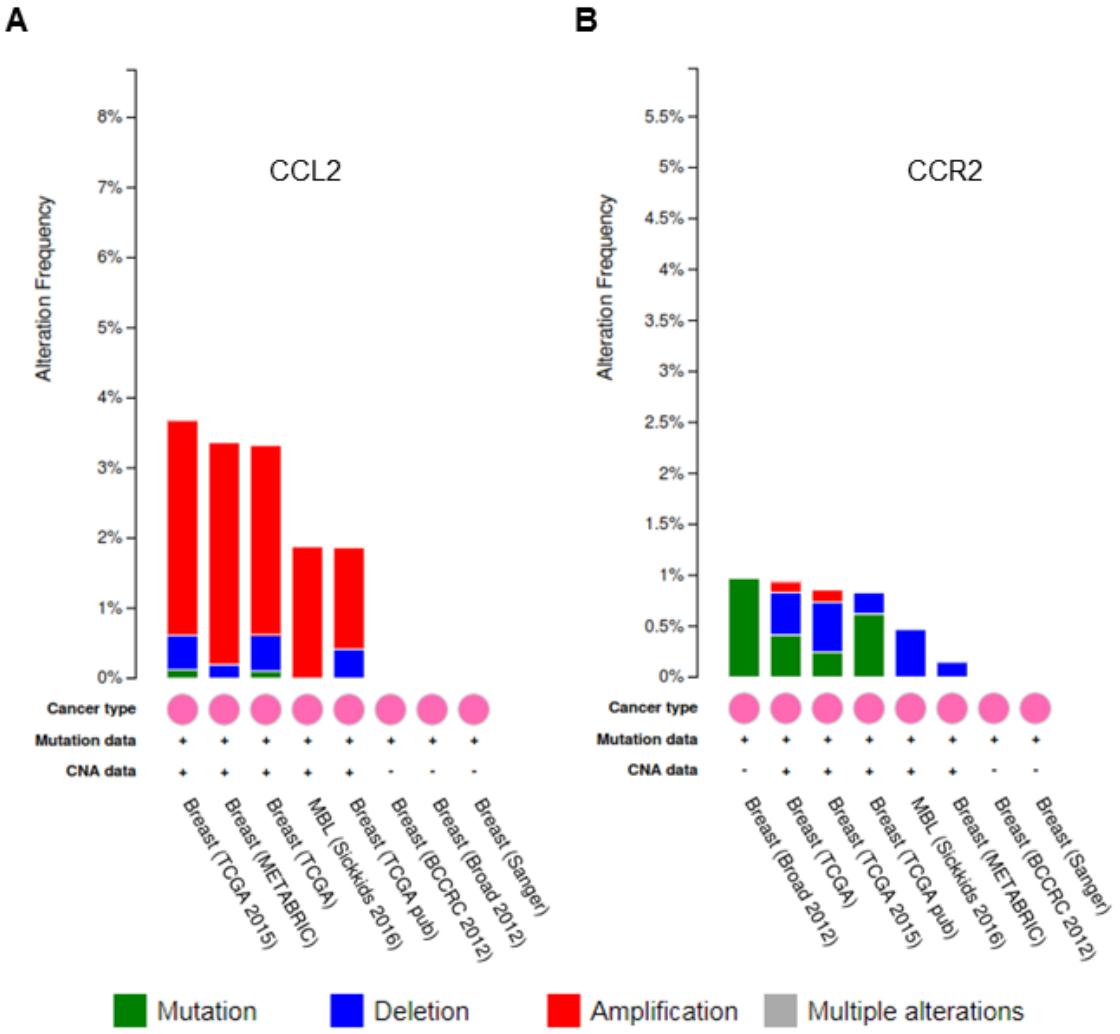

Figure 19. Genomic alternation in CCL2 and CCR2 genes in human breast cancer datasets. Color coded genomic alternation frequency in human CCL2 gene (**A**) and CCR2 gene (**B**) in breast cancer datasets. Data retrieved from cBioportal website.

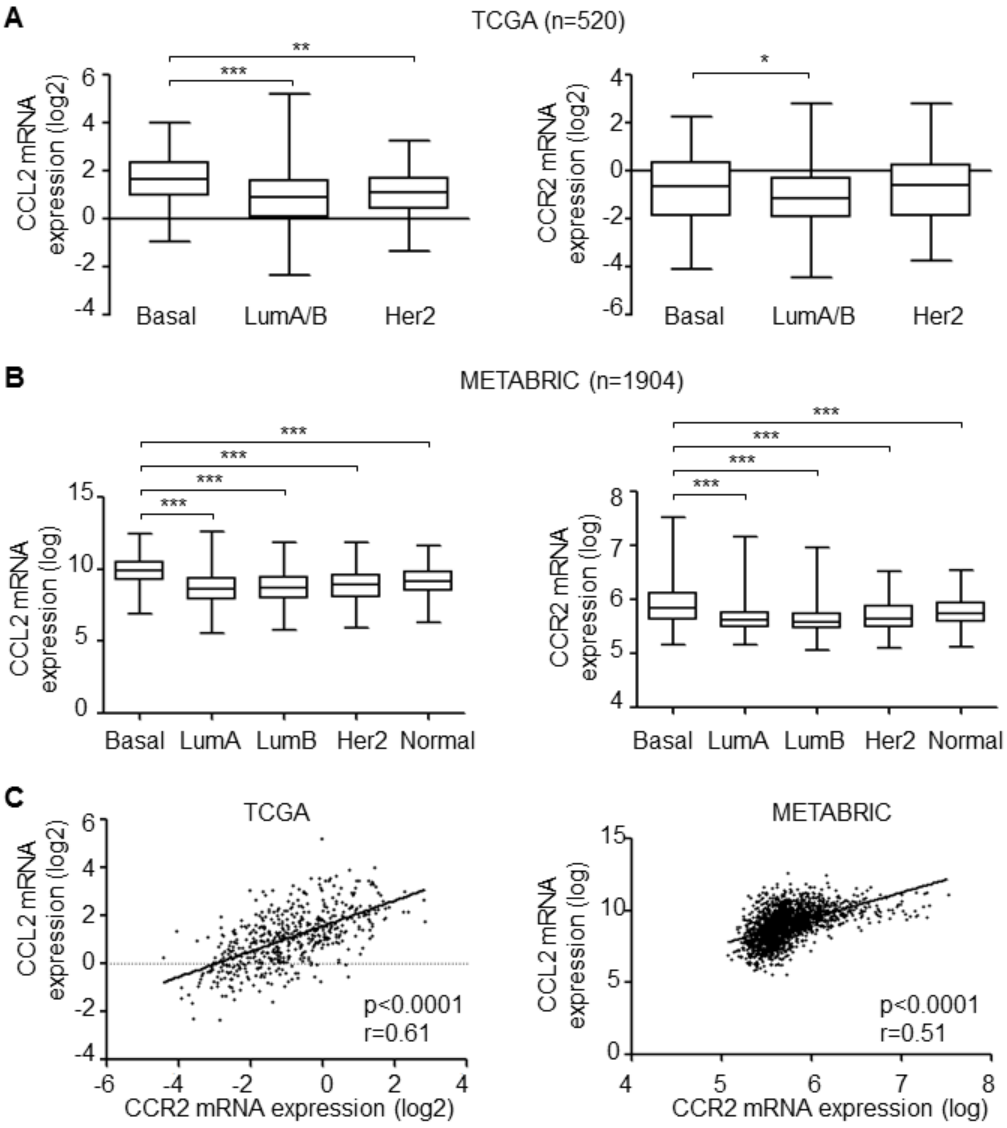

Figure 20. CCL2 and CCR2 are co-upregulated in basal-like breast cancer subtype. (A) Comparison of CCL2 and CCR2 mRNA expression among basal-like (n=96), Her2(57) and LumA/B (n=352) subtypes from TCGA dataset. (**B**) Comparison of CCL2 and CCR2 mRNA expression among basal-like (n=398), Her2(n=220), LumA (n=679), LumB (n=461) and normal-like (n=140) subtypes from METABRIC dataset. (**C**) Pearson correlation analysis of CCL2 and CCR2 expression in the two datasets.

Discussion

CCL2 is overexpressed in multiple tumor types, and is well known to regulate breast cancer progression through macrophage dependent mechanisms (32,33,36). While CCL2 is expressed in the tumor and the stroma, we report that stromal derived fibroblasts constitutes a major source of CCL2, and regulates the growth of basal-like breast cancers by signaling directly to CCR2 expressing cancer cells. Furthermore, we show that CCL2/CCR2 mediated tumor growth is regulated by PKC and SRC signaling pathways. As CCL2 and CCR2 are most highly expressed in basal-like breast cancers, the proposed pathways may represent viable therapeutic targets for this subtype.

In these studies, we noted a specific contribution from the breast CAFs in regulating breast tumor growth through CCL2 dependent expression. CCL2 is not confined to the stroma, but has been reported to be expressed in the epithelium in some breast tumors (32,33). However, CCL2 expression specifically in the stroma has been shown to be clinically relevant (35,61), correlating with poor patient prognosis for patients with basal-like breast cancers (61). The importance of the stroma may depend on the levels of epithelial CCL2. In these studies, we observed that CCL2 knockout alone in MCF10CA1d cells had minimal effects on primary tumor growth. However, these breast cancer cells expressed much lower levels of CCL2, compared to the stroma. As CCL2 knockout inhibited fibroblast mediated tumor growth, these studies indicate that the growth of MCF10CA1d cells may be dependent on the stroma. Examination of tumors over time indicates that hCAFs appear to have the most influence on growth in the first 4 weeks. This may be due to a gradual recruitment of host mouse fibroblasts and macrophage, and dilution and disappearance of grafted fibroblasts, as was reported previously (66). While murine CCL2 may also act on breast cancer cells to regulate cell behavior (39), host murine CCL2 from tumor-

bearing animals was not sufficient to rescue CCL2 deficiency in grafted cancer associated fibroblasts. These studies thus demonstrate a key importance for human fibroblasts in mediating growth of breast tumor xenografts through CCL2 dependent mechanisms.

The MCF10 breast epithelial model system has long been used as a xenograft model of breast cancer progression (63,64). While hCAFs have been shown to increase invasiveness of other breast tumor models (38,84), hCAFs had no significant effects on local invasion or metastasis of MCF10CA1d breast cancer cells, potentially due to the low metastatic ability of the cell line (64). In our studies, we demonstrated that hCAF derived CCL2 was important for the growth of MCF10CA1d breast cancer cells and the less invasive derivative cell line, DCIS.com (63). CCL2 had no effects on growth of other basal-like breast cancer cell lines including MDA-MB-231 and 4T1 mammary carcinoma cells, consistent with previous studies (39). It is possible that CCL2 mediated growth may depend on the genetic background as MCF10CA1d and DCIS.com breast cancer cells were derived from *in vivo* selection of tumors established from MCF10A breast epithelial cells overexpressing HRAS, an upstream regulator of SRC-MAPK signaling (63). In contrast, in 4T1 and MDA-MB-231 cells, CCL2 had no effect on PKC and SRC phosphorylation in these studies, but was shown to activate MAPK and SMAD3 to regulate cellular migration in previous studies (39). These studies indicate that CCL2 effects on breast cancer cells may depend on the cell line and ability to activate specific pathways associated with cell growth or migration. Interestingly, AKT is a key pathway that regulates breast tumor growth, survival and invasion, and is activated by many cytokines (79). In these studies, CCL2 had no effect on AKT phosphorylation in MCF10CA1d, DCIS.com cell lines, although these cells exhibited high basal expression of phosphor-AKT, consistent with previous studies showing that MCF10CA1d cells possess a PI3K constitutively active mutation (H1042R) (85). CCL2 had

not effect on phosphor-AKT in any other breast cancer cell line (39). In summary, these studies suggest that CCL2/CCR2 signaling in breast cancer cells activates a specific and unique combination of pathways important for growth and migration.

Previous studies have examined patterns of CCL2 and CCR2 expression in breast cancer, but have not drawn an association between these 2 genes in breast cancer subtypes. CCL2 expression has been shown to higher in estrogen negative breast cancer compared to estrogen positive cancer (86). CCL2 expression in fibroblasts inversely correlated with recurrence free survival for patients with basal-like breast cancers (61). In other studies, CCR2 expression in breast cancer cells correlated with invasive potential (39). Here, in two independent breast cancer datasets, we show that CCL2 and CCR2 are most highly co-expressed in basal-like breast cancers, compared all other subtypes, revealing a new association between CCL2 and CCR2 in breast cancer.

The CCL2/CCR2 signaling pathway is currently a therapeutic target of interest due to its significant effects on tumor growth, survival and metastasis (32,33). Many of these effects are attributed to CCL2 mediated angiogenesis or macrophage recruitment. There is currently some controversy to the feasibility of targeting as some studies suggest a rebound in tumor growth with cessation of CCL2 inhibitor treatment, due to possible macrophage dependent and angiogenesis feedback (87). However, this rebound may be due to the use of neutralizing antibodies themselves, rather than CCL2 as a target (88). Furthermore, these present studies indicate that targeting CCL2 or CCR2 expression may provide a particular benefit to patients with a basal-like subtype, where CCL2/CCR2 may signal directly to the cancer cell. Our studies support continuing efforts to identify improved treatment strategies for patients with invasive breast cancer.

Chapter IV: Therapeutic targeting the CCL2 signaling in breast cancer model

Contents in this chapter have been published in:

Yao, M., C. Smart, Q. Hu and N. Cheng (2017). "Continuous Delivery of Neutralizing Antibodies Elevate CCL2 Levels in Mice Bearing MCF10CA1d Breast Tumor Xenografts." Transl Oncol **10**(5): 734-743.

Introduction

Neutralizing antibodies and small pharmacologic agents to target cytokines in cancer have proven successful for the treatment of various cancer types, including breast and lung cancers (89). While small pharmacologic agents are in early clinical development (90), CCL2 neutralizing antibodies have been the primary agent used to target CCL2 activity, and have been extensively studied in animal models (36,38,91,92). However, recent studies have highlighted certain controversies surrounding targeting of CCL2 in cancer. Delivery of CCL2 neutralizing antibodies in animal models of breast and prostate cancer effectively inhibited tumor growth and metastasis, and decreased recruitment of macrophages (36,38,91,92). However, one recent study showed that cessation of CCL2 neutralization in a breast cancer model, lead to a rebound in tumor growth, associated with increased macrophage recruitment and tumor angiogenesis in the primary tumor (87). In addition, clinical trials have reported limited to no therapeutic efficacy of the CCL2 neutralizing antibody CNTO888, either as a single agent, or in combination with chemotherapy for the treatment of metastatic and non-metastatic cancer (93-95). Studies have suggested that a lack of efficacy was mainly due to clearance of antibody and rapid dissociation of antibody-CCL2 complex *in vivo*, leading to rebound of CCL2 levels during the antibody treatment (96). The majority of studies have involved interval injections of CCL2 blocking reagents (antibody or inhibitor). Thus, this method of delivery could lead to fluctuations of inhibitor levels over time, possibly limiting therapeutic efficacy. Furthermore, pre-clinical studies utilized murine specific CCL2 antibodies. To date, human specific CCL2 neutralizing antibodies in mouse models have not been extensively tested.

This study sought to more fully characterize the effects of human specific CCL2 neutralizing antibodies on breast cancer progression and determine whether effectiveness was

related to method of delivery. Nude mice bearing MCF10CA1d breast tumor xenografts were implanted with osmotic pumps containing control IgG or anti-CCL2, and analyzed for CCL2 levels, and tumor progression over 4 weeks. Despite inhibiting CCL2-induced migration *in vitro*, CCL2 neutralizing antibodies did not significantly affect breast tumor growth, invasion, macrophage recruitment or tumor angiogenesis. CCL2 antibodies significantly increased human CCL2 levels in circulating blood and tumor interstitial fluid. CCL2 neutralizing antibodies reduced CCL2 levels in cultured cells short-term at high concentrations. ELISA analysis of CCL2 in cultured fibroblasts and breast cancer cells revealed that the neutralizing antibodies sequestered CCL2 in the media, and that CCL2 levels were restored once the antibodies were removed. This study demonstrates that continuous delivery of CCL2 antibodies *in vivo* is possible but reveal limitations to use of neutralizing antibodies as a targeting agent for CCL2, with important implications for translating targeted therapies to the clinic.

Materials and Methods

Cell culture

The human breast cancer cell line MCF10CA1d (CA1d) (63,64) was kindly provided by the laboratory of Dr. Fred Miller (University of Michigan). Human cancer associated fibroblasts (hCAF-2300) were isolated from an invasive ductal carcinoma tissues, and characterized previously (69,97). Cells were cultured in Dulbecco's Modified Eagle Medium (DMEM) containing 10% fetal bovine serum (FBS), 2mM L-glutamate and 1% penicillin-streptomycin. Human monocyte cell line THP-1 monocytes were kindly provided by Dr. Katherine Fields (University of Kansas Medical Center), and were cultured in Roswell Park Memorial Institute medium (RPMI) containing 10%FBS and 1% penicillin-streptomycin. DNA genotyping was

performed to confirm cell identity. Cells were tested for mycoplasma after thawing using a luciferase based mycoplasma assay (Lozona, #LT07-703).

Transwell migration assay

Transwell migration assays were carried out in 24 well plates using Boyden Chambers with 5 micron pores (VWR Inc, #10789-236). In the upper chamber, THP-1 cells were seeded at 100,000 cells per well in 100 ul of RPMI containing 0.1% BSA. At the bottom chamber, 600 ul RPMI containing 0.1% bovine serum albumin (BSA) was pipetted into the bottom chamber, in the presence or absence of recombinant CCL2 (10, 50 or 100 ng/ml), anti-CCL2 (0.1, 1 or 10 ug/ml) or IgG isotype control. Cells were incubated at 37^{o}C for up to 5 hours. Phase contrast images were captured at 10x magnification of THP-1 cells migrated to the lower chamber using an EVOS FL auto imaging system, with 28 stitched fields per well. The total number of cells for each well was quantified using Image J software.

Animal care and Orthotopic transplantation

Athymic nu/nu female nude mice (5-6 weeks old) were obtained from Charles River and maintained at the University of Kansas Medical Center animal facilities, under Institutional Animal Care and Use Committee and Association for Assessment and Accreditation of Laboratory Animal Care International approved guidelines. Breast cancer cells and cancer associated fibroblasts were co-grafted into the mammary glands of mice as previously described (69). Briefly, 100,000 MCF10CA1d cells and 250,000 hCAF-2300 cells were co-embedded into 50 ul of rat tail collagen I (Corning Inc, #354236) and cultured overnight at 37^{o}C. The mice were anesthetized with 2% isoflurane. A “Y” shape incision was made 1 cm from the base of the tail and the skin flaps were folded back to expose the inguinal mammary glands. One plug was

inserted into each of the of the #4-5 and #9-10 inguinal mammary fat pads. The wounds were closed with wound clips and mice were rehydrated with 0.9% NaCl. Mice were monitored daily for 7 to 10 days until wound clips were removed. Mice were then monitored twice weekly over for the next 3 weeks until tumors reached 1.5 cm in size, the maximum tumor size allowable. Mice were sacrificed 4 weeks (28 days) post-transplantation.

Osmotic pump implantation in mice

Osmotic pumps were purchased from ALZET (Model 2004), with a manufacture pump rate of 0.23 ul per hour over 4 weeks. Osmotic pumps were filled with 1 mg/ml monoclonal mouse anti-human CCL2 antibody (R&D system, MAB279) or mouse IgG1 isotype control antibody (R&D system, MAB002) according to manufacturer's instructions. The filled pumps were equilibrated for 48 hours by incubation in 0.9% saline at 37ºC. On the day of implantation, mice were anesthetized with 2% isoflurane. A 1 cm incision was made in the right dorsum and one pump containing IgG or anti-CCL2 was inserted in each mouse (n=5 per group). Pumps were implanted immediately after orthotopic transplantation of tumor cells. The wound was closed by wound clips. Wound clips were removed 7-10 days after surgery.

Pump rate analysis

Osmotic pump activity was characterized according to manufacturer protocol. Briefly, the pump was filled with 0.1% w/v trypan blue (Sigma), placed in 15ml 0.9% saline solution in 50 ml canonical tube and incubated at 37ºC. At day: 2, 3, 4, 7,10, 14, 21 and 28, the trypan blue in the saline solution was measured at OD590 (98). After each measurement, the pump was transferred to a new fresh tube containing 15 ml 0.9% saline solution.

Blood collection

Mice were anesthetized using 2% isoflurane. Using a 25 gauge needle, blood samples (50 ul/mouse/time point) were collected on the day before surgery (Day 0), week 2 and week 4 post-transplantation through the submandibular vein. To prepare blood samples for ELISA, 0.5 M Ethylenediaminetetraacetic acid were added to blood samples at 10% of total volume. Blood samples were centrifuged at 2000xg for 15 minutes at 4^{o}C, and the supernatant containing plasma proteins were collected for analysis.

Preparation of tumor tissues for interstitial fluid analysis

Interstitial fluid was collected from tumor tissues using a procedures previously described (99). 40-100 mg samples from primary tumor tissues were weighed, and homogenized with a pellet pestle in PBS added at a ratio of 3 ul: 1 mg. The supernatant was collected after two rounds of centrifugation at 16,000g for 15 minutes at 4^{o}C.

Enzyme-linked immunosorbent assay (ELISA) of CCL2 antibody levels

To prepare plates for ELISA analysis of CCL2 antibodies, 96 well high-protein binding plates were incubated with 100 ul/well with 10 ng/ml recombinant human CCL2 (Peprotech, #300-04) diluted in PBS overnight. Plates were washed with PBS/0.05% Tween-20 and then wells were blocked with PBS containing 10% BSA for 2 hours. Wells were coated with CCL2 antibodies as standards, which were diluted to final concentrations of: 10 ug/ml, 1 ug/ml, 500 ng/ml, 100 ng/ml, 10 ng/ml and 1 ng/ml in PBS/2% BSA. As a negative control, wells were coated with IgG1 isotype control at a final concentration of 1 ug/ml. Wells were incubated with 100 ul of plasma or tumor interstitial fluid samples diluted 1:100 in PBS/2% BSA. Samples were incubated for 2 hours at room temperature, washed with PBS/0.05% Tween-20 and then incubated with 0.5 ug/ml biotinylated goat anti-mouse detection antibody (Vector Laboratories,

#VA-9200) for 2 hours. Samples were then incubated with streptavidin conjugated to horse radish peroxidase (Vector Laboratories, #900-K31) for 30 minutes. Reactions were catalyzed with TMB substrate (Thermo Scientific, #34028), stopped with 2N HCl, and read at OD450. CCL2 antibody levels were normalized to wells incubated with 2% BSA non-specific binding control.

CCL2 ELISA

Plasma samples were diluted 1:4 in phosphate buffered saline (PBS) containing 0.1%BSA and 0.05% tween-20. Tumor interstitial fluid samples were diluted 1:20. Samples were assayed using mouse CCL2 ELISA kit (Peprotech, #900-K59) or human CCL2 ELISA kit (Peprotech, # 900-K31) according to manufacturer protocol.

To generate conditioned medium, MCF10CA1d or hCAF-2300 cells were seeded at 10,000 cells per well, in triplicate in a 24 well plate. Cells were then incubated with 500 ul of DMEM/10% FBS in the presence or absence of control IgG or CCL2 antibody (1 or 10 ug/ml) for 24 hours. The medium containing IgG or anti-CCL2 were collected and assayed for CCL2 levels by ELISA (Peprotech, #900-K31). To analyze for CCL2 levels post-antibody treatment, the cells were washed once with PBS and re-incubated in serum free medium without IgG or antibody treatment for an additional 24 hours. The samples were collected and assayed for CCL2 levels by ELISA.

Tissue embedding and histology

Tumor samples were fixed in 10% neutral buffed formalin overnight, and then dehydrated in a series of: 70%, 90% and 100% ethanol for 30 minutes each. Tissues were further dehydrated in isopropanol for 1 hour, 50:50 isopropanol: wax at 60^{o}C for 1 hour, and in wax

overnight at 60^{o}C. Tissues were mounted on cassettes and sectioned into 5 micron thin slices onto glass slides. For H&E stain, slides were dewaxed in two changes of xylenes at 5 minutes each and rehydrated in a series of ethanol (100%, 90%, 70%, 50%) at 3 minutes each. Slides were stained with Mayer's hematoxylin for 2 minutes and eosin for 1.5 minutes, dehydrated and then mounted with Cytoseal under glass coverslips.

Co-Immunofluorescent staining and immunohistochemistry

For co-immunofluorescent staining, dewaxed slides were subject to antigen retrieval using 10 mM sodium citrate buffer pH 6.0 for 20 minutes in pressure cooker under low pressure setting for antigen retrieval. Samples were blocked for endogenous mouse IgG using the M.O.M kit (Vector Lab., #BMK-2202), and then incubated with mouse anti-cytokeratin 5 (CK5) at a 1:50 dilution (Thermo Fisher Scientific, #MA5-12596) and with rat anti-F4/80 (Abcam, #ab6640) at a 1:100 dilution in PBS 3%FBS. After overnight staining at 4^{o}C, slides were washed three times in PBS containing 0.05% Tween-20, incubated with Alexa Fluor 568 goat anti-rat dilution (Invitrogen, #A11077) and Alexa Fluor 488 goat anti-mouse at a 1:100 dilution (Invitrogen, #A11001) for 2 hours. Slides were counter-stained with 4',6-diamidino-2-phenylindole (DAPI) at a 1:500 dilution, and then mounted in PBS containing 50% glycerol. Eight high power images for each slide were acquired using the FL Auto EVOS imaging system at 20x magnification. For image analysis, F4/80 positive cells per image were quantified using Image J particles analysis with threshold set above background. For compartmental analysis, the stroma at the tumor periphery was defined as the area bordering the tumor that was negative for CK5 staining. The tumor core was defined as areas positive for CK5 expression. F4/80 cells in each of the compartments were quantified and normalized to area size.

For immunohistochemistry staining, dewaxed slides were subject to antigen retrieval in treated in sodium citrate buffer, and blocked for endogenous peroxidase activity in deionized water (80%): methanol (10%): hydrogen peroxide (10%) for 10 minutes. After blocking for 1 hour in PBS/5% FBS, slides were incubated with rabbit anti-von Willebrand Factor 8 (vWF8) at a 1:100 dilution (Chemicon International, #AB7356) overnight. Slides were washed in PBS 3 times for 10 minutes each, incubated with biotinylated anti-rabbit secondary antibody at a 1:500 dilution and then incubated with peroxidase conjugated to streptavidin (Vector Lab., #PK-6100) for 30 minutes. Protein expression was detected using 3,3'-diaminobenzidine (*DAB)* substrate (Vector Lab., #SK-4100) . Slides were counter-stained with Mayer's hematoxylin for 2 minutes, dehydrated and mounted with Cytoseal (Thermo Fisher, #348976). Eight images per samples were acquired under 10x magnification using the FL Auto EVOS imaging system. Expression was quantified by Image J software using procedures previously described (61).

Lung whole mount staining

Lung metastasis was analyzed by whole mount staining as described previously (38). Briefly, lung tissues were fixed in neutral buffered formalin overnight at 4^{o}C, and dehydrated on 70%, 95% and 100% ethanol for 1 hour each. Lung tissues were cleared in xylene overnight, rehydrated through a series of 100%, 95% and 70% ethanol, and counter-stained with hematoxylin for 5 minutes. Tissues were de-stained in 1% HCl and incubated with tap water for 10 to 20 minutes. Micro-metastases were counted using a Motic AE31 inverted microscope at 20x magnification.

Statistical analysis

Statistical analysis was performed using Graphpad software. Two tailed Student T test was used for two group comparisons. One Way ANOVA with Bonferroni post-hoc comparison was used for multiple group comparisons. Statistical significance was determined by $p<0.05$. *$p<0.05$, **$p<0.01$, ***$p<0.001$, ns=not significant ($p>0.05$).

Results

Neutralizing antibodies specifically block cell migration induced by human recombinant CCL2

Multiple studies have utilized murine CCL2 neutralizing antibodies to demonstrate that targeting CCL2 activity inhibits mammary tumor progression (36,38,91,92). Murine CCL2 exhibits a 70% protein homology to human CCL2, indicating high degree of conservation (27). The difference in sequence homology could affect receptor binding and activity. While the goal is to develop clinically active neutralizing antibodies for patients, i.e. antibodies that target human tissues, there have been few studies characterizing the effectiveness of human specific CCL2 neutralizing antibodies on cancer progression in mouse models, relative to endogenous and exogenous CCL2 levels. To address this issue, we obtained human specific CCL2 neutralizing antibodies from a commercial source (R&D systems) and first analyzed the specificity of neutralization of murine and human CCL2. THP-1 human monocytes were cultured *in vitro,* stimulated with increasing dosages of murine or human CCL2 and analyzed for transwell migration. Both murine and human CCL2 were found to increase migration of THP-1 cells at 10 ng/ml, indicating cross reactivity between mouse CCL2 and human CCR receptors. Chemotaxis decreased at 50 and 100 ng/ml, possibly reflecting desensitization of chemokine receptors at excess ligand concentrations. Human CCL2 induced migration with a wider range of concentration compared to murine CCL2 (Figure 21A), indicating higher sensitivity of human

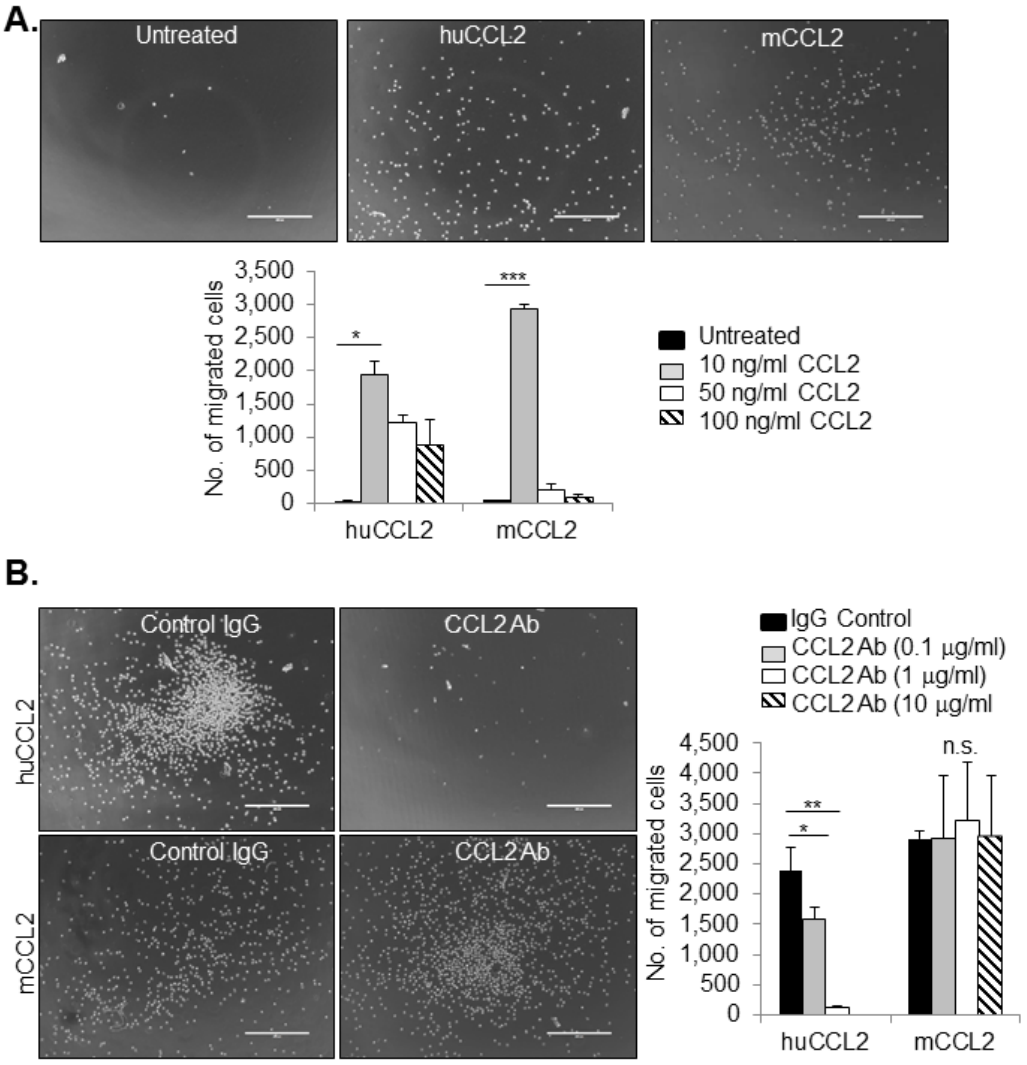

Figure 21. Neutralizing antibodies inhibit THP1 cell migration induced by recombinant human CCL2 protein. A. THP1 cells were stimulated with increasing concentrations of human (hCCL2) or mouse (mCCL2) recombinant CCL2 protein and analyzed for transwell migration after 2 hours. Representative images of cells migrated into lower chamber are shown. **B.** THP1 cells were stimulated with 10 ng/ml hCCL2 or mCCL2 in the presence or absence of increasing doses of CCL2 neutralizing antibodies or control IgG, and analyzed for transwell migration. Representative images of cells treated with CCL2 and 1 ug/ml control IgG or CCL2 neutralizing antibodies. Statistical analysis was performed using One Way ANOVA test, with Bonferroni post-hoc comparison. Statistical significance was determined by *$p<0.05$, ***$p<0.01$, and n.s=not significant. Mean $\pm$ SEM are shown. Scale bar= 400 microns.

cells to human CCL2, compared to murine CCL2. Treatment of THP-1 cells with 1 ug/ml CCL2 neutralizing antibodies inhibited migration induced by human CCL2 but not mouse CCL2 (Figure 21B), indicating that CCL2 neutralizing antibodies specifically block human CCL2.

CCL2 neutralizing antibodies delivered by osmotic pumps penetrate primary MCF10CA1d breast tumor xenografts

As the majority of studies involving CCL2 antibody delivery *in vivo* involved interval injections, we asked whether continuous delivery of CCL2 antibodies would increase therapeutic effectiveness. Osmotic pump delivery of CCL2 antibodies could stabilize drug levels and avoiding dosage fluctuations caused by interval drug injections (100-102). We obtained mini-osmotic pumps (Alzet) capable of continuous drug delivery for 4 weeks in tumor bearing mice. To characterize their long-term function, osmotic pumps were filled with trypan blue dye, placed in 50 ml conical tube containing sterile saline solution in cell culture incubator (Figure 22A). Pump activity was monitored over 4 weeks through sampling of saline and absorbance

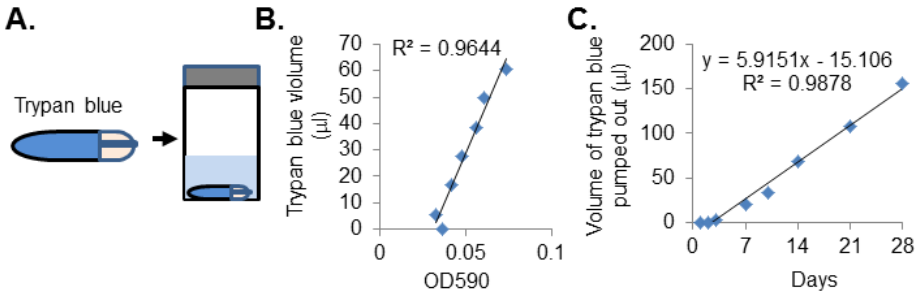

Figure 22. Characterization of osmotic pump rate *in vitro*. A. Diagram of how osmotic pump activity was tested *in vitro* using trypan blue dye. Osmotic pumps were filled with trypan blue dye and placed in 50 ml conical tubes containing saline solution. Activity was determined by measuring the optical density (OD590) of trypan blue in saline over 4 weeks**. B.** The levels of trypan blue effluxed into saline solution was plotted against OD590. **C.** Volume of trypan blue pumped out was plotted over time.

measurement of trypan blue (Figure 22B). After 3 days of incubation, the pump rate was found to be stable over 4 weeks, with an average rate of 5.9 ul per day (Figure 22C). This rate was close to the expected pump rate of 5.52 ul per day.

In previous studies, we had shown that breast stromal fibroblasts and cancer cells expressed high levels of CCL2, and CCL2 expression in basal-like breast cancers correlated with poor patient prognosis in basal-like breast cancers (38,69). Therefore, we analyzed the

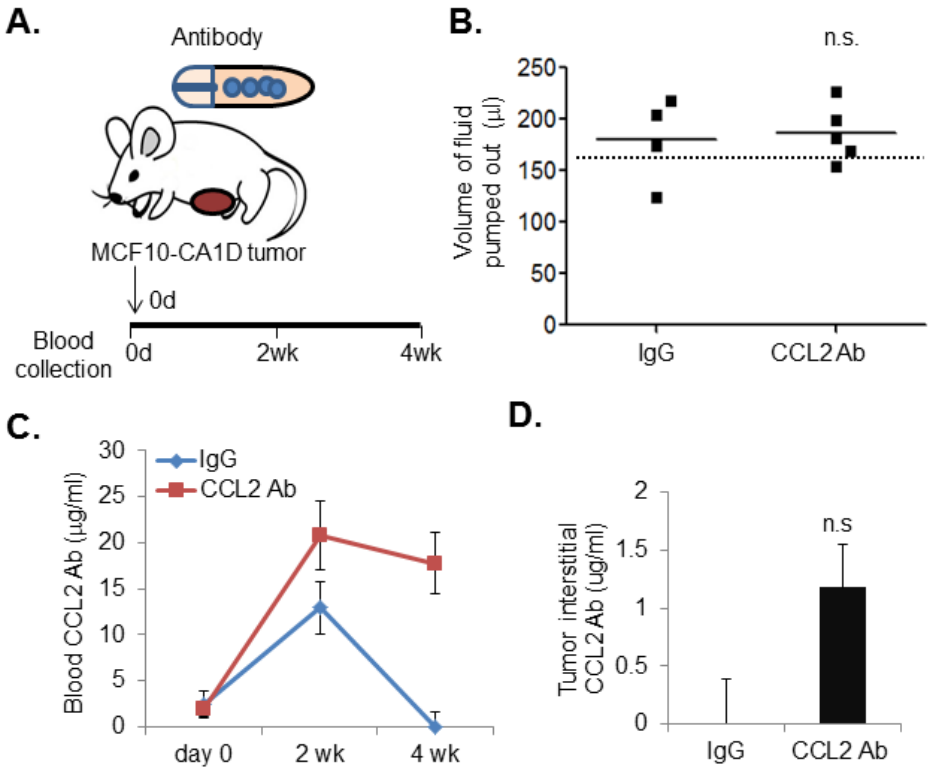

Figure 23. Osmotic pump delivery of CCL2 neutralizing antibodies in the MCF10CA1d breast tumor xenograft model. A. Diagram of pump implantation. Mice orthotopically transplanted with fibroblasts and MCF10CA1d breast cancer cells were implanted with osmotic pumps containing CCL2 neutralizing antibodies or isotype control IgG1 for 4 weeks (N=5/group). **B.** The volume of fluid pumped out was determined by subtracting the residual volume from initial volume after 4 weeks *in vivo* implantation. Dotted line indicates the expected volume pumped out (155 ul). **C.** Measurement CCL2 antibody concentration in blood by ELISA. **D.** ELISA analysis of tumor interstitial CCL2 antibody concentration in harvested tumor samples after 4 weeks of implantation. Statistical analysis was performed using Two Tailed Student T test. Statistical significance was determined by $p<0.05$. n.s=not significant. Mean $\pm$ SEM are shown.

effectiveness of osmotic pump delivery of CCL2 neutralizing antibodies on tumor growth and progression using the MCF10CA1d model of basal-like breast cancer (63,64). MCF10CA1d breast cancer cells were co-grafted with human breast cancer associated fibroblasts in the mammary glands of nude mice. Osmotic pumps with an expected delivery of rate of 0.3 mg/kg/day will filled with 1 mg/ml control IgG or anti-CCL2, and then implanted subcutaneously immediately after cellular transplantation (Figure 23A).

Mice were treated for 4 weeks until the control tumor reached 1.5 cm in size, the maximum allowable tumor size. We determined the efficiency of osmotic pump activity by measuring the volume of IgG and anti-CCL2 delivered. The residual volumes in the pumps were subtracted from the starting volume of 234±2 ul. In the anti-CCL2 treated group, osmotic pumps delivered 186±13 ul compared to 180±20 ul of control IgG delivered, indicating consistent pump activity between groups (Figure 23B). To determine the levels of anti-CCL2 in blood circulation, anti-CCL2 levels were measured by ELISA from blood sampled at day 0, the day before surgery,

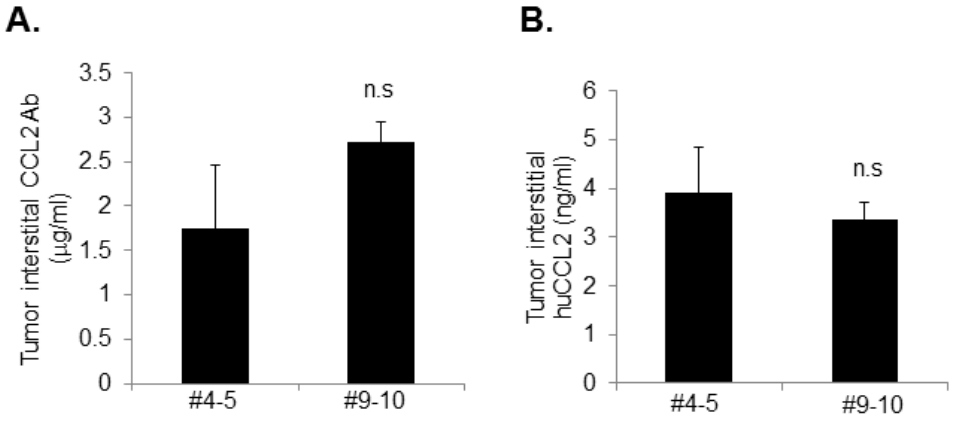

Figure 24. Location of breast tumor xenografts is not a factor in CCL2 antibody uptake or CCL2 levels. MCF10CA1D breast tumors grafted into the #4-5 and #9-10 inguinal mammary glands. Tumor tissues from anti-CCL2 treated animals were analyzed for levels of **A.** CCL2 antibodies and **B.** human CCL2 by ELISA. Statistical analysis was performed using Two Tailed Student T test. Statistical significance was determined by $p<0.05$. n.s=not significant.

2 weeks and 4 weeks post-surgery. Anti-CCL2 levels were undetectable before implantation, but 21 ug/ml were detected at week 2, and 18 ug/ml at week 4, indicating systemic delivery over time (Figure 23C). To determine whether anti-CCL2 penetrated the primary tumor, antibody levels in the tumor interstitial fluid were measured by ELISA. Approximately 1.1 ug/ml of anti-CCL2 were detected within the tumor, relative to control IgG treated mice (Figure 23D). Placement of the tumor in either the #4-5 or #9-10 inguinal mammary gland did not affect antibody penetration or CCL2 levels (Figure 24). In summary, these data indicate osmotic pump delivery of CCL2 neutralizing antibodies lead to stable antibody levels and penetrate tumor tissues.

CCL2 neutralizing antibodies do not significantly affect progression of MCF10CA1d breast tumor xenografts

To determine the effect of anti-CCL2 on tumor growth and invasion, mice were measured for tumor growth on a weekly basis for up to 4 weeks. Compared to control IgG treated mice, anti-CCL2 treated tumors did not show significant changes in tumor growth over time or tumor mass 4 weeks post-treatment (Figure 25A-B). By H&E stain, primary tumors from IgG and anti-CCL2 treated mice appeared to be high grade tumors, exhibiting extensive necrosis and tumor invasion into the fat pad (Figure 25C). By whole mount staining and H&E stain of lung tissues, there were no significant differences in lung metastasis between IgG and anti-CCL2 treated mice (Figure 25D-E). We examined for possible changes in tumor angiogenesis and macrophage recruitment by immunostaining of primary tumors. Sections were co-immunofluorescent stained for antibodies to F4/80, a macrophage marker, with human specific CK5 to distinguish MCF10CA1d breast cancer cells. Macrophages were primarily detected at the edge of the tumor, with few macrophages within the tumor tissue (Figure 26A).

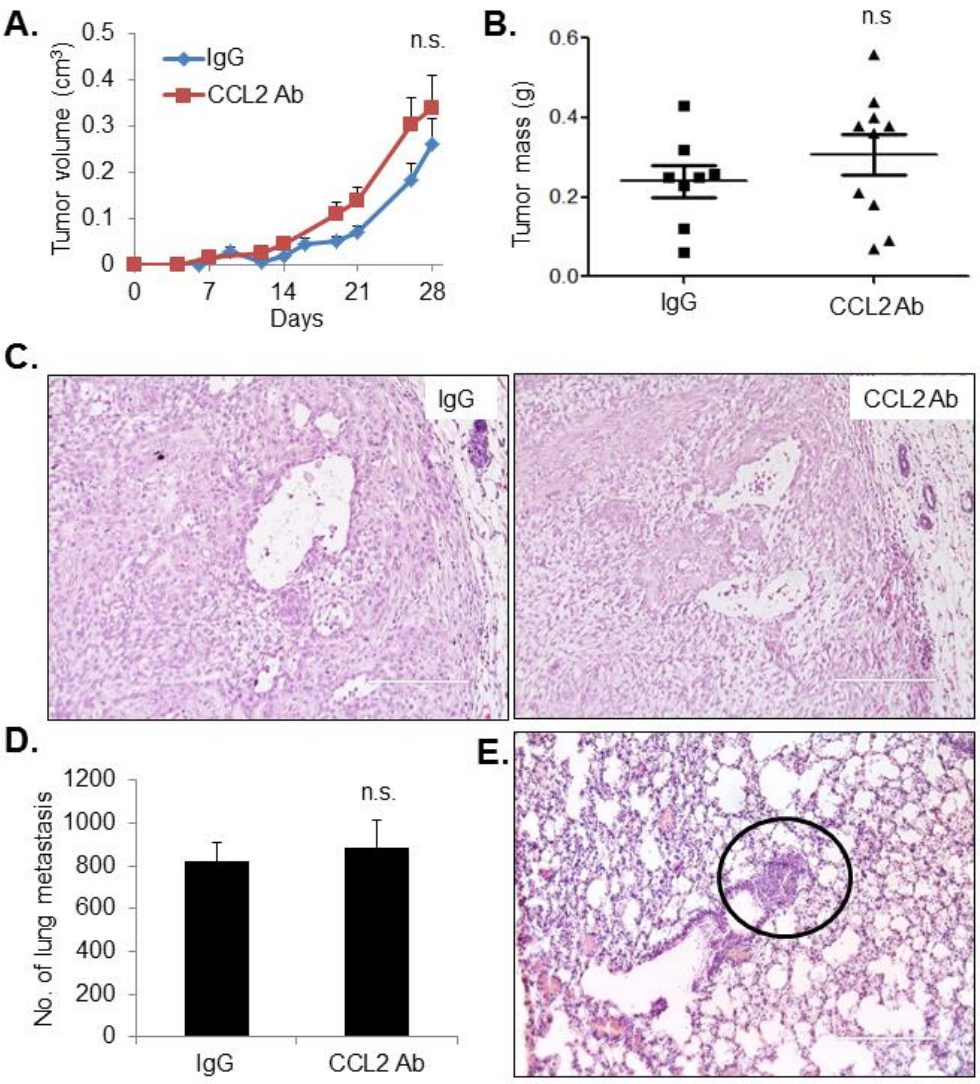

Figure 25. CCL2 neutralizing antibodies do not significantly affect progression of MCF10A1D breast tumor xenografts. IgG control or CCL2 antibody treated mice were analyzed for: **A.** tumor growth over time, **B.** tumor mass at 28 days, **C.** malignancy as assessed by H&E stain of primary tumor tissues and **D.** lung metastasis, which was assessed by lung whole mount staining. **E.** Lung metastasis was validated by H&E stain. Representative metastatic lesion is circled. Statistical analysis was performed using Two Tailed Student T test. Statistical significance was determined by $p<0.05$. n.s=not significant. Mean±SEM are shown. Scale bar= 200 microns.

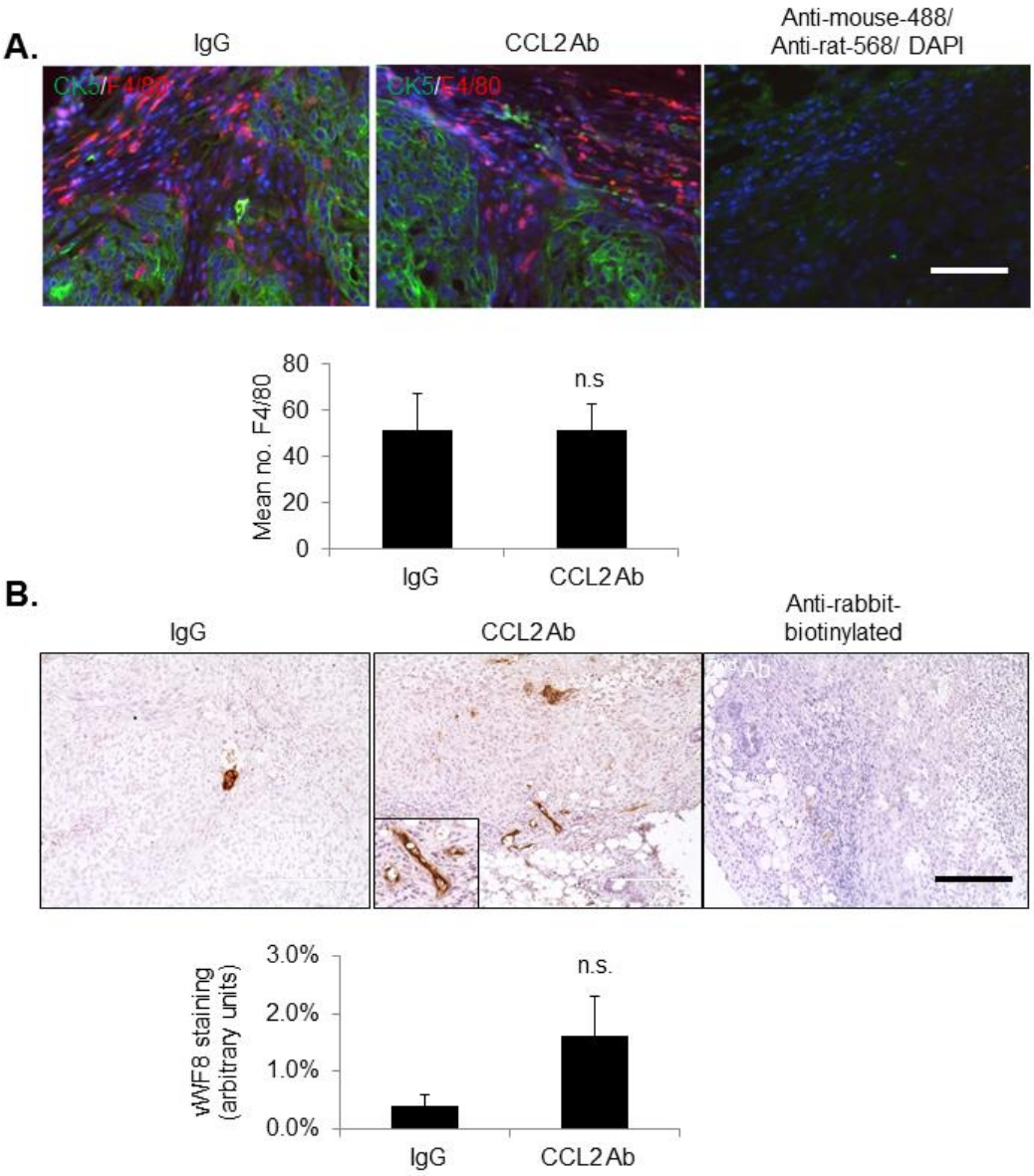

Figure 26. Delivery of CCL2 neutralizing antibodies do not significantly affect macrophage infiltration or tumor angiogenesis. A. Primary tumor tissues were co-immunofluorescent stained for Cytokeratin 5 (CK5, green) and F4/80 (red). Secondary antibody controls overlayed with DAPI are shown. **B.** Primary tumor tissues were immunostained for von Willebrand Factor 8 (vWF8). Magnified insert shows positive staining. Staining was quantified by Image J. Statistical analysis was performed using Two Tailed Student T test. Statistical significance was determined by $p<0.05$. n.s=not significant. Mean$\pm$SEM are shown. Scale bar=200 microns.

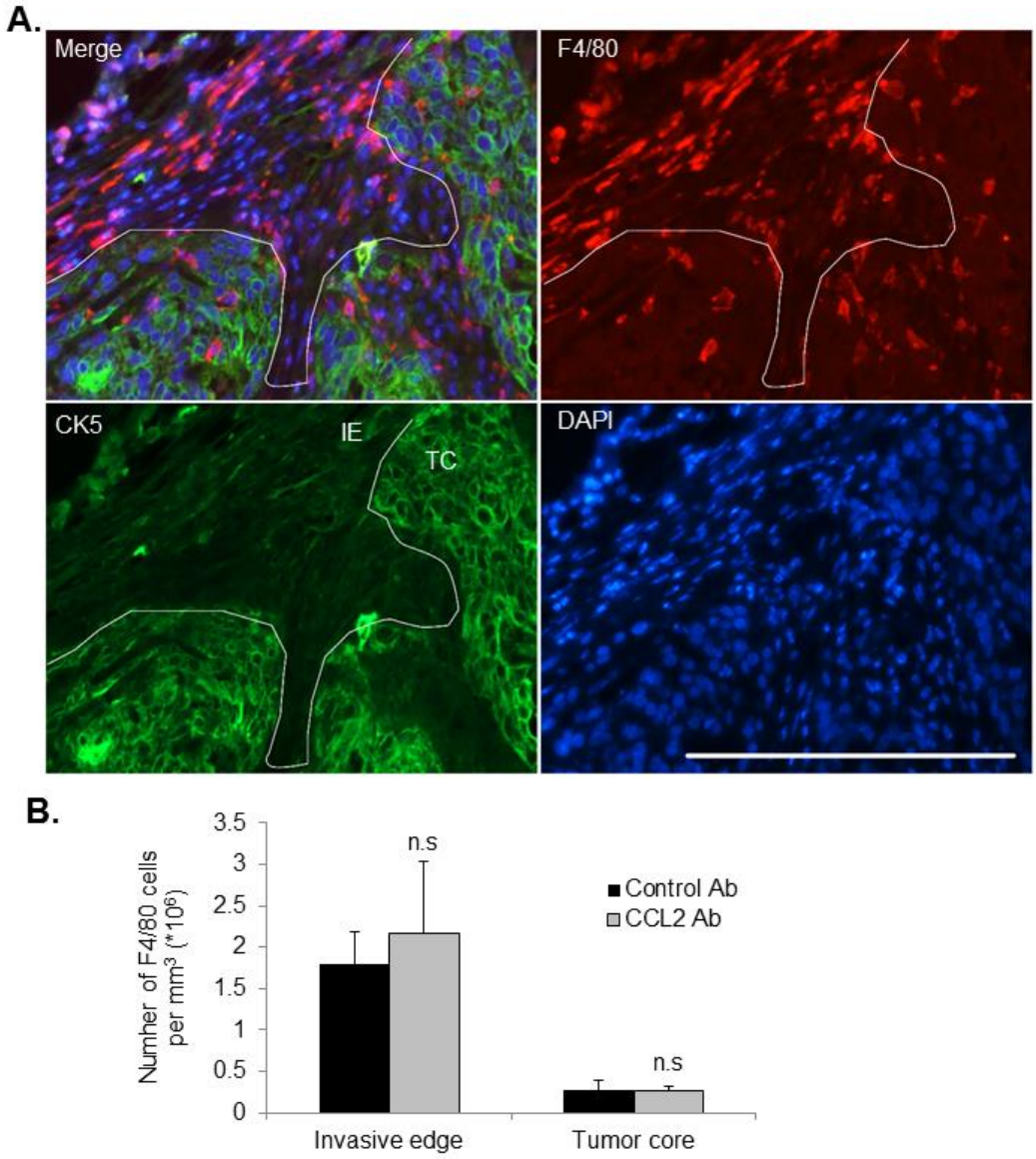

Figure 27. Quantification of F4/80 macrophage infiltration in MCF10CA1D primary tumor tissues. A. Primary breast tumor xenografts were co-immunofluorescent stained for Cytokeratin 5 (CK5) and F4/80. F4/80+ cells were localized at the invasive edge (IE) and within the tumor core (TC). Representative image is shown. Scale bar=200 microns. **B.** F4/80 cells were quantified at the invasive edge and tumor core per mm^3 using Image J software. Statistical analysis was performed using Two Tailed Student T test. Statistical significance was determined by $p<0.05$. n.s=not significant. Mean±SEM are shown.

There were no differences in total levels of macrophages regardless of localization, between IgG and anti-CCL2 treated mice (Figure 26A and 27). By vWF8 staining, there were no significant differences in tumor angiogenesis between IgG and anti-CCL2 treated mice (Figure 26B).

CCL2 neutralizing antibodies increase CCL2 levels in mice bearing MCF10CA1d breast tumor xenografts

Given the lack of therapeutic efficacy with neutralizing antibodies, we examined for CCL2 expression levels in tumor bearing mice. CCL2 levels were measured from blood samples and tumor interstitial fluid by ELISA. Mice treated with CCL2 antibodies showed significantly higher levels of human CCL2 in blood samples with a mean concentration of 603 ng/ml, compared to 346 ng/ml in IgG treated mice (Figure 28A). Anti-CCL2 treatment also increased expression of human CCL2 in the tumor interstitial fluid with a mean concentration of 3.5 ng/ml compared to 1.2 ng/ml in the control IgG group (Figure 28B). Furthermore, blood samples from

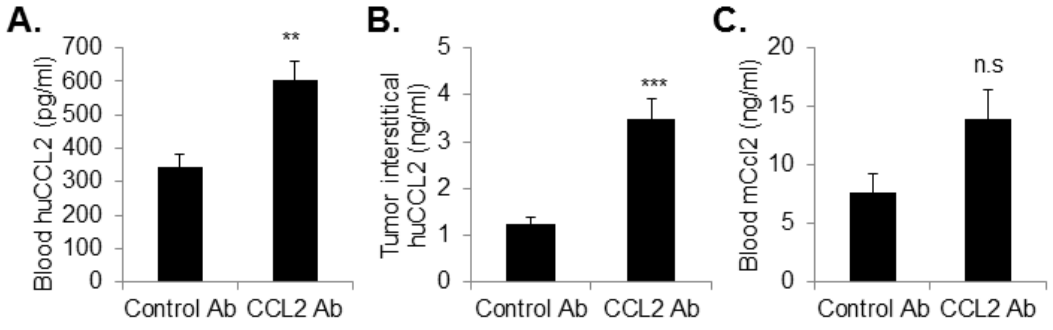

Figure 28. Delivery of CCL2 neutralizing antibodies to tumor bearing mice increases the levels of human CCL2 in blood and in primary tumor tissues. Tumor bearing mice were treated with control IgG or CCL2 neutralizing antibodies. 4 weeks post-transplantation, ELISAs were performed to measure the levels of: **A**. human CCL2 in blood, **B** human CCL2 in tumor interstitial fluid, and **C.** murine CCL2 in blood. Statistical analysis was performed using Two Tailed Student T test. Statistical significance was determined by $p<0.05$. **$p<0.01$, ***$p<0.001$, n.s=not significant.

anti-CCL2 treated mice showed a modest but not statistically significant increase in murine CCL2 expression (Figure 28C).

We addressed the possibility that anti-CCL2 treatment led to compensatory upregulation of CCL2 in breast cancer cells and fibroblasts, thereby increasing the levels found in circulation and in tumor tissues. MCF10CA1d breast cancer cells and fibroblasts were cultured in the presence or absence of anti-CCL2 or control IgG and measured for CCL2 secretion by ELISA. CCL2 expression in fibroblasts was twice as high compared to MCA10CA1D cancer cells. Increasing the concentration of anti-CCL2 to10 ug/ml reduced the levels of CCL2 in fibroblasts

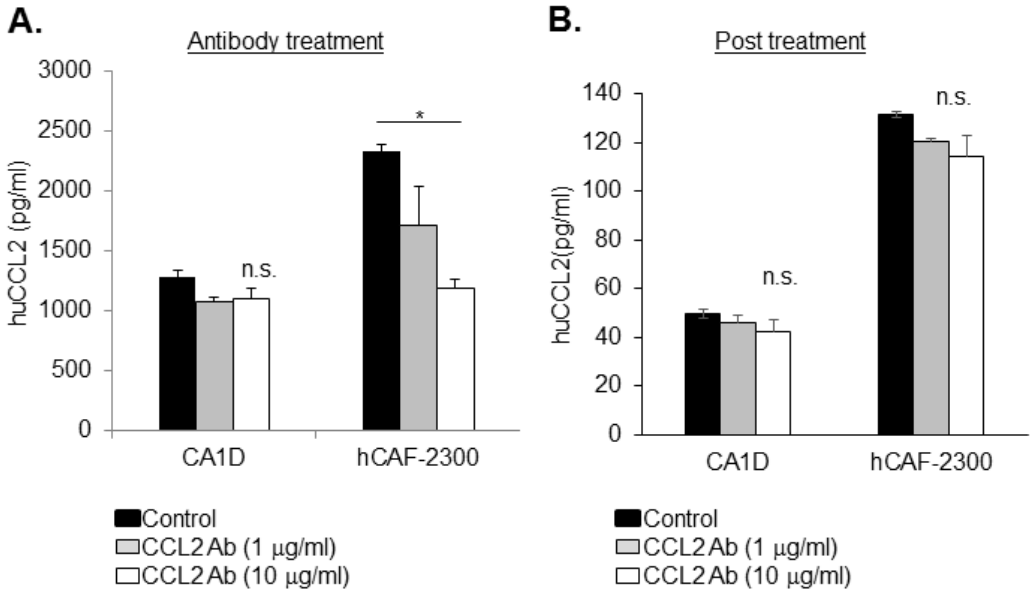

Figure 29. CCL2 levels in cultured cells are dependent on the presence of neutralizing antibodies. Cultured MCF10CA1d breast cancer cells or hCAF-2300 fibroblasts were treated with control IgG or CCL2 neutralizing antibodies for 24 hours. **A.** Medium was analyzed for CCL2 expression by ELISA. **B.** Cells were washed to remove antibodies and incubated in serum free condition medium for an additional 24 hours. CCL2 levels in conditioned medium were analyzed by ELISA. Statistical analysis was performed using One Way ANOVA test with Bonferroni post-hoc comparison. Statistical significance was determined by $p<0.05$.*$p<0.05$, n.s=not significant.

from 2300 pg/ml to 1000 pg/ml, and resulted in a small but not statistically significant decrease in CCL2 levels in breast cancer cells to 1000 pg/ml (Figure 29A). The presence of neutralizing antibodies inhibited detection of recombinant CCL2, indicating that the ELISAs detected free CCL2 secreted from cells, but not CCL2 bound to neutralizing antibodies. To further determine how the presence of anti-CCL2 affected CCL2 levels in cultured cells, the antibody containing medium was removed, and cells were incubated in fresh medium for 24 hours to generate conditioned medium. When the conditioned medium was examined for CCL2 by ELISA, there were no significant differences in CCL2 levels in fibroblasts or breast cancer cells compared to IgG treatment (Figure 29B). In summary, these data indicate that neutralizing antibodies are capable of binding and sequestering free CCL2, but a continuous presence of CCL2 antibodies is required to maintain this sequestration.

Discussion

CCL2 is a therapeutic target of interest for the treatment of cancer, and the effectiveness of CCL2 targeting alone, or in combination with other agents, is currently being determined in multiple clinical trials (93-95). However, human specific CCL2 antibodies have not been well characterized in pre-clinical studies. Furthermore, the primary method for targeting CCL2 has involved bolus injections of neutralizing antibodies. In these studies, we tested whether continuous delivery of human specific CCL2 neutralizing antibodies in animals bearing breast tumor xenografts, would be an effective therapeutic strategy. Our studies showed that stable delivery of CCL2 neutralizing antibodies over 4 weeks results in little therapeutic efficacy and increased CCL2 levels over time.

Previous studies have demonstrated that drugs delivered via osmotic pumps enhance therapeutic efficacy compared to bolus injections (101,103-105). For example, osmotic pump

delivery of carboplatin to mouse models of ovarian cancer inhibited tumor growth more effectively than intraperitoneal injection and resulted in fewer toxic side effects (105). In another study, osmotic pump delivery of Interleukin13 drug conjugates significantly slowed tumor growth and increased survival in animals with pancreatic cancer (104). These therapeutic effects are in part due to stable drug delivery modulated by osmotic pumps (101). In previous studies, we found that interval injections of CCL2 antibodies in mice resulted in a 1/3 decline of antibody levels within 24 hours (38). Here, we found that osmotic pump delivery of CCL2 neutralizing antibodies resulted in stable levels of antibody approximately 18 to 20 ug/ml in circulation over several weeks, while 10 ug/ml was shown to be inhibitory *in vitro*. However, osmotic pump delivery of CCL2 neutralizing antibodies did not significantly affect primary tumor growth or invasiveness. One possible factor limiting the effectiveness of the neutralizing antibody is tissue penetration. Approximately 1.1 ug/ml of antibodies were detected in tumor tissues, compared to 18-20 ug/ml in blood circulation. These data indicate that significantly lower levels of antibodies penetrated tumor tissues. Difficulties in drug penetration have been reported in animal models and in patients, and have been attributed to a number of factors including: leaky vasculature that does not extend into the tumor, tumor interstitial pressure, and a basement membrane that provides a barrier to drug entry (106). It would be of interest in the future to further investigate the mechanisms preventing antibody uptake, in order to enhance therapeutic efficacy.

In order to test the effectiveness of human specific CCL2 therapeutic antibodies in pre-clinical models involving human and mouse cells, it was necessary to determine how the antibody would cross react with other species. Previous studies have shown that murine specific CCL2 antibodies inhibited tumor growth and metastasis transplanted with murine mammary or prostate carcinoma cells (38,107). One study showed that murine specific CCL2 neutralizing

antibodies inhibited the growth of MDA-MB-231 breast tumor xenografts and macrophage recruitment in mice (35). The limited effectiveness of human specific CCL2 antibodies observed in our studies could be due in part to binding specificity. Human and mouse CCL2 share a 70% homology in amino acids (27) enabling human cells to respond to recombinant protein from both species. While both murine and human CCL2 stimulated human cells *in vitro*, the neutralizing antibodies inhibited human but not murine CCL2 induced cell migration. Antibody treatment of tumor bearing mice increased the levels of human CCL2, and also murine CCL2 in circulation, although the increase in murine CCL2 was not statistically significant. CCL2 is expressed by a variety of murine cell types found within the primary breast tumor, including endothelial cells and bone marrow derived cells (27). It is possible that the combined increase in human and murine CCL2 abrogated the effects of CCL2 antibody neutralization.

The CCL2 antibody concentrations detected in blood circulation and in tumor tissues were associated with increased human CCL2 levels and slight increase in murine CCL2 levels, indicating a physiological effect of CCL2 antibody delivery. These phenotypes are consistent with previous studies characterizing the effects of antibody targeting of ligands. Delivery of the CCL2 neutralizing antibody, CNTO0800 resulted in elevated CCL2 levels in patients during clinical trials (94,95). Mathematical modeling studies indicated that antibody binding prevented clearance of CCL2, and that a rapid disassociation of antibodies from the ligand contributed to the increased levels of free CCL2 (96). In our studies we found a 2-3 fold increase in CCL2 levels with antibody treatment in animals. Treatment of cultured cells with CCL2 antibodies reduced the levels of free CCL2 in fibroblasts and slightly decreased levels in breast cancer cells. However, 1000 pg/ml of CCL2 was still detectable even with 10 ug/ml of antibody present. This may potentially be due to the equilibrium between bound and unbound of CCL2. After removal

of antibodies, we found the CCL2 expression levels in cultured cells were similar to control treatment, ruling out of compensatory CCL2 production. Thus, the increased level of CCL2 observed *in vivo* could be potentially due to the enhanced stability of CCL2 by antibody binding, and a constant equilibrium between binding and dissociation of CCL2-antibody complexes. It would be of interest in the future to conduct studies on the pharmacokinetics of CCL2 antibodies in animal models of breast cancer.

In these studies, we delivered CCL2 neutralizing antibodies at a dosage of approximately 0.3 mg/kg/day. This dosage was based on previous studies reporting effectiveness of CCL2 neutralizing antibodies when delivered at dosages ranging from 0.4 mg/kg/day to 2.9 mg/kg/day (36,38,87). The slightly lower dosage was due to limitations in pump rate from an osmotic pump capable of drug delivery over 4 weeks. It is possible that a higher concentration of CCL2 antibodies might induce an anti-cancer effect, or might further elevate CCL2 levels, contributing to a rebound effect that promotes tumor progression. These studies would require a higher pump rate with shorter pump time, requiring more frequent pump replacement in the MCF10CA1d tumor model, increasing physical stress to the animals. From a clinical perspective, this would require long-term continuous delivery of high dosages of anti-CCL2 to prevent a possible rebound effect caused by decreased CCL2 antibody levels.

Conclusions

In summary, our studies report limitations in the use of human specific CCL2 neutralizing antibodies for the treatment of breast cancer in mouse models. Previous studies have shown that knockdown of CCL2 in breast tumor xenografts effectively inhibited tumor growth and metastasis, and significantly reduced CCL2 levels (54,69). These studies suggest that CCL2 remains viable therapeutic target in anti-cancer treatment. Strategies to inhibit CCL2

expression, rather than CCL2 activity only, may be a more effective approach to target CCL2. Alternatively, CCR2 inhibitors, which are in the pre-clinical pipeline (90) may overcome limitations caused by CCL2 targeting. Furthermore, the development of more physiologically relevant pre-clinical models may in turn improve the design of anti-cancer drugs.

Chapter V: Conclusion and Discussion

Overall conclusion

In this thesis study, we found that the chemokine CCL2/CCR2 signaling played an important role in mediating cancer associated fibroblasts and cancer cells interaction in basal-like breast cancer progression (Figure 30). We started by analysis the expression of CCL2 and its receptor CCR2 in breast cancer samples. We found that the chemokine CCL2 was highly expressed in invasive ductal carcinoma, and positively correlated with expression of fibroblasts maker Fsp1. High stromal CCL2 expression associated with reduced recurrence free survival in basal-like subtype. Further data mining in the breast cancer TCGA and METABRIC datasets revealed that CCL2 and CCR2 expressed highest in the basal-like subtypes, and were positively correlated. Those studies indicate the CCL2/CCR2 signaling potentially function as an important signaling pathway in the progression of basal-like breast cancer.

We confirmed that CAFs isolated from primary human and mouse breast cancer samples generally expressed high level of CCL2. CAFs promoted basal-like breast cancer cell line MCF10A-CA1D xenograft growth in the fibroblast-cancer cell co-graft model. Depletion of CCL2 expression from CAFs significantly reduced their cancer promotion ability. In contrast, CCL2 derived from cancer cells, which was expressed in much lower level, did not significantly contribute. Those studies indicate that CAFs are a major cellular source of CCL2 in the breast cancer model.

To determine the mechanism of CCL2 in tumor promotion, we found that fibroblasts conditional medium or recombinant CCL2 promoted breast cancer cell growth *in vitro*. Mutation of the CCR2 receptor in CA1D cancer cell significantly reduced cancer cells growth *in vitro* and *in vivo* in response to CCL2 stimulation. We further identified that the PKC and SRC pathways functioned downstream of CCL2/CCR2 signaling and contributed to CCL2 mediated growth

promotion. Those results provide a functional evidence of the importance of direct CCL2 signaling to basal-like breast cancer cells.

We aimed to test the therapeutic effect of blocking CCL2 in breast cancer mouse model through continuous delivery of CCL2 neutralizing antibody using the osmotic pump. Despite the steady delivery of the antibody, CCL2 blocking did not significantly affect tumor progression. Examination of CCL2 level in blood and tumor site revealed that CCL2 blocking significantly induced higher free CCL2 level, which may contribute to lack of efficacy. This study pointed out a potential unexpected effect in targeting CCL2 signaling by blocking antibody, consistent with earlier observations in human patients (94,95). This failed pre-clinical trial does not devaluate the CCl2 signaling as potential therapeutic targets, rather it points out optimized targeting strategies are needed. Alternative CCL2 signaling targeting approaches, such as by CCR2 inhibitor, may provide better therapeutic efficacy.

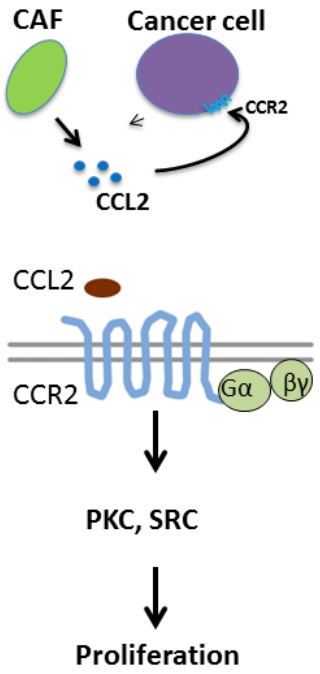

Figure 30. Overall conclusions and models.

In summary, our studies reveal that cancer associated fibroblasts are an important cellular source of CCL2 in breast cancer. The CCL2/CCR2 signaling promotes the basal-like breast cancer promotion, through directly signaling to the CCR2 receptor in cancer cells (Figure 30). Thus, the CCL2/CCR2 signaling can serve as potential therapeutic targets in basal-like breast cancer.

Significance and Innovation

Basal-like breast cancer represents about 12% of total invasive breast cancer, with estimated 30, 325 cases in 2017 in U.S. women (1). Basal-like breast cancer is the most aggressive breast cancer subtype with the worst patient outcome (1). This is mainly due to lack of targeted therapies, compared to other breast cancer subtypes. Conventional prognostic indicators such as grade and stage do not accurately predict patient prognosis for basal-like breast cancer subtypes (50,51), indicating the need to identify prognostic factors unique to each subtype. In these studies, we have identified that stromal CCL2 is an independent prognosis factor. In both univariable and multivariable analysis, stromal CCL2 significantly associated with recurrence free survival, with high hazard ratio. In comparison, other traditional prognosis factors, including TNM stage, grade and treatment options, did not significantly associated with patient outcome (Table 8). Thus, we have identified an additional critical prognosis factor that can be potentially used for basal-like breast cancer subtype. In addition, we report in these studies that the chemokine CCL2 and its receptor CCR2 express highest in basal-like breast cancer, and function importantly in promoting basal-like breast cancer progression. Thus the CCl2/CCR2 signaling can potentially serve as new therapeutic targets in basal-like breast cancer.

The stromal environment has emerged as a critical player in tumor progression (14). CAFs are the most abundant stroma cells present in cancers. Previous studies have suggested CAFs play important roles in tumor growth and metastasis (15). Thus, targeting CAFs has been proposed as promising alternative therapeutic strategy (108). However, directly targeting CAFs is difficult, due to lack of CAFs unique molecular markers (15). Thus, targeting cancer promoting factors derived from fibroblasts may serve as alternative approaches. In these studies, we report that CAFs are a major cellular source of CCL2, and CCL2 plays an important role in

breast cancer progression. Our studies provide a new molecular mechanism of cancer associated fibroblasts in cancer promotion through CCL2, which can potentially serve as a therapeutic target.

Chemokine CCL2 expression has been shown to elevate in various cancer types, including breast cancer and prostate cancer (32). The mechanistic role of CCL2, however, has been most studied in the focus of monocyte/macrophage recruitment in cancer (36). It is largely unknown whether CCL2 can directly signal into breast cancer cells. In this study, we have identified a novel mechanism of CCL2 function through directly signaling to cancer cells through CCR2. Mutation of CCR2 receptor in cancer cells significantly reduces tumor growth *in vivo* in response to fibroblasts derived CCL2. Our studies provide the first *in vivo* evidence on the importance of direct CCL2 signaling into breast cancer.

Conceptually, our studies address the role of tumor stroma in cancer progression, and specifically focus on CCL2/CCR2 signaling mediated fibroblast and breast cancer cell interaction. In addition, our studies uncover a novel mechanism of CCL2 function by directly signaling to breast cancer cells through CCR2 receptor.

In this study, we have generated valuable materials for CCL2 signaling studies. We have derived multiple primary breast CAFs cell lines. We have generated multiple CCL2 and CCR2 mutant or knockdown cell lines. All of those will provide valuable resources for the laboratory and the scientific community. We have also used innovative tools to address those questions through *in vitro* and *in vivo* models, such as the 3-dimensional culture model and co-graft tumor model. Taken together, our studies have been carried out using innovative and convincing approaches to address important questions in breast cancer.

Clinical application

The CCL2/CCR2 signaling has been continually pursued as therapeutic targets in both immune disease and cancer. In earlier clinical trials, CCL2 blocking antibody had been tested in primary and metastatic cancers, either used as a single agent or in combination with chemotherapy. Unfortunately, in all the trials, CCL2 inhibition by blocking antibody did not result in objective responses in cancer patients (93-95). Analysis of CCL2 level in patient blood samples revealed that the blocking antibody was not able to suppress CCL2 level overcome time (96). More recently, a new clinical trial with CCR2 inhibitor showed promising efficacy. In a stage I clinical trial in localized pancreatic cancer, treatment with the combination of CCR2 inhibitor PF-04136309 and chemotherapy led to 49% objective response (90). In contrast, chemotherapy alone treatment did not result in any objective response. Many other ongoing clinical trials are designed to combine CCR2 inhibition with checkpoint blockade therapy in immunotherapy.

Our studies indicate that the CCL2 signaling functions importantly in basal-like breast cancer progression. We also uncover a novel mechanism of CCL2 function through directly signaling to breast cancer cells. These studies will provide rationale in potentially targeting CCL2 signaling in basal-like breast cancer in clinic. In addition, CCL2 inhibition in clinical can potentially lead to a dual anti-cancer mechanism--blocking tumor promoting myeloid cells recruitment and blocking direct cancer cells signaling (Figure 31).

In our pre-clinical trial mouse model, we have attempted to develop an alternative approach to overcome the previous failure of CCL2 antibody in clinical trials. We ration that continual delivery of CCL2 blocking antibody would lead to steady antibody level and better therapeutic efficacy, compared to traditional interval injection used in earlier clinical trials.

However, our studies result in similar failure in controlling tumor progression in mouse model. We have observed an increased free CCL2 level with CCL2 blocking antibody, consistent with earlier reports (95). So those studies indicate a potential problem in targeting CCL2 with blocking antibody. Alternatively, targeting CCL2 signaling with CCR2 inhibitors may provide better clinical efficacy.

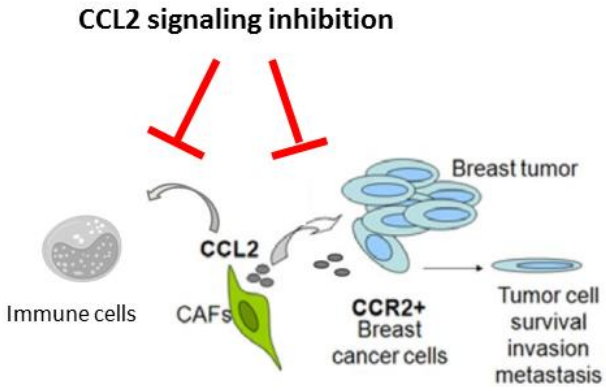

Figure 31. Clinical application of CCL2/CCR2 signaling targeting in breast cancer.

Limitations and future directions

While our studies provide valuable insights on CCL2 signaling in basal-like breast cancer progression, the studies are limited by methods and experimental models used. Future studies with additional tumor models will provide a further understanding of CCL2 signaling and stromal fibroblast functions in breast cancer.

First of all, the fibroblast-cancer cell co-graft model provides a useful system to facilitate genetic modulation of individual factors in fibroblasts or cancer cells. However, the grafted fibroblasts have limited proliferation capacity *in vivo*, and can be compensated by mouse stromal fibroblasts recruited into the tumor. In our experience, the effect of grafted fibroblasts in tumor growth promotion was most prominent in the first four weeks. After that, the tumor growth slope was similar to CA1D cancer cells grafted alone. Histology analysis revealed that cancer cells recruited mouse stromal fibroblasts infiltration/proliferation, which may compensate for the function of grafted fibroblasts. This is relevant because mouse Ccl2 derived from mouse

fibroblasts can also signal to human CCR2 in cancer cells and promote tumor progression. To overcome this, a mouse genetic model with conditional knockout CCL2 in fibroblast lineage is a more desirable tumor host. This can be potentially achieved by crossing mouse strain with CCL2 flox allele (109) with Cre recombinase expressed in fibroblasts lineage, such as Fsp1-cre mice (22). We expect that conditional knockout of CCL2 in fibroblasts will reduce grafted tumor growth more dramatically compared to our co-graft model. However, none of the current fibroblasts expressing Cre mouse lines are truly fibroblasts specific. For example, the Cre from Fsp1-cre mouse also expresses in immune cells such as macrophages (110). The depletion of CCL2 from macrophages can potentially confound the results. Similarly, the Cre from aSMA-Cre mouse expresses in endothelial cells besides CAFs (111), and endothelial cells are also implicated in CCL2 function. To overcome those, a more complicated mouse model may be needed, such as by creation of bone marrow chimeric mouse in Fsp1-Cre;$CCL2^{flox}$ with wildtype bone marrow. This will eliminate the confounding effect of CCL2 function on macrophages.

Secondly, we have used the immune-comprised nude mice as tumor host, to facilitate the study of human breast cancer cells. However, CCL2 has been indicated in tumor immunity regulation through MDSC recruitment (41). Thus, an immunocompetent mouse model is needed to address the potential dual function of CCL2 in immune cells recruitment and direct cancer cell signaling. Toward this, we have initiated a pilot project in developing a syngeneic mouse model by grafting mammary tumor cell line 4T1 into its cognate Balb/c mouse (112). Preliminary data indicated that the 4T1 tumor grew rapidly and spontaneously metastasized to the lung. Given that CCR2 is also highly expressed in 4T1 cell line (39), this mouse model will provide a valuable tool to study the effect of CCL2 in breast cancer in immunocompetent condition. This model will also provide opportunities to address the CCL2/CCR2 signaling in breast cancer metastasis.

To translate our studies into a potential clinical application, additional pre-clinical studies are needed. It will be critical to utilize additional CCL2/CCR2 signaling targeting reagents, such as CCR2 inhibitor, to test their efficacy in a preclinical mouse model. A few pharmaceutic companies have CCR2 inhibitors in clinical trials (113). A potential collaboration with them will enable us access to those drug candidates. In the potential pre-clinical studies, we will first test the efficacy of those CCR2 inhibitors in a panel of breast cancer cell lines, with especially focusing on basal-like cell lines. It will also be interesting to compare the sensitivity of basal-like breast cancer cells vs. cell lines from other subtypes in response to CCR2 inhibition. Lastly, CCR2 inhibition will be studied *in vivo* using mouse model of basal-like breast cancer. Success of these studies will provide confirmative supports in pursuing CCL2/CCR2 as therapeutic targets in basal-like breast cancer.

In addition, most of our studies have focused on targeting CCL2/CCR2 signaling alone. To achieve a durable clinical response, a potential strategy is developing a combinational therapy with CCL2/CCR2 inhibition. Our studies indicate that the CCL2 signaling potentially interacts with RAS signaling pathways in promoting cancer progression. Thus, it will be rational to test the efficacy to inhibition CCL2 signaling and RAS pathways in combination. In addition, CCL2 has been reported to promote cell survival in breast cancer cells in response to chemotherapy (39). CCL2 expression *in vivo* has also promoted cancer recurrence in response to radiation therapy (114). Currently, clinical trials have been focusing on combining CCR2 inhibition with combination of immunotherapy. Thus, it will be critical to determine the best combination strategy in targeting CCL2 signaling.

In this study, our focus is mostly on how fibroblasts promote breast cancer progression. It is also interesting to determine the influence of cancer cells on stromal fibroblasts. Cancer

associated fibroblasts stay in an activated status (15). Those indicate that there is a continuous activation signal, most likely, coming from cancer cells, to maintain fibroblast activation status (115,116). We have observed the chemokine CCL2 expression is generally higher in CAFs compared to NAFs, indicating an activation related feature. CAFs are also known expressing high level of other chemokines, such as CXCL12 (117). It will be interesting to determine whether there are common upstream signaling pathways that are induced by cancer cells, and promote chemokine production. Common inflammatory signaling pathways, such as NF-κβ, can serve as potential candidates (115,118). Those interactions can be studied by analyzing CCL2 expression regulation in fibroblasts, in context of responding to cancer cell stimulation. Inhibition of a common upstream pathway in CAFs can be a potential strategy to overcome secretion of cancer promotion factors in cancer associated fibroblasts.

Reference

1. Society. AC. 2015 Breast Cancer Facts & Figures 2015-2016. Atlanta: American Cancer Society, Inc. <http://www.cancer.org/acs/groups/content/@research/documents/document/acspc-042725.pdf>.
2. Vargo-Gogola T, Rosen JM. Modelling breast cancer: one size does not fit all. Nature reviews Cancer 2007;7(9):659-72.
3. Li CI, Anderson BO, Daling JR, Moe RE. Trends in incidence rates of invasive lobular and ductal breast carcinoma. JAMA 2003;289(11):1421-4.
4. Barroso-Sousa R, Metzger-Filho O. Differences between invasive lobular and invasive ductal carcinoma of the breast: results and therapeutic implications. Ther Adv Med Oncol 2016;8(4):261-6.
5. Cancer AJCo. Breast. New York: Springer; 2010. 347-69 p.
6. Perou CM, Sorlie T, Eisen MB, van de Rijn M, Jeffrey SS, Rees CA, et al. Molecular portraits of human breast tumours. Nature 2000;406(6797):747-52.
7. Sorlie T, Perou CM, Tibshirani R, Aas T, Geisler S, Johnsen H, et al. Gene expression patterns of breast carcinomas distinguish tumor subclasses with clinical implications. Proceedings of the National Academy of Sciences of the United States of America 2001;98(19):10869-74.
8. Caan BJ, Sweeney C, Habel LA, Kwan ML, Kroenke CH, Weltzien EK, et al. Intrinsic subtypes from the PAM50 gene expression assay in a population-based breast cancer survivor cohort: prognostication of short- and long-term outcomes. Cancer Epidemiol Biomarkers Prev 2014;23(5):725-34.
9. Dowsett M, Sestak I, Lopez-Knowles E, Sidhu K, Dunbier AK, Cowens JW, et al. Comparison of PAM50 risk of recurrence score with oncotype DX and IHC4 for predicting risk of distant recurrence after endocrine therapy. J Clin Oncol 2013;31(22):2783-90.
10. Guiu S, Michiels S, Andre F, Cortes J, Denkert C, Di Leo A, et al. Molecular subclasses of breast cancer: how do we define them? The IMPAKT 2012 Working Group Statement. Ann Oncol 2012;23(12):2997-3006.
11. Badve S, Dabbs DJ, Schnitt SJ, Baehner FL, Decker T, Eusebi V, et al. Basal-like and triple-negative breast cancers: a critical review with an emphasis on the implications for pathologists and oncologists. Modern pathology : an official journal of the United States and Canadian Academy of Pathology, Inc 2011;24(2):157-67.
12. Perou CM. Molecular stratification of triple-negative breast cancers. Oncologist 2011;16 Suppl 1:61-70.
13. Blows FM, Driver KE, Schmidt MK, Broeks A, van Leeuwen FE, Wesseling J, et al. Subtyping of breast cancer by immunohistochemistry to investigate a relationship between subtype and short and long term survival: a collaborative analysis of data for 10,159 cases from 12 studies. PLoS medicine 2010;7(5):e1000279.
14. Quail DF, Joyce JA. Microenvironmental regulation of tumor progression and metastasis. Nature medicine 2013;19(11):1423-37.
15. Kalluri R. The biology and function of fibroblasts in cancer. Nature reviews Cancer 2016;16(9):582-98.

16. Augsten M. Cancer-associated fibroblasts as another polarized cell type of the tumor microenvironment. Frontiers in oncology 2014;4:62.
17. Sugimoto H, Mundel TM, Kieran MW, Kalluri R. Identification of fibroblast heterogeneity in the tumor microenvironment. Cancer biology & therapy 2006;5(12):1640-6.
18. Surowiak P, Murawa D, Materna V, Maciejczyk A, Pudelko M, Ciesla S, et al. Occurence of stromal myofibroblasts in the invasive ductal breast cancer tissue is an unfavourable prognostic factor. Anticancer Res 2007;27(4C):2917-24.
19. Paulsson J, Sjoblom T, Micke P, Ponten F, Landberg G, Heldin CH, et al. Prognostic significance of stromal platelet-derived growth factor beta-receptor expression in human breast cancer. The American journal of pathology 2009;175(1):334-41.
20. Schoppmann SF, Berghoff A, Dinhof C, Jakesz R, Gnant M, Dubsky P, et al. Podoplanin-expressing cancer-associated fibroblasts are associated with poor prognosis in invasive breast cancer. Breast cancer research and treatment 2012;134(1):237-44.
21. Ariga N, Sato E, Ohuchi N, Nagura H, Ohtani H. Stromal expression of fibroblast activation protein/seprase, a cell membrane serine proteinase and gelatinase, is associated with longer survival in patients with invasive ductal carcinoma of breast. International journal of cancer Journal international du cancer 2001;95(1):67-72.
22. Bhowmick NA, Chytil A, Plieth D, Gorska AE, Dumont N, Shappell S, et al. TGF-beta signaling in fibroblasts modulates the oncogenic potential of adjacent epithelia. Science 2004;303(5659):848-51.
23. Kraman M, Bambrough PJ, Arnold JN, Roberts EW, Magiera L, Jones JO, et al. Suppression of antitumor immunity by stromal cells expressing fibroblast activation protein-alpha. Science 2010;330(6005):827-30.
24. Rhim AD, Oberstein PE, Thomas DH, Mirek ET, Palermo CF, Sastra SA, et al. Stromal elements act to restrain, rather than support, pancreatic ductal adenocarcinoma. Cancer cell 2014;25(6):735-47.
25. Ozdemir BC, Pentcheva-Hoang T, Carstens JL, Zheng X, Wu CC, Simpson TR, et al. Depletion of carcinoma-associated fibroblasts and fibrosis induces immunosuppression and accelerates pancreas cancer with reduced survival. Cancer cell 2014;25(6):719-34.
26. Griffith JW, Sokol CL, Luster AD. Chemokines and chemokine receptors: positioning cells for host defense and immunity. Annual review of immunology 2014;32:659-702.
27. Deshmane SL, Kremlev S, Amini S, Sawaya BE. Monocyte chemoattractant protein-1 (MCP-1): an overview. Journal of interferon & cytokine research : the official journal of the International Society for Interferon and Cytokine Research 2009;29(6):313-26.
28. Charo IF, Myers SJ, Herman A, Franci C, Connolly AJ, Coughlin SR. Molecular cloning and functional expression of two monocyte chemoattractant protein 1 receptors reveals alternative splicing of the carboxyl-terminal tails. Proceedings of the National Academy of Sciences of the United States of America 1994;91(7):2752-6.
29. Kurihara T, Warr G, Loy J, Bravo R. Defects in macrophage recruitment and host defense in mice lacking the CCR2 chemokine receptor. The Journal of experimental medicine 1997;186(10):1757-62.
30. Lu B, Rutledge BJ, Gu L, Fiorillo J, Lukacs NW, Kunkel SL, et al. Abnormalities in monocyte recruitment and cytokine expression in monocyte chemoattractant protein 1-deficient mice. The Journal of experimental medicine 1998;187(4):601-8.

31. Tsou CL, Peters W, Si Y, Slaymaker S, Aslanian AM, Weisberg SP, et al. Critical roles for CCR2 and MCP-3 in monocyte mobilization from bone marrow and recruitment to inflammatory sites. J Clin Invest 2007;117(4):902-9.
32. Hembruff SL, Cheng N. Chemokine signaling in cancer: Implications on the tumor microenvironment and therapeutic targeting. Cancer therapy 2009;7(A):254-67.
33. Soria G, Ben-Baruch A. The inflammatory chemokines CCL2 and CCL5 in breast cancer. Cancer letters 2008;267(2):271-85.
34. Zhang J, Patel L, Pienta KJ. CC chemokine ligand 2 (CCL2) promotes prostate cancer tumorigenesis and metastasis. Cytokine & growth factor reviews 2010;21(1):41-8.
35. Fujimoto H, Sangai T, Ishii G, Ikehara A, Nagashima T, Miyazaki M, et al. Stromal MCP-1 in mammary tumors induces tumor-associated macrophage infiltration and contributes to tumor progression. Int J Cancer 2009;125(6):1276-84.
36. Qian BZ, Li J, Zhang H, Kitamura T, Zhang J, Campion LR, et al. CCL2 recruits inflammatory monocytes to facilitate breast-tumour metastasis. Nature 2011;475(7355):222-5.
37. Yoshimura T, Howard OM, Ito T, Kuwabara M, Matsukawa A, Chen K, et al. Monocyte chemoattractant protein-1/CCL2 produced by stromal cells promotes lung metastasis of 4T1 murine breast cancer cells. PLoS One 2013;8(3):e58791.
38. Hembruff SL, Jokar I, Yang L, Cheng N. Loss of transforming growth factor-beta signaling in mammary fibroblasts enhances CCL2 secretion to promote mammary tumor progression through macrophage-dependent and -independent mechanisms. Neoplasia 2010;12(5):425-33.
39. Fang WB, Jokar I, Zou A, Lambert D, Dendukuri P, Cheng N. CCL2/CCR2 chemokine signaling coordinates survival and motility of breast cancer cells through Smad3 protein- and p42/44 mitogen-activated protein kinase (MAPK)-dependent mechanisms. The Journal of biological chemistry 2012;287(43):36593-608.
40. Rajaram M, Li J, Egeblad M, Powers RS. System-wide analysis reveals a complex network of tumor-fibroblast interactions involved in tumorigenicity. PLoS Genet 2013;9(9):e1003789.
41. Chun E, Lavoie S, Michaud M, Gallini CA, Kim J, Soucy G, et al. CCL2 Promotes Colorectal Carcinogenesis by Enhancing Polymorphonuclear Myeloid-Derived Suppressor Cell Population and Function. Cell Rep 2015;12(2):244-57.
42. Vande Broek I, Leleu X, Schots R, Facon T, Vanderkerken K, Van Camp B, et al. Clinical significance of chemokine receptor (CCR1, CCR2 and CXCR4) expression in human myeloma cells: the association with disease activity and survival. Haematologica 2006;91(2):200-6.
43. Lu Y, Cai Z, Xiao G, Liu Y, Keller ET, Yao Z, et al. CCR2 expression correlates with prostate cancer progression. Journal of cellular biochemistry 2007;101(3):676-85.
44. Zhang XW, Qin X, Qin CY, Yin YL, Chen Y, Zhu HL. Expression of monocyte chemoattractant protein-1 and CC chemokine receptor 2 in non-small cell lung cancer and its significance. Cancer immunology, immunotherapy : CII 2013;62(3):563-70.
45. Tsuyada A, Chow A, Wu J, Somlo G, Chu P, Loera S, et al. CCL2 mediates cross-talk between cancer cells and stromal fibroblasts that regulates breast cancer stem cells. Cancer research 2012;72(11):2768-79.

46. Sorlie T, Tibshirani R, Parker J, Hastie T, Marron JS, Nobel A, et al. Repeated observation of breast tumor subtypes in independent gene expression data sets. Proc Natl Acad Sci U S A 2003;100(14):8418-23.
47. Sorlie T, Perou CM, Tibshirani R, Aas T, Geisler S, Johnsen H, et al. Gene expression patterns of breast carcinomas distinguish tumor subclasses with clinical implications. Proc Natl Acad Sci U S A 2001;98(19):10869-74.
48. Cheang MC, Chia SK, Voduc D, Gao D, Leung S, Snider J, et al. Ki67 index, HER2 status, and prognosis of patients with luminal B breast cancer. J Natl Cancer Inst 2009;101(10):736-50.
49. Aleskandarany MA, Green AR, Benhasouna AA, Barros FF, Neal K, Reis-Filho JS, et al. Prognostic value of proliferation assay in the luminal, HER2-positive, and triple-negative biologic classes of breast cancer. Breast Cancer Res 2012;14(1):R3.
50. Munzone E, Curigliano G, Colleoni M. Tailoring adjuvant treatments for the individual patient with luminal breast cancer. Hematol Oncol Clin North Am 2013;27(4):703-14, vii-viii.
51. Hudis CA, Gianni L. Triple-negative breast cancer: an unmet medical need. The oncologist 2011;16 Suppl 1:1-11.
52. Ueno T, Toi M, Saji H, Muta M, Bando H, Kuroi K, et al. Significance of macrophage chemoattractant protein-1 in macrophage recruitment, angiogenesis, and survival in human breast cancer. Clin Cancer Res 2000;6(8):3282-9.
53. Valkovic T, Fuckar D, Stifter S, Matusan K, Hasan M, Dobrila F, et al. Macrophage level is not affected by monocyte chemotactic protein-1 in invasive ductal breast carcinoma. Journal of cancer research and clinical oncology 2005;131(7):453-8.
54. Fang WB, Yao M, Jokar I, Alhakamy N, Berkland C, Chen J, et al. The CCL2 chemokine is a negative regulator of autophagy and necrosis in luminal B breast cancer cells. Breast Cancer Res Treat 2015;150(2):309-20.
55. Zou A, Lambert D, Yeh H, Yasukawa K, Behbod F, Fan F, et al. Elevated CXCL1 expression in breast cancer stroma predicts poor prognosis and is inversely associated with expression of TGF-beta signaling proteins. BMC Cancer 2014;14:781.
56. Abadi A, Yavari P, Dehghani-Arani M, Alavi-Majd H, Ghasemi E, Amanpour F, et al. Cox models survival analysis based on breast cancer treatments. Iran J Cancer Prev 2014;7(3):124-9.
57. Kwan ML, Kushi LH, Weltzien E, Maring B, Kutner SE, Fulton RS, et al. Epidemiology of breast cancer subtypes in two prospective cohort studies of breast cancer survivors. Breast Cancer Res 2009;11(3):R31.
58. Rezai M, Kellersmann S, Knispel S, Lax H, Kimmig R, Kern P. Translating the concept of intrinsic subtypes into an oncoplastic cohort of more than 1000 patients - predictors of recurrence and survival. Breast 2015;24(4):384-90.
59. Dehqanzada ZA, Storrer CE, Hueman MT, Foley RJ, Harris KA, Jama YH, et al. Correlations between serum monocyte chemotactic protein-1 levels, clinical prognostic factors, and HER-2/neu vaccine-related immunity in breast cancer patients. Clin Cancer Res 2006;12(2):478-86.
60. Park SY, Kim HM, Koo JS. Differential expression of cancer-associated fibroblast-related proteins according to molecular subtype and stromal histology in breast cancer. Breast Cancer Res Treat 2015;149(3):727-41.

61. Yao M, Yu E, Staggs V, Fan F, Cheng N. Elevated expression of chemokine C-C ligand 2 in stroma is associated with recurrent basal-like breast cancers. Mod Pathol 2016.
62. Fang WB, Jokar I, Chytil A, Moses HL, Abel T, Cheng N. Loss of one Tgfbr2 allele in fibroblasts promotes metastasis in MMTV: polyoma middle T transgenic and transplant mouse models of mammary tumor progression. Clin Exp Metastasis 2011;28(4):351-66.
63. Strickland LB, Dawson PJ, Santner SJ, Miller FR. Progression of premalignant MCF10AT generates heterogeneous malignant variants with characteristic histologic types and immunohistochemical markers. Breast cancer research and treatment 2000;64(3):235-40.
64. Santner SJ, Dawson PJ, Tait L, Soule HD, Eliason J, Mohamed AN, et al. Malignant MCF10CA1 cell lines derived from premalignant human breast epithelial MCF10AT cells. Breast cancer research and treatment 2001;65(2):101-10.
65. Guy CT, Cardiff RD, Muller WJ. Induction of mammary tumors by expression of polyomavirus middle T oncogene: a transgenic mouse model for metastatic disease. Mol Cell Biol 1992;12(3):954-61.
66. Cheng N, Bhowmick NA, Chytil A, Gorksa AE, Brown KA, Muraoka R, et al. Loss of TGF-beta type II receptor in fibroblasts promotes mammary carcinoma growth and invasion through upregulation of TGF-alpha-, MSP- and HGF-mediated signaling networks. Oncogene 2005;24(32):5053-68.
67. Morales CP, Holt SE, Ouellette M, Kaur KJ, Yan Y, Wilson KS, et al. Absence of cancer-associated changes in human fibroblasts immortalized with telomerase. Nature genetics 1999;21(1):115-8.
68. Lambert D, Cheng N. Mammary transplantation of stromal cells and carcinoma cells in C57BL/6 mice. Journal of Visualized Experiments 2011 (54).
69. Fang WB, Yao M, Brummer G, Acevedo D, Alhakamy N, Berkland C, et al. Targeted gene silencing of CCL2 inhibits triple negative breast cancer progression by blocking cancer stem cell renewal and M2 macrophage recruitment. Oncotarget 2016.
70. Tiscornia G, Singer O, Verma IM. Production and purification of lentiviral vectors. Nat Protoc 2006;1(1):241-5.
71. Sanjana NE, Shalem O, Zhang F. Improved vectors and genome-wide libraries for CRISPR screening. Nature methods 2014;11(8):783-84.
72. Heckl D, Kowalczyk MS, Yudovich D, Belizaire R, Puram RV, McConkey ME, et al. Generation of mouse models of myeloid malignancy with combinatorial genetic lesions using CRISPR-Cas9 genome editing. Nat Biotechnol 2014;32(9):941-6.
73. Lee GY, Kenny PA, Lee EH, Bissell MJ. Three-dimensional culture models of normal and malignant breast epithelial cells. Nature methods 2007;4(4):359-65.
74. Cancer Genome Atlas N. Comprehensive molecular portraits of human breast tumours. Nature 2012;490(7418):61-70.
75. Curtis C, Shah SP, Chin SF, Turashvili G, Rueda OM, Dunning MJ, et al. The genomic and transcriptomic architecture of 2,000 breast tumours reveals novel subgroups. Nature 2012;486(7403):346-52.
76. Pereira B, Chin SF, Rueda OM, Vollan HK, Provenzano E, Bardwell HA, et al. The somatic mutation profiles of 2,433 breast cancers refines their genomic and transcriptomic landscapes. Nat Commun 2016;7:11479.
77. Hsu PD, Lander ES, Zhang F. Development and applications of CRISPR-Cas9 for genome engineering. Cell 2014;157(6):1262-78.

78. Salcedo R, Ponce ML, Young HA, Wasserman K, Ward JM, Kleinman HK, et al. Human endothelial cells express CCR2 and respond to MCP-1: direct role of MCP-1 in angiogenesis and tumor progression. Blood 2000;96(1):34-40.
79. Thelen M. Dancing to the tune of chemokines. Nat Immunol 2001;2(2):129-34.
80. Hanke JH, Gardner JP, Dow RL, Changelian PS, Brissette WH, Weringer EJ, et al. Discovery of a novel, potent, and Src family-selective tyrosine kinase inhibitor. Study of Lck- and FynT-dependent T cell activation. The Journal of biological chemistry 1996;271(2):695-701.
81. Zhu X, Kim JL, Newcomb JR, Rose PE, Stover DR, Toledo LM, et al. Structural analysis of the lymphocyte-specific kinase Lck in complex with non-selective and Src family selective kinase inhibitors. Structure 1999;7(6):651-61.
82. Gschwendt M, Dieterich S, Rennecke J, Kittstein W, Mueller HJ, Johannes FJ. Inhibition of protein kinase C mu by various inhibitors. Differentiation from protein kinase c isoenzymes. FEBS Lett 1996;392(2):77-80.
83. Gould CM, Antal CE, Reyes G, Kunkel MT, Adams RA, Ziyar A, et al. Active site inhibitors protect protein kinase C from dephosphorylation and stabilize its mature form. The Journal of biological chemistry 2011;286(33):28922-30.
84. Zhang XH, Jin X, Malladi S, Zou Y, Wen YH, Brogi E, et al. Selection of bone metastasis seeds by mesenchymal signals in the primary tumor stroma. Cell 2013;154(5):1060-73.
85. Kadota M, Yang HH, Gomez B, Sato M, Clifford RJ, Meerzaman D, et al. Delineating genetic alterations for tumor progression in the MCF10A series of breast cancer cell lines. PLoS One 2010;5(2):e9201.
86. Chavey C, Bibeau F, Gourgou-Bourgade S, Burlinchon S, Boissiere F, Laune D, et al. Oestrogen receptor negative breast cancers exhibit high cytokine content. Breast cancer research : BCR 2007;9(1):R15.
87. Bonapace L, Coissieux MM, Wyckoff J, Mertz KD, Varga Z, Junt T, et al. Cessation of CCL2 inhibition accelerates breast cancer metastasis by promoting angiogenesis. Nature 2014;515(7525):130-3.
88. Yao M, Smart C, Hu Q, Cheng N. Continuous Delivery of Neutralizing Antibodies Elevate CCL2 Levels in Mice Bearing MCF10CA1d Breast Tumor Xenografts. Transl Oncol 2017;10(5):734-43.
89. Scott AM, Wolchok JD, Old LJ. Antibody therapy of cancer. Nat Rev Cancer 2012;12(4):278-87.
90. Nywening TM, Wang-Gillam A, Sanford DE, Belt BA, Panni RZ, Cusworth BM, et al. Targeting tumour-associated macrophages with CCR2 inhibition in combination with FOLFIRINOX in patients with borderline resectable and locally advanced pancreatic cancer: a single-centre, open-label, dose-finding, non-randomised, phase 1b trial. Lancet Oncol 2016;17(5):651-62.
91. Loberg RD, Ying C, Craig M, Day LL, Sargent E, Neeley C, et al. Targeting CCL2 with systemic delivery of neutralizing antibodies induces prostate cancer tumor regression in vivo. Cancer Res 2007;67(19):9417-24.
92. Zhu X, Fujita M, Snyder LA, Okada H. Systemic delivery of neutralizing antibody targeting CCL2 for glioma therapy. J Neurooncol 2011;104(1):83-92.
93. Brana I, Calles A, LoRusso PM, Yee LK, Puchalski TA, Seetharam S, et al. Carlumab, an anti-C-C chemokine ligand 2 monoclonal antibody, in combination with four

chemotherapy regimens for the treatment of patients with solid tumors: an open-label, multicenter phase 1b study. Target Oncol 2015;10(1):111-23.
94. Pienta KJ, Machiels JP, Schrijvers D, Alekseev B, Shkolnik M, Crabb SJ, et al. Phase 2 study of carlumab (CNTO 888), a human monoclonal antibody against CC-chemokine ligand 2 (CCL2), in metastatic castration-resistant prostate cancer. Invest New Drugs 2013;31(3):760-8.
95. Sandhu SK, Papadopoulos K, Fong PC, Patnaik A, Messiou C, Olmos D, et al. A first-in-human, first-in-class, phase I study of carlumab (CNTO 888), a human monoclonal antibody against CC-chemokine ligand 2 in patients with solid tumors. Cancer Chemother Pharmacol 2013;71(4):1041-50.
96. Fetterly GJ, Aras U, Meholick PD, Takimoto C, Seetharam S, McIntosh T, et al. Utilizing pharmacokinetics/pharmacodynamics modeling to simultaneously examine free CCL2, total CCL2 and carlumab (CNTO 888) concentration time data. J Clin Pharmacol 2013;53(10):1020-7.
97. Fang WB, Mafuvadze B, Yao M, Zou A, Portsche M, Cheng N. TGF-beta Negatively Regulates CXCL1 Chemokine Expression in Mammary Fibroblasts through Enhancement of Smad2/3 and Suppression of HGF/c-Met Signaling Mechanisms. PLoS One 2015;10(8):e0135063.
98. Uliasz TF, Hewett SJ. A microtiter trypan blue absorbance assay for the quantitative determination of excitotoxic neuronal injury in cell culture. J Neurosci Methods 2000;100(1-2):157-63.
99. Haslene-Hox H, Oveland E, Berg KC, Kolmannskog O, Woie K, Salvesen HB, et al. A new method for isolation of interstitial fluid from human solid tumors applied to proteomic analysis of ovarian carcinoma tissue. PLoS One 2011;6(4):e19217.
100. Rosen H, Abribat T. The rise and rise of drug delivery. Nat Rev Drug Discov 2005;4(5):381-5.
101. Patra CN, Swain S, Sruti J, Patro AP, Panigrahi KC, Beg S, et al. Osmotic drug delivery systems: basics and design approaches. Recent Pat Drug Deliv Formul 2013;7(2):150-61.
102. Chen J, Pan H, Ye T, Liu D, Li Q, Chen F, et al. Recent Aspects of Osmotic Pump Systems: Functionalization, Clinical use and Advanced Imaging Technology. Curr Drug Metab 2016;17(3):279-91.
103. Vassileva V, Allen CJ, Piquette-Miller M. Effects of sustained and intermittent paclitaxel therapy on tumor repopulation in ovarian cancer. Mol Cancer Ther 2008;7(3):630-7.
104. Shimamura T, Fujisawa T, Husain SR, Joshi B, Puri RK. Interleukin 13 mediates signal transduction through interleukin 13 receptor alpha2 in pancreatic ductal adenocarcinoma: role of IL-13 Pseudomonas exotoxin in pancreatic cancer therapy. Clin Cancer Res 2010;16(2):577-86.
105. Zhidkov N, De Souza R, Ghassemi AH, Allen C, Piquette-Miller M. Continuous intraperitoneal carboplatin delivery for the treatment of late-stage ovarian cancer. Mol Pharm 2013;10(9):3315-22.
106. Minchinton AI, Tannock IF. Drug penetration in solid tumours. Nat Rev Cancer 2006;6(8):583-92.
107. Mizutani K, Sud S, McGregor NA, Martinovski G, Rice BT, Craig MJ, et al. The chemokine CCL2 increases prostate tumor growth and bone metastasis through macrophage and osteoclast recruitment. Neoplasia 2009;11(11):1235-42.

108. Engels B, Rowley DA, Schreiber H. Targeting stroma to treat cancers. Seminars in cancer biology 2012;22(1):41-9.
109. Shi C, Jia T, Mendez-Ferrer S, Hohl TM, Serbina NV, Lipuma L, et al. Bone marrow mesenchymal stem and progenitor cells induce monocyte emigration in response to circulating toll-like receptor ligands. Immunity 2011;34(4):590-601.
110. Osterreicher CH, Penz-Osterreicher M, Grivennikov SI, Guma M, Koltsova EK, Datz C, et al. Fibroblast-specific protein 1 identifies an inflammatory subpopulation of macrophages in the liver. Proceedings of the National Academy of Sciences of the United States of America 2011;108(1):308-13.
111. Wendling O, Bornert JM, Chambon P, Metzger D. Efficient temporally-controlled targeted mutagenesis in smooth muscle cells of the adult mouse. Genesis 2009;47(1):14-8.
112. Pulaski BA, Ostrand-Rosenberg S. Mouse 4T1 breast tumor model. Curr Protoc Immunol 2001;Chapter 20:Unit 20 2.
113. Nywening TM, Wang-Gillam A, Sanford DE, Belt BA, Panni RZ, Cusworth BM, et al. Targeting tumour-associated macrophages with CCR2 inhibition in combination with FOLFIRINOX in patients with borderline resectable and locally advanced pancreatic cancer: a single-centre, open-label, dose-finding, non-randomised, phase 1b trial. Lancet Oncol 2016.
114. Kalbasi A, Komar C, Tooker GM, Liu M, Lee JW, Gladney WL, et al. Tumor-Derived CCL2 Mediates Resistance to Radiotherapy in Pancreatic Ductal Adenocarcinoma. Clinical cancer research : an official journal of the American Association for Cancer Research 2017;23(1):137-48.
115. Erez N, Truitt M, Olson P, Arron ST, Hanahan D. Cancer-Associated Fibroblasts Are Activated in Incipient Neoplasia to Orchestrate Tumor-Promoting Inflammation in an NF-kappaB-Dependent Manner. Cancer cell 2010;17(2):135-47.
116. Mitra AK, Zillhardt M, Hua Y, Tiwari P, Murmann AE, Peter ME, et al. MicroRNAs reprogram normal fibroblasts into cancer-associated fibroblasts in ovarian cancer. Cancer Discov 2012;2(12):1100-8.
117. Orimo A, Gupta PB, Sgroi DC, Arenzana-Seisdedos F, Delaunay T, Naeem R, et al. Stromal fibroblasts present in invasive human breast carcinomas promote tumor growth and angiogenesis through elevated SDF-1/CXCL12 secretion. Cell 2005;121(3):335-48.
118. Grivennikov SI, Greten FR, Karin M. Immunity, inflammation, and cancer. Cell 2010;140(6):883-99.